STUDY OF FDM BASED ADDITIVE MANUFACTURING PROCESS THROUGH OPTIMIZED DEEP LEARNING STRATEGY

Thesis Submitted for the Award of the Degree of

DOCTOR OF PHILOSOPHY

in

Mechanical engineering

By

Nitin Narayan Gotkhindikar

Registration Number: 41900738

Supervised By

Dr. Mahipal

Associate Professor, School of Mechanical Engineering, Lovely Professional University, Phagwara, Punjab, India

Co-Supervised by

Dr. Ravinder Kataria

Assistant Professor, Department of Fashion Design, National Institute of Fashion Technology, Jammu, India

LOVELY PROFESSIONAL UNIVERSITY, PUNJAB

2024

DECLARATION

I, hereby declared that the presented work in the thesis entitled "Study of FDM Based Additive Manufacturing Process through Optimized Deep Learning Strategy" in fulfilment of degree of **Doctor of Philosophy (Ph. D.)** is outcome of research work carried out by me under the supervision of Dr. Mahipal, working as Associate professor, in the School of Mechanical Engineering of Lovely Professional University, Punjab, India. In keeping with general practice of reporting scientific observations, due acknowledgements have been made whenever work described here has been based on findings of other investigator. This work has not been submitted in part or full to any other University or Institute for the award of any degree.

(Signature of Scholar)

Name of the scholar: Nitin Narayan Gotkhindikar

Registration No.: 41900738

Department/school: School of mechanical engineering

Lovely Professional University,

Punjab, India

CERTIFICATE

This is to certify that the work reported in the Ph. D. thesis entitled Study of FDM Based Additive Manufacturing Process through Optimized Deep Learning Strategy" submitted in fulfillment of the requirement for the award of degree of **Doctor of Philosophy (Ph.D.)** in the School of mechanical engineering, is a research work carried out by Mr. Nitin Narayan Gotkhindikar, (Registration No.) 41900738, is bonafide record of his original work carried out under my supervision and that no part of thesis has been submitted for any other degree, diploma or equivalent course.

(Signature of Supervisor)

Name of supervisor: Dr. Mahipal

Designation: Associate professor

Department/school: Mechanical engineering

University: LPU, Punjab, India

(Signature of Co-Supervisor)

Name of Co-Supervisor: Dr. Ravinder Kataria

Designation: Assistant professor

Department/school: Fashion design

University: NIFT, Jammu, India

ABSTRACT

The process, which is designed as 3D digital data to create component layers using depositing elements are termed as Additive Manufacturing (AM). Moreover, this AM mechanism is the competitive model for the conventional manufacturing scheme, because several complex design processes are widely difficult and impossible using conventional model. Fused deposition modeling (FDM) is a model of AM which uses layer by layer-based methodology to fabricate a component. Today in the digital manufacturing era FDM process is widely used as it can construct intricate and complex part geometries in short time as compared to conventional manufacturing, its simplicity and economical bahaviour. Hence, the FDM strategy is primarily used to fabricate the products in an attractive manner; these kinds of products are mainly worn in real life. FDM is well-known with guests in a type of industries, from automotive sector to items bought by consumer's production. These guests use FDM throughout their output growth, prototyping and manufacturing processes. FDM is having uniqueness in term of no loose powder and material used in the form of filament offers adaptability and reduces the resident time into sight the melting chamber. In FDM the process parameters are dominant determinants for reconstructing the part characteristics and minimizing the build time and cost. Though evidently several researches have been carried out regarding optimisation of input parameters to enhance the mechanical properties of FDM printed parts, eventually various studies reported the flimsy nature of 3D printed materials which should be taken care of. Despite of many advantages, literature argued various machine learning approaches adopted to increase the performance of FDM addressing the issues of irregularities in part properties, accuracy, and reliability due to challenging task of best parametric selection.

Nowadays, AM process is incorporated with several real-time applications and rapidly increased in many fields. Considering other methods, the AM with FDM printing technology is low cost and easy to use. However, compare the existing techniques various complexity and lower prediction capabilities were reviewed. In

addition, mismatch connection during the designing process may reduce the prediction accuracy rate; therefore, the prediction is very important regarding those issues and parameter selection. The main aim of this ML with AM technique is to select the best parameter combination in the 3D printing design. During the printing process, the input data is carried randomly then it leads to cause the overflow issue. These problems have been motivated this present research work.

In this context, the present study proposed a deep neural network strategy to predict the best parametric combination with optimized mechanical properties of printed parts. In the present research, less analysed design variables parameters like nozzle diameter, width of print line, layer thickness and print speed were considered as input parameters with their levels values that were trained to the proposed system. The selection of values was based on previous literature and customized 3D printed FDM machine. Adhering to ASTM standards with predefined dimensions total 256 experiments have been carried for each output, in which 204 result data used for training and 52 for testing the model using PYTHON programming language. Subsequently, the proposed model has gained the accuracy of 88.46% and RMSE value 0.3396 and R^2 value 0.8796 is validated by relating the performance with existing models. Nozzle diameter was influential parameter for tensile strength, flexural strength and layer thickness dominates compressive strength predicted by Taguchi analysis.

In this research, a deep learning model was developed for detecting the best connection between process parameters. For example, high dimensional accuracy, high surface finish and better tensile strength can be achieved by setting low layer thickness but can affect the compressive strength adversely. Print speed affects the mechanical properties; build time affects the overall cost of product. Hence, the efficient outcomes of the developed model have been verified by gaining the best combination of process parameters and Taguchi analysis interpreted their influence on the mechanical strength of FDM printed parts.

Taguchi L16 array of specific subset of input parameters combinations was utilized to conduct the experimentation for case study. Tensile strength, compressive strength

and flexural strength were analysed by multi optimization using Taguchi and Grey relation analysis combined with principal component analysis. PCA assigns weight to each measurable significant response which affects the GRG. PCA determined the contribution of tensile strength (43.22%), flexural strength (30.52%) and compressive strength (26.26%) respectively. WGRG values depicted the most influential factor as print speed followed by nozzle diameter, layer thickness and width of each print layer successively. Optimum combination of input parameters was analysed by GRA associated with PCA approach as nozzle diameter 0.3 mm, print speed 60 mm/s, layer thickness 0.2 mm and width of each layer 0.9 mm which was classified into class 1 in DNN. Confirmatory experimental values for flexural strength were 60.7 Mpa, tensile strength 37.7 Mpa and compressive strength 26.1 Mpa which demonstrated 4.71 % improvement in predicted WGRG. Validation of proposed case study was carried out with experimental confirmation to find out significance of optimized parameters to enhance the mechanical behaviour of printed parts.

When the data fed is more this model will gain higher prediction accuracy. Limitation of this study is huge number of data is needed to accurately process the neural network model. This could be challenging and resource-intensive, particularly in cases where obtaining sufficient data may be difficult or expensive. In future this model can be used analyse the best combination for the optimization of other mechanical properties. Theoretically speaking depending upon the objective of the application this model can be processed and tuned (like number of neurons and layers, activation functions, optimizers, dropouts, normalization, batch size) to select optimized parametric combination to achieve different aims in terms of part quality characteristics, build time, cost etc. In futuristic direction other AI techniques like Big data, Cloud computing, IoT (Internet of Things) can be implemented. This study limits its use as standard test parts fabrication was used adhering to ASTM standards. In futuristic direction the optimum combination of FDM process design variables can be used to build smart manufacturing based real time components using highly customized 3D printers.

Keywords: *Additive manufacturing (AM), Fused deposition modelling (FDM), Grey relation analysis (GRA), Principal component analysis (PCA), Artificial intelligence*

(AI), Machine learning (ML), Deep neural network (DNN), IoT (Internet of Things), American society of testing materials (ASTM), Taguchi analysis, Mechanical properties, Big data, Cloud computing.

ACKNOWLEDGEMENT

I would like to extend my sincere gratitude to my thesis supervisor, Dr. Mahipal and co-supervisor Dr. Ravinder Kataria, for their invaluable guidance, unwavering support, and insightful advice throughout my research journey. Their mentorship, motivation, and expertise have been instrumental in shaping my work and helping me navigate through the challenges of my thesis. I am truly grateful for their dedication and encouragement, which have inspired me to strive for excellence. Thank you, Dr. Mahipal and Dr. Ravinder Kataria for being exceptional mentors who stood with me in hard times and for believing in my potential.

I am thankful to the entire family of Lovely Professional University, School of Mechanical Engineering for their administrative support during the various phases of my research work. Special thanks to Dr. Neha Munjal, Dr. Vishal Francis and Dr. Rekha for their timely guidance on necessary activities.

I extend my sincere thanks Auto Cluster Pvt. Ltd and 3DeoMetry solutions Pvt. Ltd for providing many specific amenities for conduction of research work.

I am highly obliged to Shri Malojiraje Chhatrapati (Chairman AISSMS COE), Dr. D. S. Bormane (Principal AISSMS COE), Dr. S. V. Chiatanya (Head Mechanical department) and all the colleagues for their moral support to my endeavour.

I must not forget to acknowledge almighty God, my parents, my wife Mrs Ketaki, son Nishiket for amazing support, encouragement, patience and advice during this journey.

TABLE OF CONTENTS

LIST OF TABLES

LIST OF FIGURES

LIST OF ABBREVIATIONS

Abbreviation	Description
3D	Three dimensional
ABS	Acrylonitrile butadiene styrene
ADT	Anderson darling test
AI	Artificial intelligence
AM	Additive manufacturing
ANF	Artificial neural framework
ANN	Artificial neural network
ANOVA	Analysis of variance
ASTM	American society of testing materials
CAD	Computer aided design
CFR-PLA	Carbon fibre-filled polylactide
CLIP	Continuous Liquid Interface Production
DFM	Design for manufacturing
DL	Deep learning
DNN	Deep Neural Network
DSD	Definitive screening design
FDM	Fused deposition modelling
FFF	Fused filament fabrication
GA	Genetic Algorithm
GRA	Grey regression analysis

GRG	Grey relational grade
IoT	Internet of Things
KNN	K-Nearest Neighbour
LOM	Laminated Object Manufacturing
LSTM	Long Short-Term Memory
MAM	Metal Additive Manufacturing
ML	Machine learning
NB	Naïve Bayes
PC	Polycarbonate
PCA	Principle component analysis
PEI	Polyetherimide
PLA	Polylactic acid
PPSF	Polyphenylsulfone
PSP	Process structure property
QC	Quality control
RELU	Rectified Linear Unit
RF	Random Forest
RMSE	Root Mean Squared Error
RSM	Response surface methodology
S/N	Signal to noise
SEM	Scanning electron microscopy
SLA	Stereo lithography
SLM	Selective Laser Melting

SLS	Selective Laser Sintering
SRC	Sparse representation-based Classification
SSE	Residual Sum of Squares
SST	Total Sum of Squares
STL	Standard Tessellation Language
SVR	Support Vector Regression
WGRG	Weighted grey relational grade

CHAPTER 1

INTRODUCTION

1.1 Pretext

The process, which is designed as 3D digital data to create component layers using depositing elements is termed Additive Manufacturing (AM) [1]. Moreover, this AM mechanism is the competitive model for the conventional manufacturing scheme, because several complex design processes are widely difficult and impossible using the traditional model [2]. Nowadays, AM is a distinguished boom-driving force in some of the biggest international industries Aeronautical, medical, and protection industries are also utilizing AM production in spiralling costs. Figure 1.1 depicts the fundamental concept of the FDM process which comes under AM processes for effective implementation of process parameters depending upon the various aims to make the product compatible in the working environment.

Even in the remaining decade, additive production solutions have come in an extended manner. The advancements in today's 3D printing systems have revolutionized AM, offering numerous benefits and capabilities compared to earlier technologies. Modern 3D printing systems boast enhanced energy efficiency and reliability, resulting in more consistent and dependable performance. Improved print speeds enable faster production of parts, contributing to increased efficiency and productivity. Larger maximum part sizes allow for the creation of larger and more complex components, expanding the range of applications for 3D printing technology. Enhanced surface finishes contribute to higher-quality printed parts, reducing the need for post-processing and improving overall aesthetics. Today's 3D printing software is designed to be user-friendly, with intuitive interfaces and streamlined workflows. Unlike earlier AM systems that required specialized knowledge and training, modern 3D printing software does not demand extensive expertise, lowering the learning curve for users. Modern 3D printing systems offer various compatible materials, including traceable and aerospace-grade composite substances.

The introduction of metal fused filament fabrication (FFF) technology has made it possible to 3D print metal parts faster, safer, and more cost-effective than ever before. Cloud connectivity enables seamless communication between users and sets of printers, facilitating distributed manufacturing operations. Users can initiate print jobs across multiple 3D printers located in different geographic locations, ensuring accessibility and availability of parts whenever and wherever needed. Industry 4.O connectivity allows for integration with core systems in manufacturing facilities, enabling automated and data-driven production workflows. Requests for component manufacturing can be initiated directly from factory systems, streamlining the production process and enhancing overall efficiency. The scalability of modern 3D printing systems is facilitated by cloud-enabled interconnectivity and the availability of diverse printers tailored to different production needs. From metal and industrial-grade 3D printers to desktop 3D printers, a wide range of options is available.

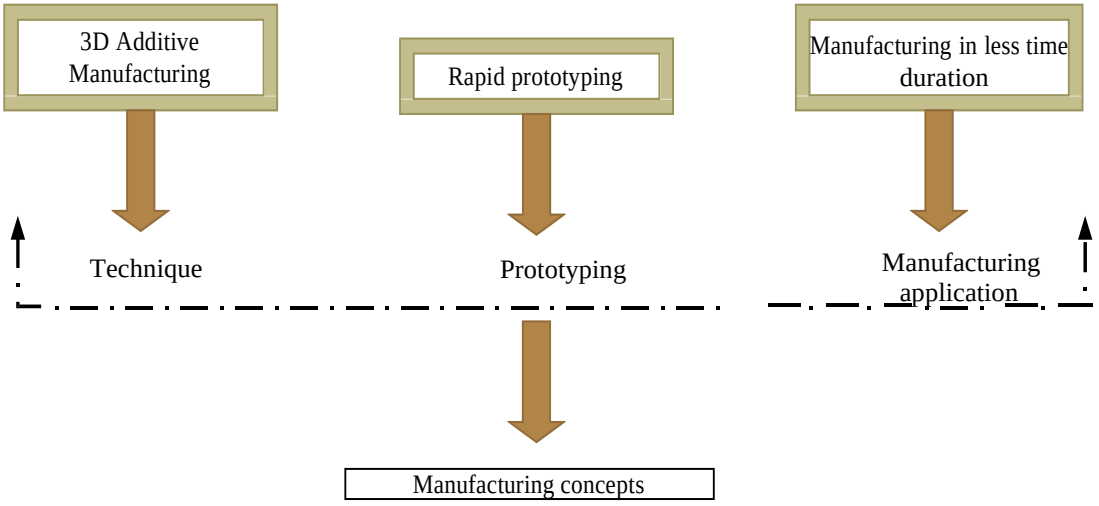

Figure 1.1 Fundamentals of FDM (Source: Developed by own)

1.2 AM techniques

AM falls under different categories,

- AM based on liquid
- AM based solid state substances
- AM based powder particles

Stereo lithography (SLA) or Vat Photo polymerization

This technique is known for its speed and affordability, remained a popular and widely used 3D printing technology It operates by utilizing a bath of photosensitive liquid, which solidifies layer by layer through exposure to a computer-monitored ultraviolet (UV) light [3].

Selective Laser Sintering (SLS)

Compatible with metal as well plastic prototyping, SLS constructs prototypes using a powder bed, with each layer built up using a laser to heat and sinter the powder based material. However, the strength of SLS parts is typically inferior to those produced by SLA, and the surface finish may be rough, often requiring additional finishing work [3].

FDM or Material Jetting

This cost-effective and user-friendly process is prevalent in non-industrial type desktop 3D printers. FDM employs a spool of thermoplastic material after melting within a printing nozzle before being deposited layer wise according to a computerized print program [3]. While early results of FDM had less resolution and strength, advancements have rapidly improved its performance making it ideal for product development due to its speed and affordability.

Selective Laser Melting (SLM) or Powder Bed Fusion

This process is commonly used in aeronautical, automotive, and medical industries, SLM is favoured for producing high-strength, intricate parts. The fusion process using powder bed utilizes a finely dispersed metal powder melted layer wise using a higher initiation of electron or laser operated beam to construct prototype or production parts. Generalised materials in SLM include titanium, aluminum, stainless steel and cobalt chrome alloys [3].

Laminated Object Manufacturing (LOM)

LOM is a cost-effective method that doesn't require controlled conditions. It builds up thin laminates accurately part off using laser beams or other cutting devices to form the CAD design. Each layer is delivered and bonded atop the previous one until the part is complete.

Continuous Liquid Interface Production (CLIP)

A variant of DLP, CLIP continuously pulls the part from a vat without using layers. As the part emerges it leads to cross a light, altering its set up to create the required dimensional design pattern over the plastic [3].

Binder Jetting

This technique allows for the simultaneous printing of one or multiple parts, although the resulting parts may not be as strong as those from SLS. Then an inkjet printhead selectively deposits liquid binding agents onto the powdered layer, binding the particles together to form the desired shape of the part. After compaction the part may be cured in an oven to fuse the powder into a coherent final part [3].

1.3 Fused Deposition Modelling

In FDM process, STL file is importing into pre-processing software, slicing the model into thin layers and generating a control file for the machine as shown in Figure 1.2.

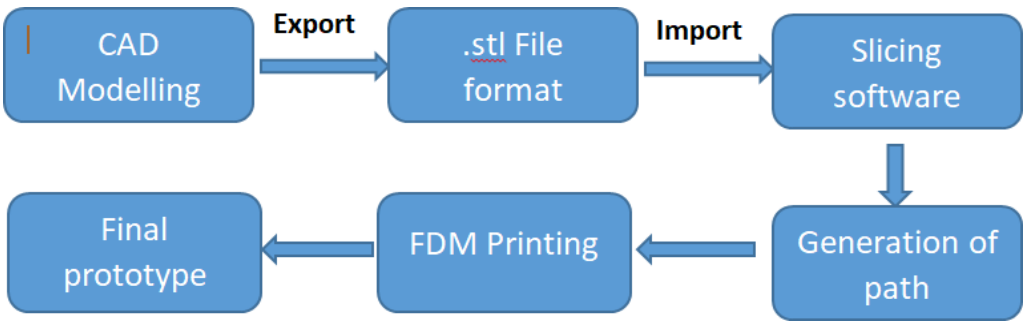

Figure1.2 Basic steps for FDM process (Source: Developed by own)

The FDM is a kind of 3D printing process that employs filament-type thermoplastics. In this technique a printer head heats the filament to melting temperatures enabling the creation of a structure layer by layer from the bottom up. The printer nozzle moves in accordance with the design specified in the STL file format progressively adding filament until the entire structure is formed. Notably, FDM serves as a precursor to one of the most widely used bio printing methods, known as extrusion-based printing. Figure 1.3 shows the illustration of FDM process. In FDM, 3D structures are constructed layer by layer by heating both the build material and supporting material through extrusion nozzle attached to the liquefier head. Initially, supporting material is deposited to establish a foundation for the main polymeric material. The nozzle moves along predefined paths, depositing the melted material layer by layer to build up the object. The material solidifies almost immediately after extrusion forming each layer of the object.

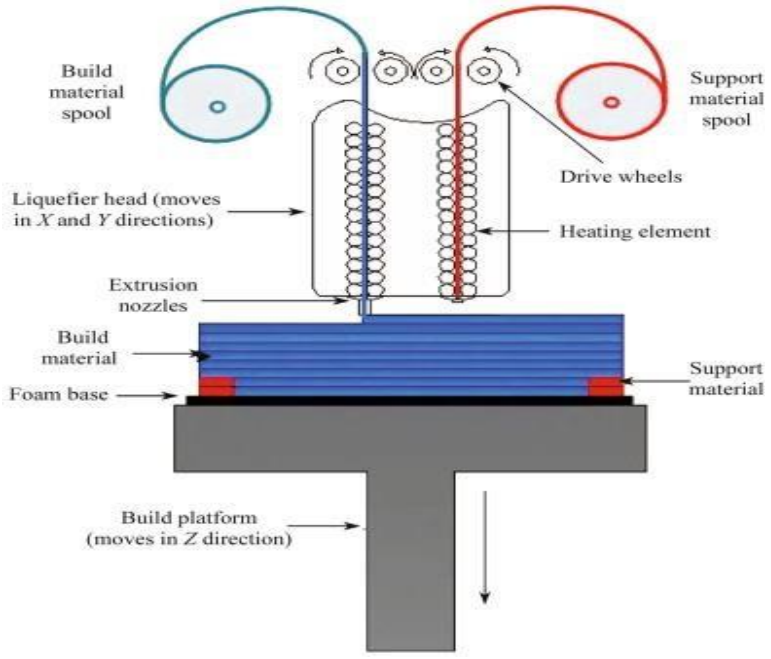

Figure 1.3 Illustration of FDM Process [3]

Support structures may also be generated during the printing process to provide stability for overhanging features. These supports are typically made of the same material as the main object and are removed after printing is complete, often by manually breaking them away or using tools. After the printing process is finished,

the object is allowed to cool and harden before being removed from the build platform. There's typically no need for a water-based cleaning solution to remove supporting material as FDM printers generally do not use support structures that require post-processing removal in the same way as vat polymerization.

The FDM process involves dispensing two materials, one for building the part and the other for a disposable support structure, from plastic filament rolls. The filament is fed into a temperature-controlled extrusion head heated to a semi-liquid state and extruded in ultra-thin layers onto a base. FDM operates in x, y and z axes building the model layer by layer. Support structures are generated automatically for overhanging geometries and removed later.

The primary material for FDM is Polylactic acid (PLA) and acrylonitrile butadiene styrene (ABS), a commonly used thermoplastic found in numerous consumer products, ranging from LEGO bricks to white-water canoes. Additionally, FDM machines can use other thermoplastics like Polycarbonate (PC) or Polyetherimide (PEI), with support materials typically being water-soluble wax or brittle thermoplastics like Polyphenylsulfone (PPSF). Thermoplastics, known for their ability to withstand heat, chemicals and mechanical stress make them ideal for printing prototypes subjected to testing.

Polylactic acid (PLA) is extensively employed in a diverse array of engineering and medical applications owing to its distinctive advantage of biodegradability. Despite PLA being a conventional material widely utilized in engineering applications compatible with most open-source FDM machines [4], several studies have highlighted the inherent frailty of 3D-printed materials, warranting careful consideration. Established in the late 1980, FDM has evolved with machines like FDM Titan, FDM Dimension, FDM Vantage, FDM Maxum, FDM 3000, and FDM Prodigy Plus.

1.4 Why FDM?

FDM has gained popularity across various industries, including automotive (Hyundai, BMW, Lamborghini) and consumer goods manufacturing (Nestle, Black and Decker,

Dial). Industries in these sectors leverage FDM throughout their product development, prototyping and manufacturing processes. FDM has capability to produce highly detailed objects also makes it a preferred choice for engineers testing parts for fit for use. Beyond prototyping, FDM is employed to manufacture customer end parts, specifically fine, detailed components and special production tools. Some thermoplastics used in FDM can even meet food and drug packaging standards, making it a prevalent 3D printing method in the medical industry. Professional FDM printers positioning them as cost-effective choice for businesses investing in complete 3D printing systems. FDM serves various purposes, including the creation of concept models in early product development, fabrication of functional prototypes for testing, production of end-use parts, and manufacturing tools. The technology significantly reduces the time and cost associated with traditional tooling or machining processes. The technique is also applied in the field of tissue engineering scaffold production through the melt extrusion method, using a layer-by-layer approach with thermoplastic polymers. While FDM presents advantages such as no unbound loose powder and flexibility in material processing [3].

FDM, well known material extrusion method, is the most popular AM technology, allowing the manufacturing of products using higher strength thermoplastics such as polycarbonate, polyphenylsulfone, polylactic acid, ULTEM and ABS. The aerospace industry has adopted FDM for producing lightweight yet durable parts, demonstrating its versatility from rapid prototyping to end-use applications. FDM's economic advantages and the absence of chemical post-processing make it an ideal choice for various applications.

1.5 FDM process parameters

The significant process parameters in the FDM are being highlighted through Figure 1.4. All the process parameters of FDM can be changed to achieve different goals. While changing these parameters (e.g. print speed, layer height, filament extrusion speed and path distance in a layer), the connection between paths (lines) in a layer will be changed.

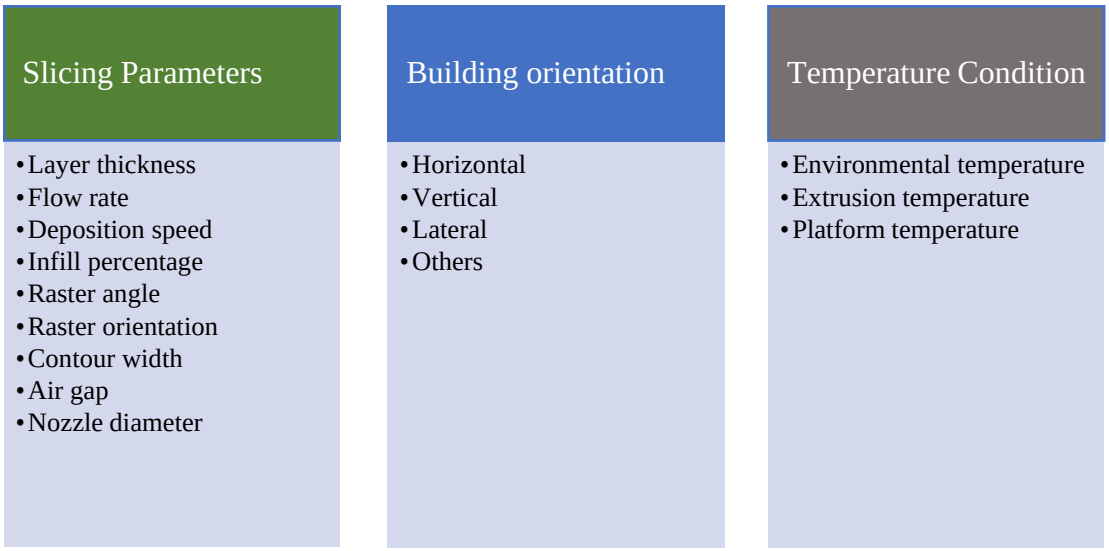

Figure 1.4 Dominant process parameters in FDM process [5]

Nozzle diameter: The diameter of the extruder tip, known as the nozzle diameter, is a crucial factor influenced by the type of nozzle utilized. It directly affects the behaviour of the extruded melt flow [6].

Extrusion temperature: The extrusion temperature refers to the temperature required to covert the solid-state filament into a melting stage prior to the process of extrusion. This temperature is contingent upon both the material type being used and the printing speed. It is typically determined based on the melting point of the filament material [7].

Print speed: The print speed in FDM refers to the distance travelled by the nozzle tip per unit time, usually measured in millimetres per second (mm/s), during the printing process. The ideal print speed is associated with various factors including the material being used, the extrusion temperature, and the desired resolution. Finding the optimum printing speed involves balancing these factors to achieve the desired print quality and structural integrity of the final object [8].

Build orientation: The build orientation in AM refers to the position of the part on the build platform relative to the X, Y, and Z axes. It can be represented as either a quantitative parameter, such as the angle of the axis or a categorical parameter indicating specific orientations (e.g. upright, flat, angled).

Layer thickness: The layer thickness in AM refers to the vertical resolution of each printed layer and is determined by factors such as the material being used, the diameter and type of the nozzle, and the printing parameters. It plays a crucial role in influencing various aspects of the printed object, including mechanical strength, quality of surface, dimensional accuracy, and build time [7].

Raster width: The raster width in AM, also known as road width, refers to the width of each extruded filament or line deposited by the printer's nozzle. It is determined primarily by the diameter of the nozzle. A smaller raster width, achieved with a smaller nozzle diameter, results in finer details and higher resolution in the printed object. However, using a smaller raster width typically requires more manufacturing time due to the increased number of passes required to cover the build area. Additionally, smaller raster widths generally consume less material.

Raster angle: The raster angle in AM refers to the orientation of the raster path relative to the X-axis on the printing platform. It determines the internal structure of the final printed product and can have a significant impact on both surface roughness and mechanical strength.

Air gap: An air gap in AM denotes the separation between two consecutive deposited beads or lines within the same layer of the printed object. These gaps are crucial in determining structural integrity, surface quality, and dimensional accuracy [9].

Infill density: The infill density in AM represents the proportion of material utilized to construct the internal structure of a printed object, typically expressed as a percentage. Parameters such as air gap and raster width enable users to regulate the infill density during the printing process. The density of the infill significantly impacts the weight and mechanical strength of a part produced through FDM.

Infill pattern: The infill pattern plays a crucial role in determining various aspects of the 3D printed part, including its structural integrity, mechanical properties, and overall performance. [5].

A fishbone diagram, presented in Figure 1.5, visually depicts the impacts of various process factors on various part qualities. This diagram serves as an initial overview of the survey's findings, compiled from various recent studies. It is noteworthy that

certain process variables overlap with part qualities, functioning as essential process parameters.

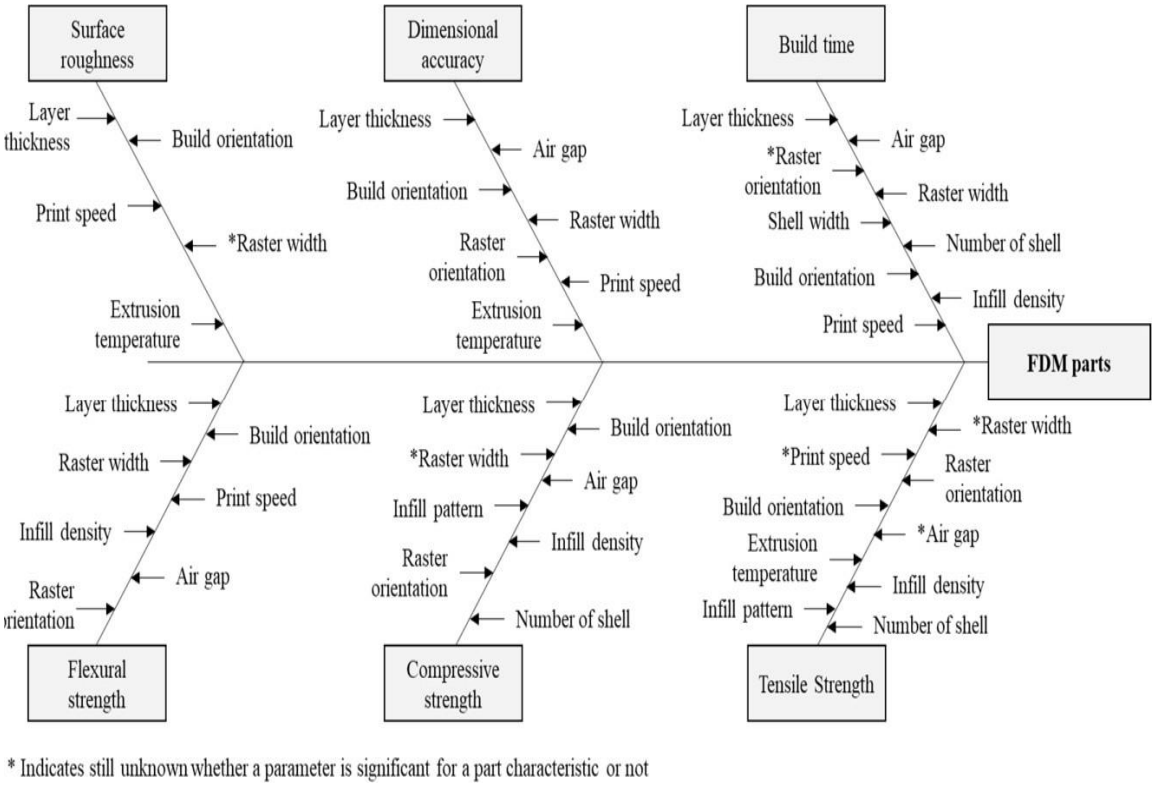

Figure 1.5 Fishbone diagram to indicate the effect of process parameters [10]

1.6 Need of study

Various process parameters in FDM can be adjusted to attain specific objectives. For instance, modifying parameters such as print speed, filament extrusion speed, layer thickness and path travel within a layer can impact the outcome of the fabricated parts. Lowering the print speed, for instance may result in higher strength in the final components. When these parameters are altered, the connectivity within paths lines in a layer is also affected, emphasizing the dynamic relationship between the chosen printing parameters and the structural characteristics of the printed object.

The AM process involves numerous data-related issues and factors, which are often assessed using machine learning (ML) or deep learning (DL) models [3, 15]. Post-manufacturing, DL and ML techniques play a crucial role in the validation process [11, 16]. Various methodologies in the past have introduced techniques such as fuzzy systems [12], DL models [13], decision trees [14] and others. However, these techniques have demonstrated suboptimal results, primarily attributed to the inherent complexity of the design.

1.7 Organization of thesis

Chapter 1 describes the background of AM process flow, different techniques, recent advancements in AM, FDM process, materials and methods, FDM process parameters, research need. Chapter 1 sets the stage for the subsequent chapters by providing readers with a comprehensive understanding of AM, particularly focusing on FDM and highlighting the context, significance and scope of the research.

Chapter 2 of the research manuscript delves into a comprehensive exploration of existing studies, techniques and algorithms relevant to the current investigation which is commonly referred to as "Literature Survey." This section aims to convey readers with a thorough understanding of the background and context surrounding the research topic. It reviews previous research, methodologies and findings in the field, highlighting key insights, trends and gaps in knowledge. Additionally, Chapter 2 delineates the objectives and scope of the research work, providing clarity on the specific goals, aims and boundaries of the study.

Chapter 3 is exhibiting the proposed methodology with detailing the approach, techniques, and methodologies to be employed in the research. This section elucidates the steps and procedures that will be undertaken to achieve the research objectives effectively. This helps to contextualize the research within a defined framework and elucidates what the study aims to achieve and the extent to which it will be pursued.

Chapter 4 provides a comprehensive overview of the fabrication and testing procedures conducted as part of the research study offering insights into the methods

used and the outcomes obtained. This part of the research manuscript focuses on the first experimental phase aimed at optimizing the process parameters.

Chapter 5 of the research manuscript is dedicated to the optimization and validation of the proposed algorithm. This chapter elaborates on various aspects related to algorithm development and its execution. A detailed exploration of the algorithm development and implementation process is included here by providing readers with insights into the methodologies, techniques, and tools employed to realize the proposed solution It serves as a critical component of the research manuscript, providing valuable insights into the practical implementation of the proposed methodology and the effectiveness of the optimized process parameters. It demonstrates the technical aspects of translating theoretical concepts into practical applications, laying the groundwork for the subsequent evaluation and analysis of the developed algorithm. This part of the research manuscript is also dedicated to discussing the findings and analysing the performance of the proposed work with existing researches. Overall, this chapter serves as a critical component of the research manuscript, providing a comprehensive evaluation and interpretation of the research findings. It helps readers understand the significance of the proposed work in the broader context of the field and provides valuable insights for advancing knowledge and practice in the relevant area of study.

Chapter 6 depicts the concluded remarks of the research work and provides a concise summary of the key findings, contributions and implications of the research. Further it is pointed towards future directions for continued exploration and inquiry.

CHAPTER 2

LITERATURE REVIEW

The literature review aims to convey a chronological overview of research efforts in the field of AM, particularly focusing on FDM technology. Over the last decade, there has been a significant expansion in the applications of FDM technology across various sectors such as automotive, medical, domestic and small industrial products. Despite these advancements, challenges persist in achieving desired part quality without the need for new materials.

This chapter examines the progressive development of FDM technology and highlights the challenges associated with different aspects of AM, especially focusing on the FDM process. It discusses the need for process optimization to achieve the desired properties of FDM products. Additionally, the chapter explores the impact of various FDM process parameters.

Furthermore, the chapter delves into modeling and optimization methods utilized to evaluate FDM process parameters. By reviewing existing literature, this chapter provides insights into the current state of knowledge and identifies areas for further research and improvement in FDM processes.

2.1 Overview

AM is the vying model for the common manufacturing blueprint, because various complex design processes are widely difficult utilizing conventional model. In FDM the process parameters are dominant determinants for reconstructing the part characteristics and minimizing the build time and cost. FDM is well-known with guests in a type of industries, from automotive sector to items bought by consumer's production. These guests use FDM throughout their output growth, prototyping and manufacturing processes. FDM is having uniqueness in term of no loose powder and material used in the form of filament offers adaptability and reduces the resident time into sight the melting chamber [17]. In this context, this study aims to explore the

materials and their increased limits to resolve enhanced parametric optimization and potentials.

Moreover, the designing process of 3D digital statistics is to generate the layers using FDM components, which are termed, AM. Here, the fabricated products are mainly damaged by real-life AM systems [18]. Part characteristics are influenced by slicing parameters, building orientation, temperature conditions of FDM manufacturing process. Many parameters like layer thickness, print speed, infill percentage, nozzle diameter, flow rate, raster angle and extrusion temperature can be changed to achieve best line connection while depositing the material which will lead to optimize part properties [8].

FDM) is a model of AM which uses layer by layer-based methodology to fabricate a component. Today in the digital manufacturing era FDM process is widely used as it can construct intricate and complex part geometries in short time as compared to conventional manufacturing, its simplicity and economical bahaviour. Despite of such advantages, literature argued various ML approaches adopted to increase the performance of FDM addressing the issues of irregularities in part properties, accuracy, and reliability due to challenging task of best parametric selection. In this context, the present study proposed strategy to predict the best parametric combination with optimized mechanical properties of printed parts.

2.2 Historical background

The concept of AM traces back to the 1960s, with early attempts made by institutions like Battelle Memorial Institute and Dynell Electronics Corp. In the late 1970s and early 1980s, researchers like H. Kodama and Charles Hull further contributed to the development of AM technologies, leading to the commercialization of the first AM systems by 3D Systems in 1987.

Throughout the 1990s, various AM techniques, such as Stereolithography (SLA), Selective Laser Sintering (SLS), and Laminated Object Manufacturing (LOM), were

commercialized by companies like Stratasys, Cubital and Helisys. The emergence of these systems marked significant milestones in the evolution of AM technologies.

In the early 2000s, advancements in AM continued with the introduction of new systems capable of processing a wider range of materials and producing multi-colour prints. Open-source initiatives like RepRap also gained momentum during this time, contributing to the democratization of AM technology.

The focus on metal AM (MAM) gained prominence in the mid-2010s, with companies like ExOne announcing capabilities for printing metal materials such as Inconel 625. Alongside technological advancements, there was a growing emphasis on environmental sustainability, waste reduction, and customization in AM processes [19].

In recent years, the AM industry has witnessed a surge in research and development efforts aimed at addressing diverse applications across sectors such as medical, automotive, aerospace, electronics and defence. The focus has shifted towards enhancing process efficiency, expanding material options, and exploring novel AM techniques. Overall, the trajectory of AM evolution reflects a continuous drive towards innovation, with advancements driven by both technological breakthroughs and market demands. The future of AM holds promise for further advancements, fuelled by ongoing research, industry collaborations, and the adoption of AM technologies in diverse applications.

It is evident from Figure 2.1 the ongoing research in extrusion-based AM is driving innovation and pushing the boundaries of what is possible, paving the way for new applications, materials, and manufacturing paradigms.

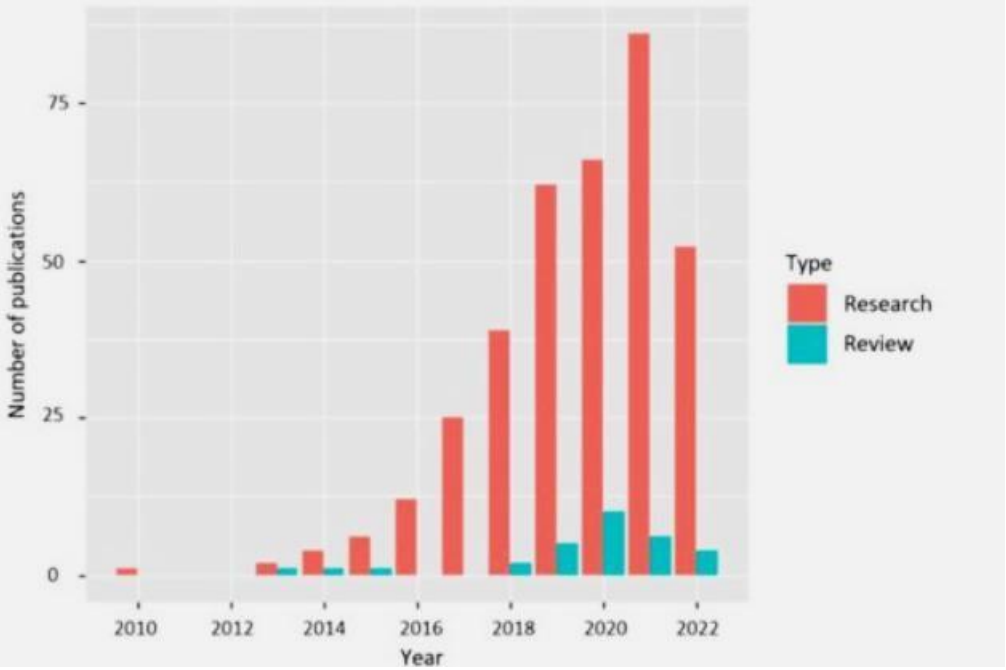

Figure 2.1 Number of publications on extrusion-based AM per year (as per Scopus database, Accessed on June 2023)

2.3 Glance at an interface between ML and AM

ML techniques offer several opportunities to enhance various aspects of the FDM process:

Process Optimization: ML algorithms can analyse sensor data from FDM machines to optimize parameters like temperature, speed, layer height, and material flow rate. By correlating these parameters with print quality, ML models can recommend optimal settings to improve efficiency and reduce defects.

Predictive Maintenance: ML models can predict equipment failures by analysing historical sensor data for patterns indicative of potential issues. This enables proactive maintenance, minimizing downtime and preventing costly breakdowns.

Quality Control: ML algorithms can inspect images of printed parts to detect defects such as warping or delamination. Trained on a dataset of defective and non -defective

parts, ML models can classify parts automatically and reject those not meeting quality standards.

Material Selection: ML techniques can analyse material properties and object requirements to recommend the most suitable material for a specific application. This helps optimize material usage and ensures printed parts meet performance criteria [20].

Support Structure Optimization: ML algorithms can analyse 3D models to predict where support structures are needed during printing. By optimizing support placement, ML models reduce material usage, post-processing efforts, and improve surface finish.

Energy Efficiency: ML models can analyse energy consumption data to identify opportunities for reducing energy usage without compromising print quality. This involves optimizing heating and cooling cycles and minimizing energy consumption during idle periods.

Customized Printing: ML techniques can analyse large datasets of 3D designs and user preferences to generate customized printing recommendations. By understanding user preferences and past designs, ML models can suggest modifications or generate entirely new designs tailored to specific requirements. By leveraging ML, FDM processes can be optimized for efficiency, quality, and customization, driving innovation in AM [21].

Figure 2.2 shows various data that can be used and processed through ML to determine process structure property (PSP) chain relationship.

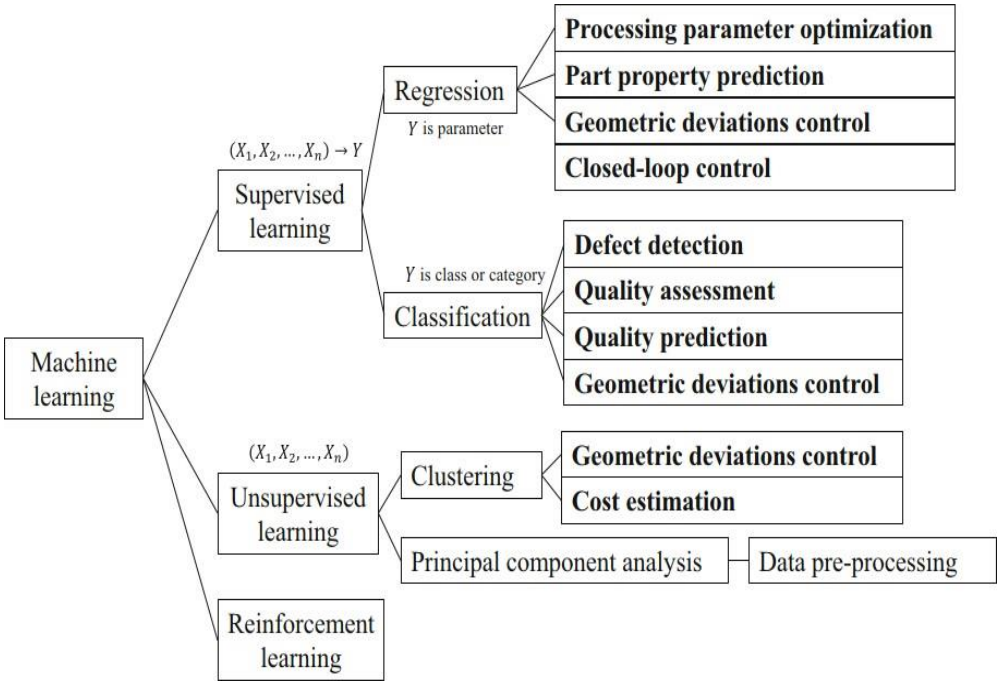

Figure 2.2 Taxonomy of ML applications in the AM field [20]

2.4 Literature review in FDM

FDM process limitations were recorded due to inconsistency in process repeatability and part characteristics [3]. Part characteristics are influenced by slicing parameters, building orientation, temperature conditions of FDM manufacturing process. To achieve different aims in terms of part quality characteristics, build time, mechanical properties, cost etc. various influential parameters like nozzle diameter, build orientation, flow rate, raster angle, extrusion temperature, layer thickness, print speed, infill percentage, air gap can be changed [22]. The selection of best combination of optimized parameters is challenging task. Carrying out more number of experiments or 3D simulations is inefficient to meticulously optimize the FDM process which is possible by integration of ML with FDM process [2]. Moreover, the AM procedure includes a lot of data issues and factors, which are estimated based on ML models [11, 16]. After completion of manufacturing, DL and ML techniques are used for validation purposes [12, 23].

In past, several techniques have been introduced in various methodologies like fuzzy systems [13], Image processing, decision tree [15], etc. Mohamed et al [24] has developed the fabrication of part dimension optimization and modelling scheme. To analyse the design properties, the artificial neural framework (ANF) was used.

V. Chowdary Boppana et al. [1] utilized an ANN coupled with Genetic Algorithms (GA) to establish the non-linear relationship between selected process parameters and tensile strength in AM. The findings indicate that these process parameters significantly impact tensile strength, with raster angle emerging as the most influential factor. Specifically, increasing the build orientation about the Y-axis resulted in specimens with more compact structures, leading to enhanced fracture resistance and ultimately higher tensile strength. This suggests that optimizing the build orientation can positively influence the mechanical properties of printed parts, particularly in terms of tensile strength.

N. Naveed et al. [7] determined the optimal raster orientation for fabricating 3D parts using thermoplastic material, specifically polylactic acid (PLA), by investigating the tensile properties of the printed parts. In addition to tensile testing, microstructural analyses are conducted on the fracture interface, outer surfaces, and inner surfaces of the 3D parts using scanning electron microscopy (SEM) to examine material failure modes, defects, and reasons for failure.

By varying the raster angles, the study explored five different orientations to understand their impact on the strength and quality of the printed parts. The objective is to identify the raster orientation that results in the strongest 3D printing parts. This information can then be used to optimize the printing process and enhance the mechanical performance of printed components.

Through detailed analysis of the microstructure and tensile properties, the study aims to provide insights into the relationship between raster orientation and part strength. By identifying the best raster orientation, manufacturers can improve the quality and reliability of their 3D printed parts, leading to better overall performance in various applications.

Chamil Abeykoon et al. [9] carried experimentation using DSC, SEM, TGA with various material combinations as PLA, ABS, CFR-PLA, CFR-ABS, CNT-ABS commented as tensile, compressive, flexural properties were best at print temperature of 215℃ , infill density of 100%, print speed of 90 mm/s, and linear infill pattern.

High strength material was CFR-PLA (J Mogan. [37]). Ganesh Chate et al.[38] investigated the effect on strain, elastic modulus stated that moisture content 10% and raster angle 90% show optimum result.

R.K Gupta et al. [13] have developed the adaptive fuzzy logic to analyse the parameters, which are used in the 3D-based FDM printing substances. Here, the fuzzy logic is initiated to the neural model to monitor the parameters of the 3D printing.

A. Gupta et al. [18] phrased product strengthening model based on ANN algorithm. The developed ANN model demonstrates its capability to predict lower average error values under various conditions, including different processing conditions, materials, and machine setups.

B.M. Castro et al. [25] have introduced the 3D printing strategy for a web-based replica to accelerate the pharmaceutical application of the ML model. Method-ML, to detect the characteristics of printing 3D design, one of the datasets was constructed. In this study, a total of 614 drug-loaded combinations were designed using 145 various pharmaceutical excipients. These formulations were 3D printed and evaluated in-house. To develop a predictive tool, a dataset was compiled, and ML models were trained and tested using a 75:25 split. Notably, the AI models achieved accuracies of 76% and 67% for predicting key fabrication parameters related to printability and filament characteristics, respectively. By the implementing this method, the fabrication data of 3D model was obtained for that particular drug.

Ravi Butola et al. [26] analysed comparison of RSM and ANN for prediction of the tensile properties of friction stir-processed surface composites, concluded that the ANN model's predictive capability is observed to be better than the RSM model in regards with tensile strength.

Ashutosh Kumar Gupta et al. [27] investigated the effect of process parameters on dimensional accuracy of FDM printed parts and results show that ANN model predicts the results with very less error in comparison of existing models.

Jayant Giri et al. [28] optimized critical process parameters like layer thickness, air gap, raster width, build orientation, raster angle, and the number of contours for enhancing the properties of FDM printed part such as tensile strength, surface roughness, and build time using ANN and concluded that the tensile strength improves with the 0^{o} build orientation of the object, low layer thickness and raster width with high range.

Mohammad Shirmohammadi et al. [29] investigated the effect of FDM 3D printing process parameters on the surface roughness of printed parts using ANN Hybrid algorithm and RSM, concluded that 0.3 mm of nozzle diameter achieves the best surface quality.

M. A. Mahmood et al. [30] reviewed ML technique has been recently validated for intricate pattern identification and the development of deterministic relationships, which eliminates the necessity of constructing and solving physical models. Among ML methods, ANN stand out as the most commonly used model as having capability to be play with large datasets and robust computational capabilities. Study provided an overview of the progress made with ANN in various aspects of 3D printing. Also addressed the challenges encountered when applying ANN in 3D printing and proposed potential solutions to overcome these challenges.

O.A.Mohmed et al. [31] investigated how various fabrication conditions in FDM affect the dimensional accuracy of cylindrical parts. To achieve this, a novel approach combining integrated second-order definitive screening design (DSD) and ANN techniques was evolved. The experimental design involved evaluating six significant operating variables that impact dimensional accuracy in FDM to determine the optimal fabrication conditions that result in improved dimensional accuracies for cylindrical parts.

Demei Lee et al. [32] the study investigated the impact of processing parameters on the mechanical properties of FDM-printed carbon fibre-filled polylactide (CFR-PLA) composites using an L18 orthogonal array model. Tensile and impact strengths were measured post-printing, and the effects of different parameters on these strengths were analysed. Experimental findings revealed that 3D-printed CFR-PLA exhibited a rougher surface morphology compared to virgin PLA. Among the selected variables, bed temperature was identified as the most influential parameter affecting the tensile strength of CFR-PLA-printed parts. This suggests that controlling the bed temperature during printing is critical for achieving desired tensile properties in CFR-PLA composites. Furthermore, bed temperature and print orientation were found to be the key parameters affecting the impact strengths of the printed composites. Parts printed at a 45° orientation demonstrated superior mechanical strengths compared to those printed at a 90° orientation. This indicates that optimizing print orientation can significantly impact the impact resistance of CFR-PLA parts, with oblique orientations yielding better performance. Print speed 55mm/s, bed temperature 70°C, infill density 60%, orientation 45°, nozzle temperature 220°C yield to optimum combination.

M. Ajay Kumar et al. [33] confirmed 0.1 mm layer height, 80% infill density, 80mm/s print speed were the best parameters for the optimisation of tensile strength. Tensile strength is inversely proportional to number of layers but directly proportional to infill density and bed temperature was insignificant parameter.

100 % infill density and hexagonal pattern print exhibits best tensile strength amongst print pattern is dominant factor (Harsh Vardhan et al [38], Ge Gao et al [70], K.N. Gunasekaran et al [24], Vishal Wankhede et al [31]).

A. R. Kafshgar et al. [34] found out optimum combination as 0/90° raster angle, 220°C extrusion temperature, 60% infill rate, 0.1 mm layer thickness for better tensile strength and toughness. Higher layer thickness part was stronger. Thermal behaviour was influenced by printing speed and infill density (N. A. Fountasa et al [74]).

P. K. Farayibi et al. [35] investigated 0.2, 0.4, 0.3 mm layer thickness, 210°C, 220°C, 215°C extrusion temperature, 50%, 30%, 50% infill density were best for impact, tensile, hardness respectively.

Pooja patil et al. [36] investigated surface roughness, printing time and filament length using grey relational analysis commented as layer thickness of 0.2 mm , triangular pattern, printing speed 100 mm/s and infill % seventy were the optimum parameters.

Various optimization techniques were utilised by researchers like, Response surface methodology (RSM) [54,55], Genetic algorithm (GA) [54,56], Taguchi orthogonal array[58,50,32-34,61,64,], Full factorial[57], Fuzzy system[59,60], Analysis of variance (ANOVA)[58,34,62], Scanning Electron Microscopy (SEM)[63], Grey regression analysis [35,36,66], ANN [56], KNN,RF,SVM [67] to optimize the design parameters to yield better mechanical properties.

Table 2.1 illustrates about the author with publication year, the specific area of focus, such as process optimization, mechanical properties, etc., the methods used in the research, including the algorithms, techniques, or strategies (e.g., machine learning, deep learning, and statistical methods). Further it incorporates the parameters that were controlled or optimized during the study (e.g., nozzle diameter, print speed, layer height) and the outcomes that were measured to evaluate performance, such as mechanical properties (e.g., tensile strength, compressive strength, accuracy). Finally it depicts the key results or conclusions drawn from the study.

Table 2.1 Literature of FDM

Reference of research, year	**Work Area (Methods, Input and Output)**	**Findings**
V. C. Bopanna et al. [1], (2023)	The ANN-GA approach is evolved to generate the non-linear performance relationship between the input process parameters and tensile strength.	Study demonstrates that the selected process parameters had prominent effect on response variable. Most influential factor was raster angle. Raising the Y axis build orientation fabricated objects with compact structures which lead to enhanced fracture resistance.
A.Karad, P. Sonawwanay [2], (2023)	The chosen infill pattern for the flexural test study was the triangular pattern, which incorporates various densities of infill percentages, specifically 25%, 50%, 75%, and 100%..	With linear patterns with 100% infill density, scanning electron microscopy analysis revealed a clear relationship between the microstructures and the rasters. The analysis showed various features such as porosity, voids, gaps between beads, and holes due to polymer being pulled out.
Wenxin Lao *et al* [4], (2020)	Artificial neural mechanism was utilized to recognize the finest nozzle shapes. The quantity of printing procedure was enhanced.	Finally, the finest shapes of nozzle were detected.

Steffen Esslinger and Rainer Gadow [10], (2020)	Technique: FDM-Slip casting, to design thermoplastic moulds using 3D printing scheme.	The measure of compressive strength was found.
D.Yadav, D.Chhabra *et al* [13], (2020).	3D experiments were done to test the tensile strength, the method used to observe the 3D printing parameter is Adaptive based neural fuzzy system	Several parameters have been validated like density, fabrication layer thickness and tensile strength
M.Goudswaard, B. Hicks, and A.Nassehi [14], (2021)	Decision models were executed using artificial neural model to value the capacity of 3D design	The capability of Artificial neural model was evaluated and the mechanical properties was reported for that specific 3D object
Kaushik Yanamandra, *et al* [15], (2020)	Imaging strategy to reconstruct the tool path. Original model was trained as input; finally, the reconstruction model was compared with original model.	High quality of composite parts was equipped successfully.
S.Dev, and R.Srivastava et al [16], (2020)	Taguchi mechanism was worn to do the experimental works. Also, genetic algorithm was used to optimize the design parameters. The optimized parameters were	At final, an intelligent model was determined to utilize in 3D design process for attaining high tensile strength

	gained as o/p.	
K. Rajan, M. Samykano, K. Kadirgama [17], (2022)	Parameters and mechanical properties with different materials have been discussed.	Various materials and their effects on mechanical properties shown PLA is flexible material for FDM processes.
Luis Suárez and Manuel Domínguez [23], (2020)	The environmental issues in fabricating AM was systematically reviewed	Finally, the issues are separated and the difficulties of equipping 3D design were described.
O.A. Mohamed, S.H.Masood, and J.L.Bhowmik [24], (2021)	For analysing the design properties Artificial neural model with screening design was utilized. Here, 3D object properties like thickness dimension, etc. was trained as input and the dimension accuracy was obtained as output.	The robustness score of Artificial neural scheme was found with wide measure of exactness rate.
M.Elbadawi, B.M. Castro *et al* [25], (2020)	Method-ML, To detect the characteristics of printing 3D design, one of the datasets was constructed. In the following steps that constructed dataset was trained to the system then the 3D painting design in medicines were worn as tested samples.	By the implementing this method, the fabrication data of 3D model was obtained for that particular drug

S. Garzon-Hernandez *et al* [26], (2020)	Technology FDM was utilized. If any fault function was recognized then an innovative constitutive was designed.	Printing parameters was calculated using numerical analysis and the fault process was recognized.
A. Gupta, M.Taufiq [27], (2022)	The part strength modeling technique based on ANN involved the development of a predictive model that correlates input parameters (such as process parameters, material properties, geometry)	The developed ANN model has demonstrated its capability to predict lower average error values under various conditions, including different processing conditions, materials, and machines.
M. Birosz, M. Ando [39], (2023)	The versatile infill scaling technique for FDM aims to optimize the infill pattern and density to improve the mechanical properties of printed parts, particularly in terms of tensile strength.	Adjusting the infill pattern and density based on specific scaling factors to achieve desired mechanical properties while minimizing material usage and print time.
Jianjing Zhang, Peng Wang, Robert X. Gao [40], (2019)	Measuring temperature and vibration data provides valuable insights into the layer-wise thermal and mechanical activities	Experimental evaluation has demonstrated that the Long Short-Term Memory (LSTM)-based predictive model surpasses the performance of various ML

	during the AM process, while also helping to identify process variations.	techniques, including Support Vector Regression (SVR) and Random Forest.
Mohammad Farhan Khan, *et al* [41], (2020)	Convolution based neural approach to value the quality of the designed 3D parts. The function of DL has monitored via 3D printer.	The process was optimized to diminish the cost and time.
Jorge Manuel *et al* [42], (2020)	Numerical analyses are designed to evaluate the mechanical characteristics of plastic materials. Moreover, the plastic Nylstrong GF-PA6 was manufactured using FDM approach.	Compressive strength was attained at high range by FDM. Also, achieved less error and high accuracy.
S. Garzon-Hernandez *et al* [43], (2020)	Here, FDM technology was used and the experimental data was worn as dataset.	The properties of manufactured 3D design were validated.
Vigneshwaran Shanmugam *et al* [45], (2021)	After manufacturing the composite, fatigue properties were calculated by FDM technique. Hence, the significant scores of fatigue properties were calculated.	Mechanical strength and fatigue properties was analysed successfully.

RuChen *et al* [46], (2020)	FDM technology with inversion stress model was modelled to estimate the chief parameters like layer number and thickness, direction of printing and density, Here, stress and strain was monitored frequently.	Residual stress measure of the designed 3D printing model was evaluated.
Luca Di Angelo *et al* [47], (2020)	The utilized algorithm was based on multi objective model, which is known as S-metric selection. Here, the data of designed 3D object has taken as input and the optimal orientation has obtained as output.	Finally, the manufacturing cost and quality of designed object was estimated with high exactness measure.
Zeqing Jin *et al* [48], (2019)	Autonomous correction scheme was upgrade in AM system to correct the fault automatically during the manufacturing process.	Faults are detected and corrected automatically in short duration and less energy cost.
Arfan Majeed *et al* [49], (2021)	Smart AM for better decision-making function, application utilized for FDM was AlSi10Mg alloy and the process, which worn for manufacturing	Manufacturing emission was reduced, the process can execute in short period.

	process is sensor melting strategy.	
Vishal Wankhede *et al* [50], (2020)	Method: Taguchi's. An engineering design has taken for the experimental process, the input variables of engineering model were trained as input and the output was obtained for each variable.	Variance analysis was developed to study the chief behaviour of variable process. Also, density and layer thickness were calculated.

2.5 Research gap and problem identification

AM process is incorporated with several real-time applications and rapidly increased in many fields. While FDM has become a prevalent method for additive manufacturing due to its cost-effectiveness and ease of use, the process is still hindered by challenges in achieving consistent part properties. Traditional approaches often fail to capture the complex and nonlinear relationships between process parameters and part performance, particularly under varying conditions. However, compared with the existing ML techniques various complexity and lower prediction capability issues are reviewed. In addition, mismatch connection during the designing process may reduce the prediction accuracy rate; therefore, the prediction is very important regarding those issues and parameter selection. The main aim of this ML with AM technique is to select the best parametric combination in the 3D printing design. During the printing process, the input data is carried randomly then it leads to cause the overflow issue. The integration of machine learning, especially deep learning (DL), into additive manufacturing remains underexplored, with limited studies investigating how DL can dynamically enhance performance characteristics in real-time.

While deep learning has proven effective in fields such as image recognition and natural language processing, its application in fault detection for FDM is still in its

infancy. Very few studies have developed deep learning models specifically tailored to monitor FDM processes and predict potential failures in real-time.

Various optimization techniques were utilised by researchers like, Response surface methodology (RSM), Genetic algorithm (GA), Taguchi orthogonal array, Full factorial, Fuzzy system, Analysis of variance (ANOVA), Scanning Electron Microscopy (SEM), Grey regression analysis, ANN, KNN,RF,SVM to optimize the design parameters to yield better part properties. However, these approaches often focus on specific aspects of the process, such as dimensional accuracy or surface roughness, without fully addressing the complex interactions between multiple mechanical properties and process parameters.

To bridge the research gap and to enhance the performance characteristics of FDM by providing strong interface between AM & ML, various FDM areas where ML applications have been implemented is shown in Fig.2.3 The pie chart shows almost 75% studies have been carried out related to quality monitoring system, mixed studies and surface roughness in the FDM process. It is evident from the chart that there is scope to analyse the effect of process parameters to improve mechanical properties of parts produced by FDM process using ML applications.

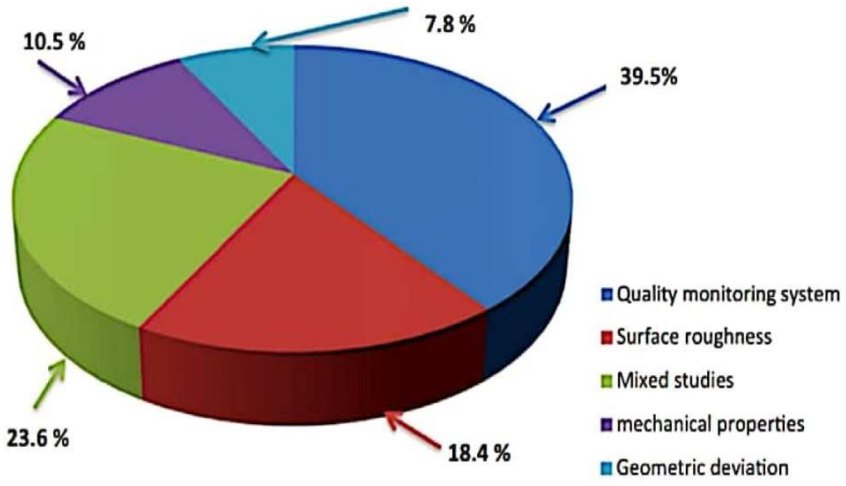

Figure 2.3 ML applications in FDM areas [21]

The primary challenge lies in establishing an effective interface between additive manufacturing processes and deep learning models that can predict and optimize key performance metrics. Existing research lacks of adjusting FDM process parameters dynamically based on real-time data to optimize mechanical properties, thereby hindering advancements in producing high-quality, reliable parts. There is a need to bridge this gap by developing models that learn from large datasets to predict and enhance the performance characteristics of FDM, ultimately improving part consistency, quality, and process efficiency.

There is a pressing need to develop an optimized deep learning model that can efficiently detect faults, monitor process behaviour and predict issues before they arise. This model should be able to handle the complexity of FDM processes and improve part quality by reducing defects and optimizing performance. Parameters such as nozzle diameter, layer thickness, print speed and extrusion temperature have received less attention compared to others like infill density, infill pattern, build orientation, raster width, or raster orientation. Future research could focus on investigating these less analyzed parameters to understand their impact on part quality and performance better.

A critical challenge is the lack of comprehensive comparative studies that evaluate deep learning-based optimization methods against traditional optimization techniques for FDM in terms of multiple performance metrics, such as prediction accuracy, tensile strength, and compressive strength.

2.6 Objectives of study

1] To study and enhance the performance characteristics of FDM by providing strong interface between AM & DL.

2] To develop the optimized deep learning model (SMbDBNS) to start the detection process for both fault and behaviour.

3] To compare the obtained parameter results with other existing approaches in terms of over flow rate, prediction accuracy, tensile strength, compressive strength etc.

CHAPTER 3

RESEARCH METHODOLOGY

3.1 Problem formulation

Today in the digital manufacturing era FDM process is widely used as it can construct intricate and complex part geometries in short time as compared to conventional manufacturing, its simplicity and economical bahaviour. Despite of such advantages, literature argued various machine learning approaches adopted to increase the performance of FDM addressing the issues of irregularities in part properties, accuracy, and reliability due to challenging task of best parametric selection. In several strategies, FDM technique was suffered a lot because of complex product design and less prediction measure. So, to enhance the AM mechanism a machine learning model is suited to implement to maximize the defeat detection rate and designed object behaviour. In this context, the present study proposed a DNN strategy to predict the best parametric combination with optimized mechanical properties of printed parts.

3.2 Research plan

This chapter represents the overview of research steps that have been followed to comply with research objectives. Many studies have delved into optimizing process parameters in FDM using a variety of methodologies. Traditional optimization methods typically involve experimental design, trial and error, or heuristic approaches. However current developments in machine learning (ML) have provided novel opportunities for process optimization in FDM. Diverse researches have evolved with the machine learning (ML) techniques, including artificial neural networks (ANNs), genetic algorithms (GAs), support vector regression (SVR), and reinforcement learning (RL), to optimize FDM process parameters.

To accomplish the research objectives certain steps were followed as shown in Figure 3.1. Based on the identified gap in the literature regarding the optimization of process

parameters in FDM associated with the ML techniques, the research objectives were formulated.

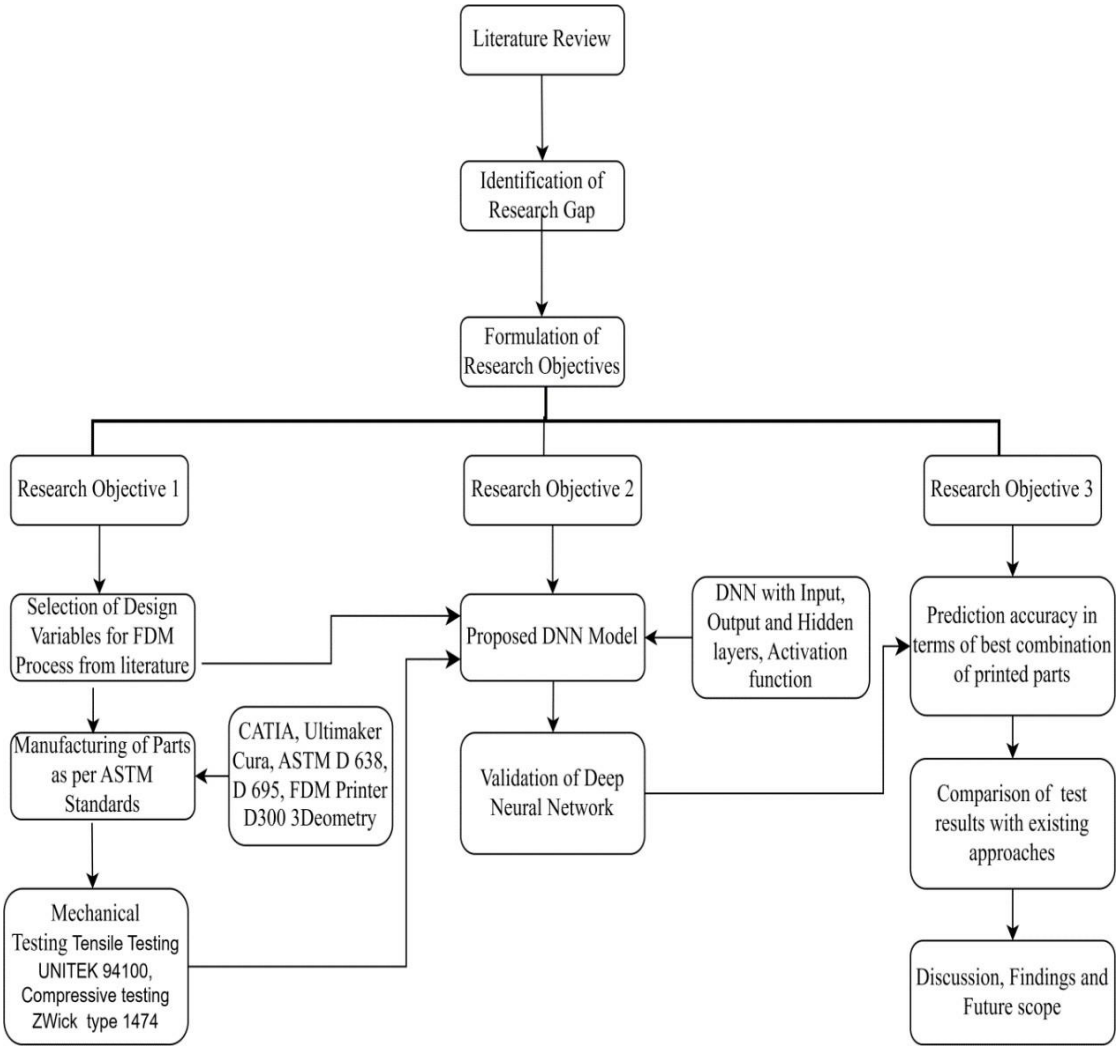

Figure 3.1 Research methodology

PLA is used in wide range engineering and medical applications due its unique advantage of biodegradability. Though conventional material like PLA is used in wide range engineering applications; was used in most of the open source FDM machines.

The characteristics of part manufactured by FDM processes are influenced by different process variables such as slicing parameters (layer thickness flow rate, deposition speed, infill percentage, raster angle, raster orientation, contour width, air

gap, nozzle diameter), Build orientation, temperature condition (environmental temperature, extrusion temperature, platform temperature) [17]. In the present research, less analysed design variables parameters like nozzle diameter, width of print line and layer thickness, print speed are considered as input parameters with their levels values. The selection of values was based on previous literature and customized 3D printed FDM machine. These specific values were chosen because they cover a broad range of commonly used settings in FDM printing. The ranges allow for comprehensive experimentation to determine optimal settings that strike a balance between competing factors like surface finish, dimensional accuracy, mechanical strength, and print time. The goal is to optimize the process parameters such that the final printed part meets the desired performance standards (e.g., tensile, compressive, and flexural strength) while minimizing production time and material waste.

Figure 3.2 depicts the schematic architecture of proposed model used to optimise the FDM process parameters. The test specimens have been manufactured with predetermined dimensions strictly adhering to ASTM standards followed by standard operating procedure for manufacturing (CAD modelling, conversion to .stl file format, slicing, generation of tool path, printing for final prototype).Experiments carried out to test the mechanical properties of manufactured parts and collected dataset from the experimental results were inscribed for training the proposed machine learning model.

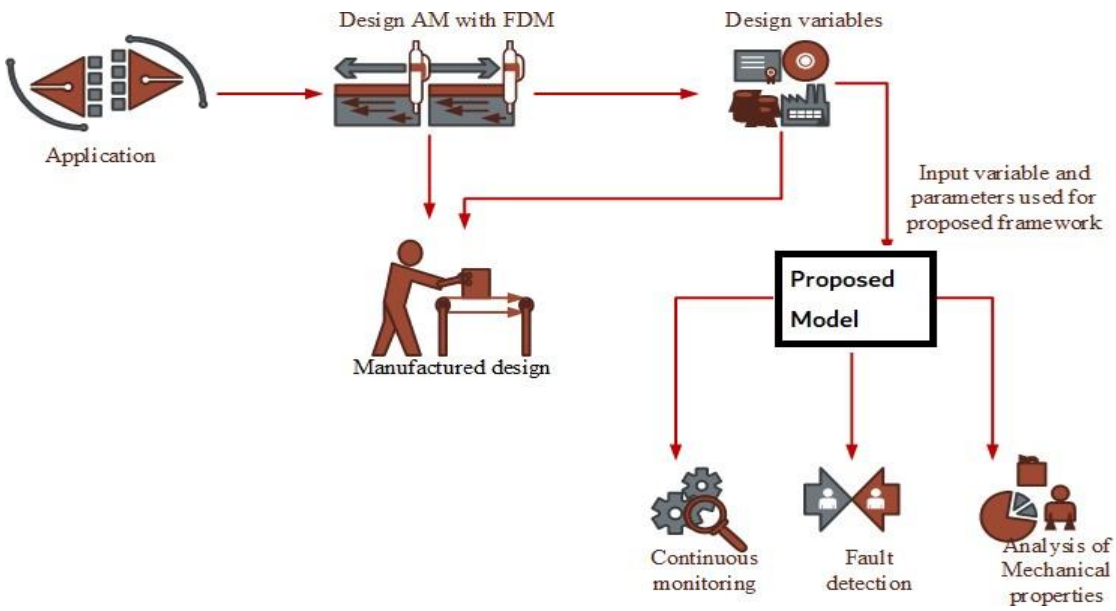

Figure 3.2 FDM with ML architecture

Proposed DNN algorithm was developed to aim the enhancement in prediction accuracy regarding best parametric selection to optimize the mechanical properties. The available dataset was converted into training 70% and rest testing sets to evaluate the performance of the model. The specific splitting ratio is around 70-80% of the data for training and rest 20-30% for testing. Then it assures that the model is trained on a enough amount of dataset to learn the underlying patterns and relationships, while also allowing for an independent evaluation of its performance on unrevealed data. Additionally, the integration of machine learning techniques allows for more efficient exploration of the parameter space and identification of optimal settings.

Training dataset was handed to fit the model's parameters, while testing data was fed to assess how well the trained model generalizes to new, unseen data. This split helps to avoid overfitting, in which though the algorithm performs best on the training dataset but may fail to reveal to new data.

DNN is characterized by its depth, which refers to the existence of various hidden layers within the input and output layers [24]. Network to learn intricate patterns and representations from the input data can be enabled by hidden layers, leading to more

sophisticated feature extraction and higher-level abstractions. DNNs consist of three or more hidden layers stacked between the input and output layers. Each hidden layer contains numerous neurons (nodes) that perform computations on the input data [40].

Activation functions like ReLU (Rectified Linear Unit), sigmoid were implied to the output of each neuron to hidden layers for introducing non-linearity and activate the network to learn complex mappings between inputs and outputs. DNNs can automatically learn hierarchical representations of the input data. Lower layers typically catch simple features such as edges and textures, while higher layers arrest increasingly abstract and intricate features such as shapes and objects.

The hyperparameters (number of neurons and layers, normalization, batch size, activation functions, optimizers, dropouts,), were tuned to find the optimal combination that maximizes the performance metrics of the model, such as accuracy, precision. Evaluation of trained model on the test set using the predefined performance metrics using classification technique.

Validation of model performance was performed using statistical analysis well in addition of performance matrix using experimental dataset. Documentation of the entire validation process was done, including data pre-processing steps, model architecture, hyperparameter tuning, and performance evaluation results.

Finally, study summarized the key findings obtained from the experimental analysis conducted. Comparison of the findings was evaluated with previous studies or literature to identify similarities, differences, or contradictions. Discussion covered how the results contribute to addressing gaps in knowledge and advancing the understanding of the research area. Limitations of the study and their potential impact on the interpretation of results stated to engrave the future research direction. Methodology also suggested potential extensions or refinements to the methodology used.

CHAPTER 4

FABRICATION AND TESTING

4.1 Overview

The adopted experimental methodology in this study is shown in Figure 4.1. The key motive of utilizing ML in AM is to find out best combination of process parameters and analyse the mechanical properties of the proposed design. In this present research work, the design variables are based on nozzle diameter, layer thickness, print speed, distance from each print line used as an input parameters to train the developed model in Deep Neural Network. Their level values were based on previous literature and customized 3D printed FDM machine. Rest parameters were kept constant. Full factorial experiments with 4 parameters and 4 levels, 4 x 4 x 4 x 4= 256 has been carried out for each output value in terms of tensile and compressive strength respectively, as more data requirement to execute deep neural network and to attain the best prediction accuracy for the continuous monitoring process.

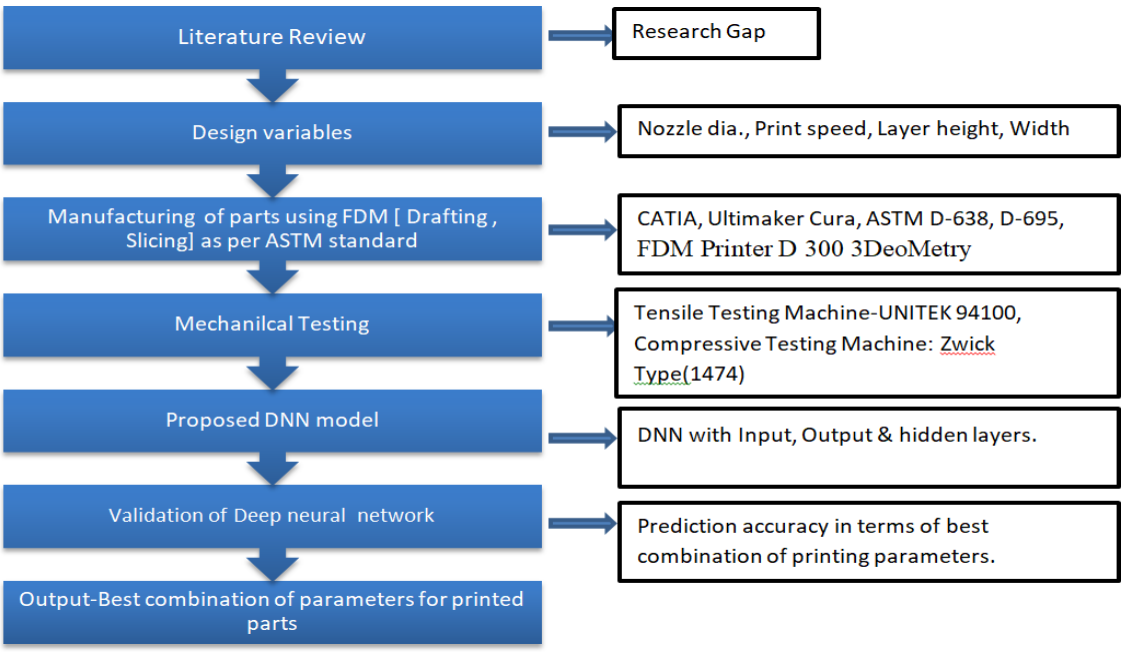

Figure 4.1 Experimental Methodology

Table 4.1 Significant Materials in FDM Process PLA and ABS [42]

Property	**PLA**	**ABS**
Printing temperature (° C)	180 to 230	210 to 250
Build platform temperature (° C)	20 to 60	80 to 110
Raft	Optional	Mandatory
Strength	High	Medium
Flexibility	Brittle	Moderately flexible
Heat resistance	Low	Moderate
Biodegradability	Yes	No
Moisture absorption	Yes	Yes

Table 4.1 elaborates the significance of discrimination of PLA (Polylactic Acid) and ABS (Acrylonitrile Butadiene Styrene) which are indeed two common thermoplastic materials used in FDM and other AM processes. PLA is a biodegradable and environmentally friendly thermoplastic derived from renewable resources such as corn starch or sugarcane. It has a relatively low melting temperature (around 180-220°C) and exhibits good dimensional stability, stiffness, and surface finish. ABS is a petroleum-based thermoplastic known for its high strength, toughness, and impact resistance. It has a higher melting temperature (around 210-250°C) compared to PLA [11].

PLA is easier to print with compared to ABS due to its lower printing temperature and minimal warping tendency. It adheres well to the print bed and typically does not require a heated build platform. PLA offers good stiffness and dimensional accuracy. PLA is easier to post-process compared to ABS. It can be sanded, painted, and glued

easily, and it does not emit strong odours during printing. Specific properties are shown in Table 4.2 [30].

PLA is considered more environmentally friendly than ABS due to its biodegradability and renewable sourcing. It is compostable under certain conditions and has a lower carbon footprint compared to ABS [11].

Table 4.2 Properties of PLA [30]

Property	Values
Specific Gravity	1–1.5
Surface Energy (dynes)	36–40
Melting Temperature (◦C)	140–210
Molecular Weight (Daltons)	Approx. 1.6×10^5
Melt Flow Index (g/ min)	4–22
Crystallinity (%)	5–35
Glass Transition Temperature (◦C)	50–75
Solubility Parameters (J/cm)	21

4.2 Experimental details

The test specimens have been manufactured with PLA Material with 1.75 mm diameter with predetermined dimensions strictly adhering to ASTM 638(type IV), ASTM D695 and ASTM 790. Figure 4.2 shows the material used for fabrication with

different colours confronting for experimentation. Density of PLA was 1.24 gm/cm^3. Test parts were fabricated using FDM Printer D 300 3DeoMetry Make: Build 300 X 300. Figure 4.3 shows the machine tool used for fabrication of parts.

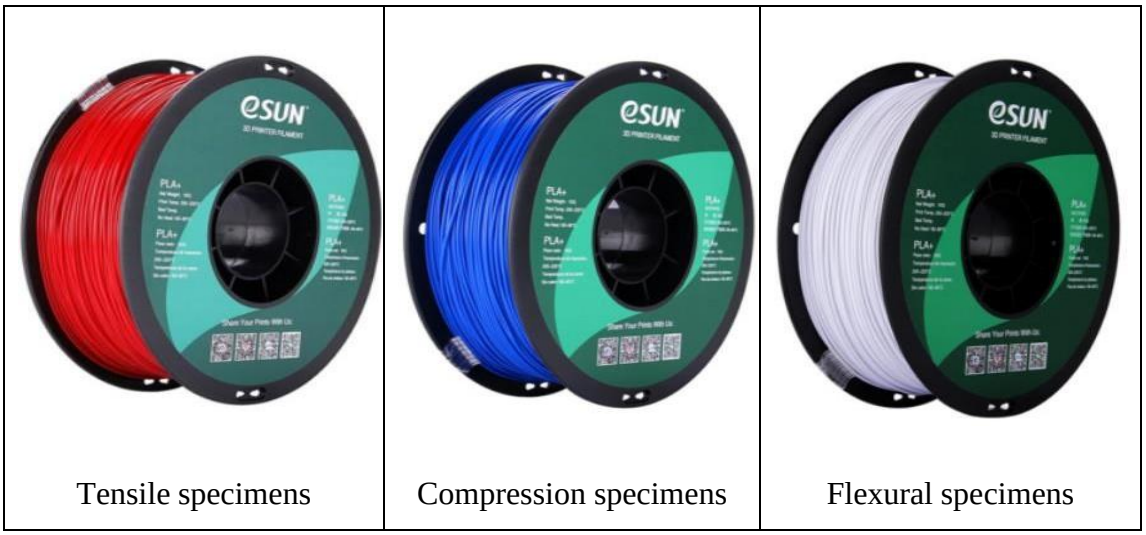

Tensile specimens	Compression specimens	Flexural specimens

Figure 4.2 PLA material used for experimentation

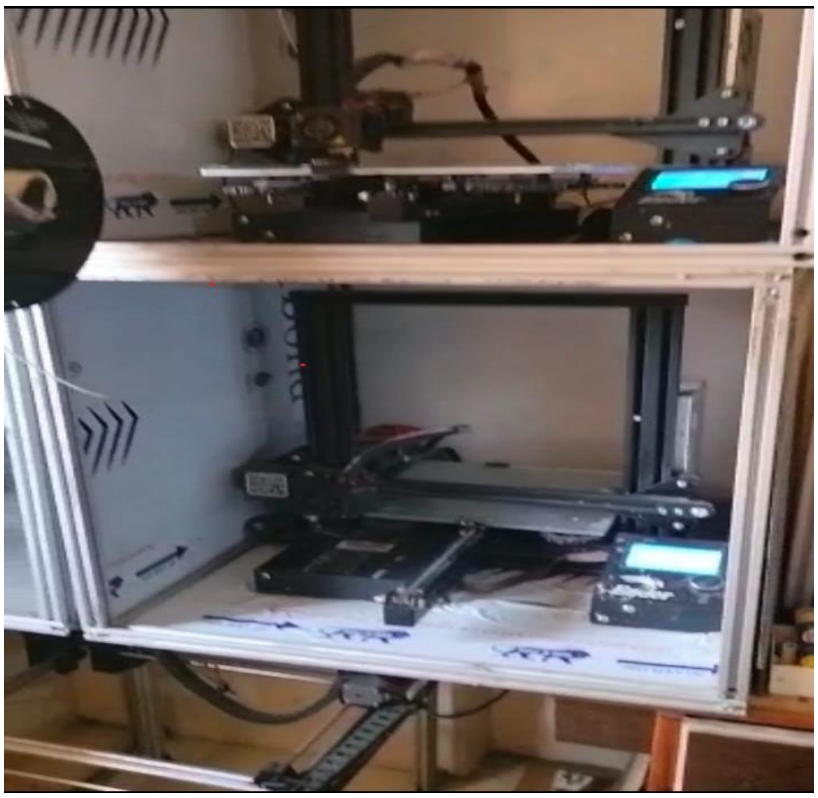

Figure 4.3 FDM printer used for fabrication

The detailed specifications of printer are depicted in Table 4.3.

Table 4.3 Specifications of FDM system

Typical Specifications	Print technology	FFF
	Type	Material extrusion
	Manufacturer	3DeoMetry
Process specifications	Build size	300 mm x 300 mm x 205 mm
	Layer resolution	0.05 mm
	Extruder	Single
	Enclosed chamber	No
	Extruder temperature limit	350°C
	Bed temperature	100°C
	Connection media	USB, SD
Raw material Specifications	Filament diameter	1.75 mm
	Materials can be print	PLA, ABS, PETG, PC
Software	Slicer (recommended)	Cura
	Allowed operating systems	Windows, Mac OSX, Linux
Electrical requirements	Input	220-240 V

Drafting of tested parts was done using CATIA 5.0 software as shown in Fig.4.4, 4.6 and 4.8.Ultimaker Cura 4.0 was used for slicing & generating G codes to adjust the mentioned parameters precisely.

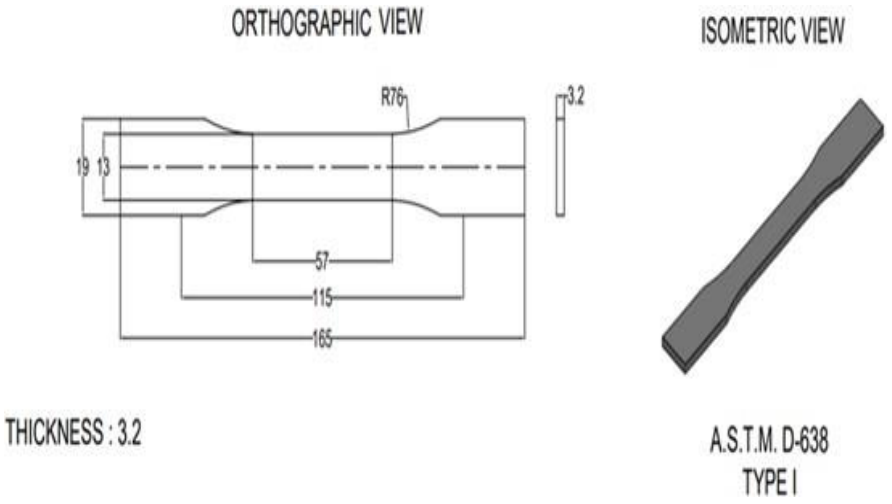

Figure 4.4 Tensile test specimen CAD model

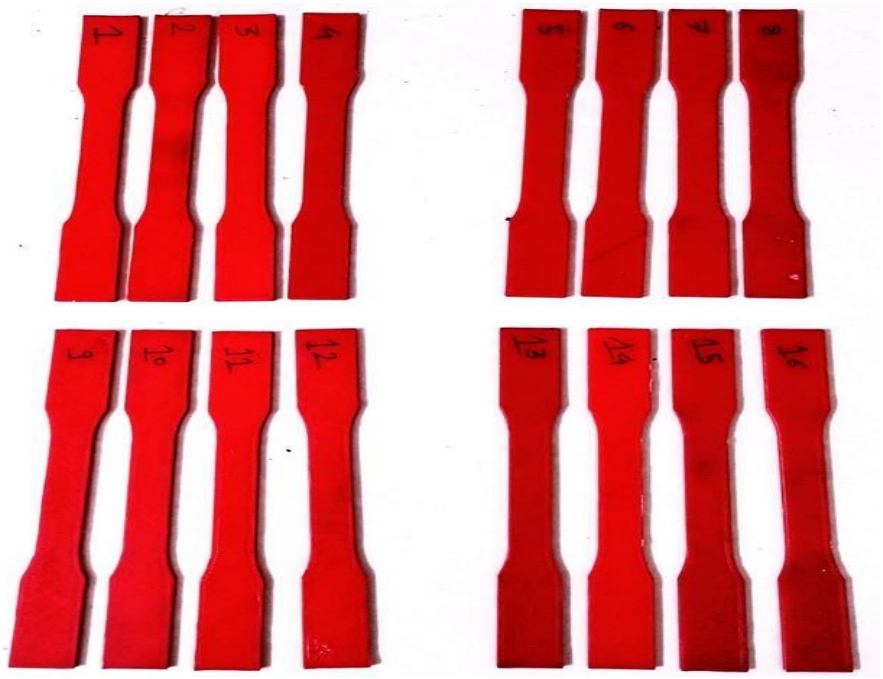

Figure 4.5 Tensile test specimens

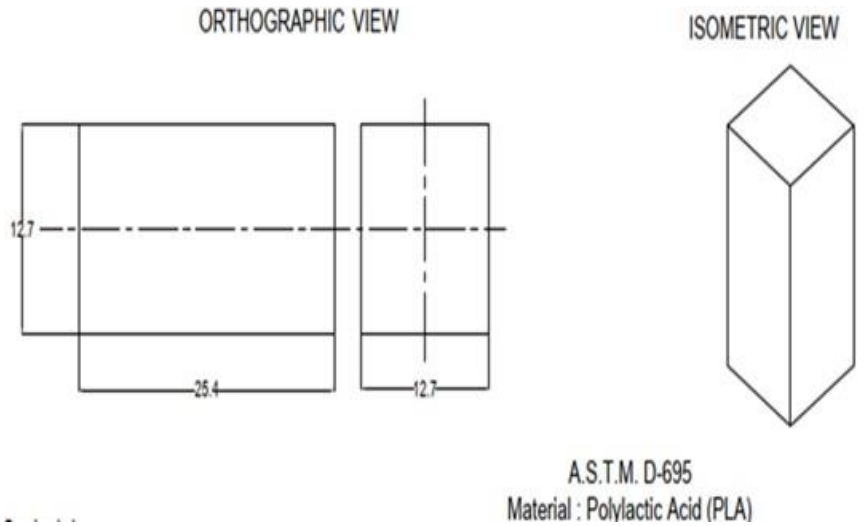

Figure 4.6 Compressive test specimen CAD model

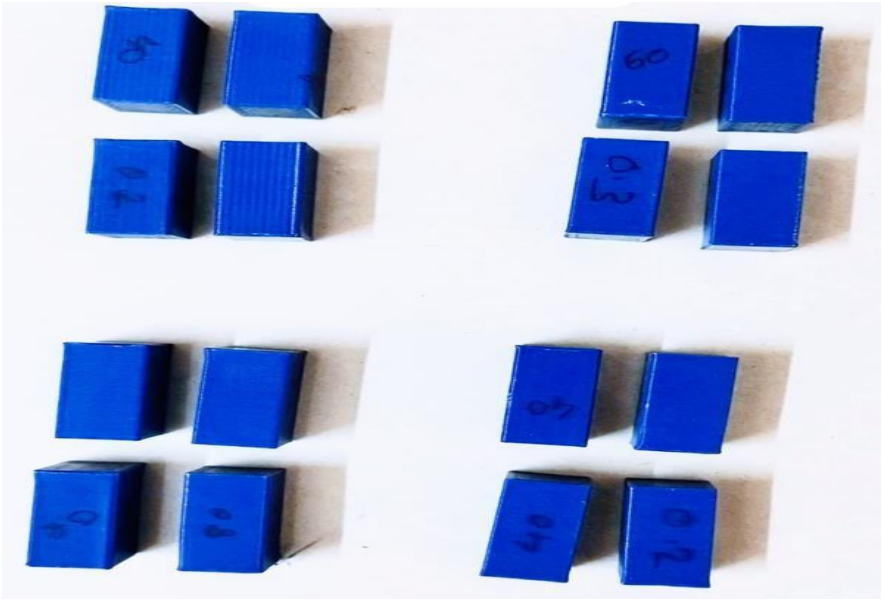

Figure 4.7 Compressive test specimens

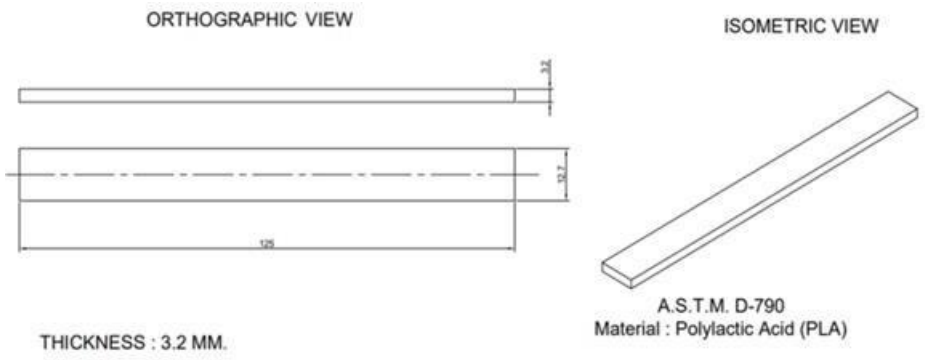

Figure 4.8 Flexural test specimen CAD model

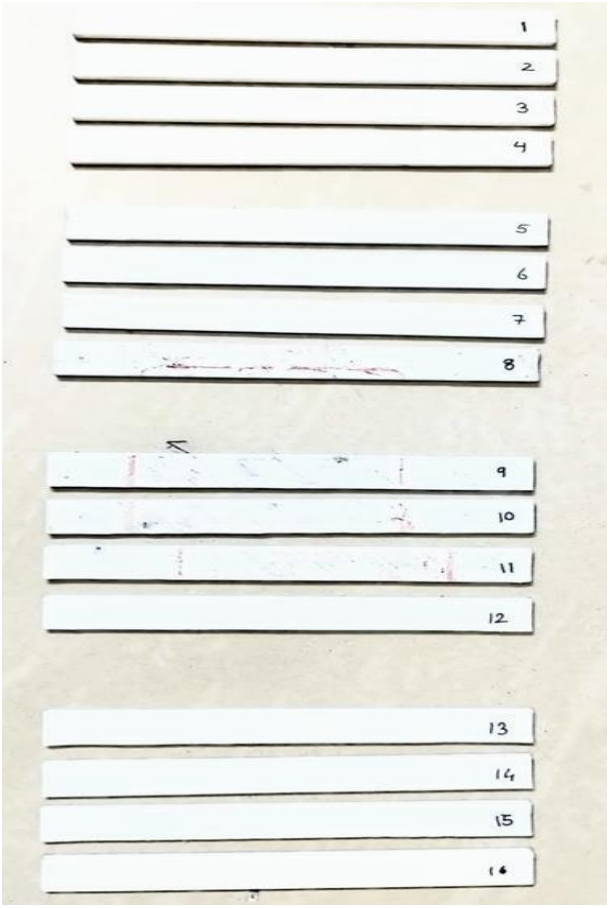

Figure 4.9 Flexural test specimens

4.2.1 Tensile test set up

Tensile testing of Type I specimens was carried out as per ASTM D638 using a Unitek 94100 universal testing machine. Type I specimens are dogbone-shaped with a narrowed central section.

Specimen Dimensions:

Gauge Length: 165 mm (6.5 inches)

Width: 19 mm (0.75 inches)

Thickness: 3.2 mm (0.125 inches)

The grips were provided for sufficient clamping force without causing premature failure or slippage during testing. The testing speed settings utilized on the Unitek 94100 machine to meet the requirements specified in ASTM D638. A common testing speed for plastics is 5 mm/min at a constant strain rate of 0.01 per sec. Tensile testing was carried out at standard temperature and humidity conditions (23°C ± 2°C and 50% ± 5% relative humidity) as recommended by ASTM D638 ensuring that the testing environment meets these conditions to ensure consistency and reproducibility of results.

Tensile strength can be calculated using the equation 4.1 given below:

Tensile strength $TS = \frac{\mathrm{F}}{\mathrm{A}CS}$ ---------- (4.1)

Where F is load applied and ACS is area of cross section before loading.

Figure 4.10 Test set up for tensile properties

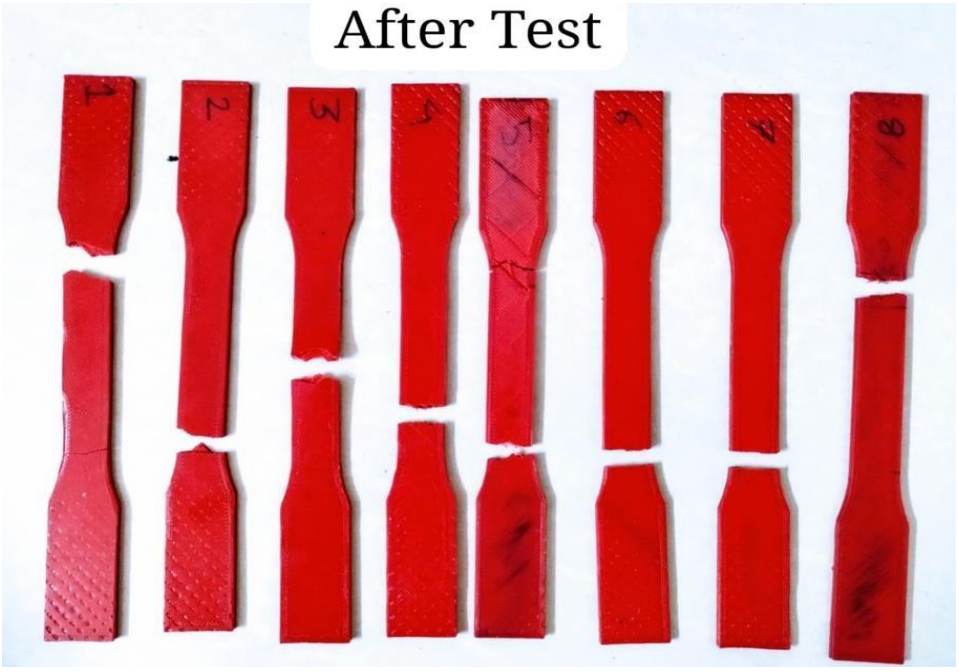

Figure 4.11 Tensile specimens after testing

4.2.2 Compression test set up

The compression strength test is conducted to evaluate how a material responds to compressive forces under specific parameter settings. In this test, cylindrical specimens are prepared according to the ASTM D695 standard. The dimensions of the specimens consist of a diameter of 12.7 mm and a height of 25.4 mm, ensuring a length-to-diameter ratio of 2:1. These specimens are subjected to compressive loads to determine their resistance to compression, providing valuable insights into the material's behaviour under such conditions. The compression test is performed on Zwick type 1474 testing machine with an initial strain rate of 10-2 s -1 with speed of testing 1.5 mm/min.

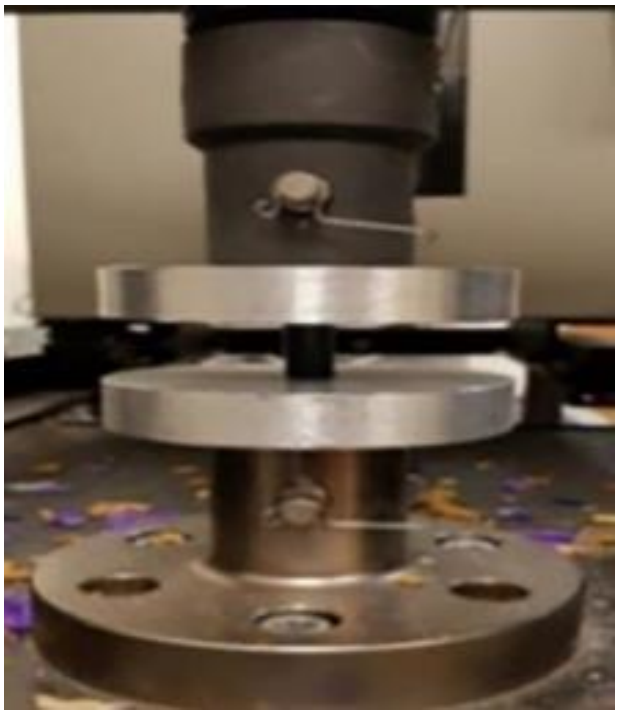

Figure 4.12 Test set up for compressive properties

Figure 4.13 Compressive specimens after testing

4.2.3 Flexural test set up

Bending test based three point technique was also performed on Tinius Olsen machine at a constant strain rate of 0.01 per sec. The specimen size followed by ASTM D790 standard with the dimensions of length = 127mm, width = 12.7mm and thickness = 3.2mm.

The calculation of stresses and Strains were done according to the loads obtained by 3-point bending machine mechanism. The equations 4.2 and 4.3 can be used for calculation of the stress and strain respectively.

Flexural stress $FS = \frac{3FL}{2bt^2}$ ------- (4.2)

Strain = $\frac{6\,\delta\,t}{L^2}$ ------- (4.3)

Figure 4.14 Test set up for flexural properties

Figure 4.15 Flexural specimens after testing

Drafting of tested parts was done using CATIA 5.0 software as shown in Figure 4.4, 4.6 and 4.8.Ultimaker Cura 4.0 was used for slicing & generating G codes to adjust the mentioned parameters precisely. Their level values are represented in Table 4.4.

Layer thickness, nozzle diameter, print speed, width of layer was considered as input parameters with four levels of each parameter. Nozzle diameter, width of each print line was less analysed parameters than others. The selection of parameter values was based on previous literature and customized 3D printed FDM machine. Rest parameters were kept constant is given as per Table 4.5. These specific values were chosen because they cover a broad range of commonly used settings in FDM printing. The ranges allow for comprehensive experimentation to determine optimal settings that strike a balance between competing factors like surface finish, dimensional accuracy, mechanical strength, and print time. The goal is to optimize the process parameters such that the final printed part meets the desired performance standards (e.g., tensile, compressive, and flexural strength) while minimizing production time and material waste.

Table 4.4 Experimental parameters and their level values

Parameters	Level 1	Level 2	Level 3	Level 4
Layer thickness (mm)	0.1	0.2	0.3	0.4
Nozzle diameter (mm)	0.15	0.2	0.25	0.3
Distance of each layer(mm)	0.3	0.5	0.7	0.9
Print speed (mm/s)	20	40	60	80

Table 4.5 Constant experimental parameters

Parameter	Value
Air gap	0
Raster angle	0º
Extrusion Temperature	210º C
Infill density	100%
Infill Pattern	Linear
Wall thickness	1 mm
Top thickness	1 mm
Bottom thickness	1 mm

4.3 Experimental values

The Table 4.6 depicts the different combinations of selected input parameters and the experimental values of mechanical properties namely Tensile and compressive strength. Full factorial experiments with 4 parameters and 4 levels, 4 x 4 x 4 x 4= 256 has been carried out for each output value in terms of tensile and compressive strength respectively, as more data requirement to execute DNN and to attain the best prediction accuracy for the continuous monitoring process. Experimental results were classified accordingly in two classes. Maximum Tensile strength in the experimental results obtained was 38.13 N/mm² and Compressive strength 27.36 N/mm².The best combinations of Tensile and Compressive strength both greater than its midrange and average values correspondingly 35.49 MPa and 25.30 MPa are taken as Class 1

combination and rest are Class 2. Class 1 was for good connection status and Class 2 for others.

Table 4.6 Experimental values for various combinations of input parameters

Nozzle diameter (mm)	Print speed (mm/s)	Layer thickness (mm)	Distance print line(mm)	Tensile strength (MPa)	Compressive Strength (Mpa)	Class
0.15	20	0.1	0.3	33.87	26.07	2
0.15	20	0.1	0.5	36.15	26.05	1
0.15	20	0.1	0.7	34.44	25.34	2
0.15	20	0.1	0.9	34.68	24.41	2
0.15	20	0.2	0.3	34.75	25.07	2
0.15	20	0.2	0.5	32.93	25.67	2
0.15	20	0.2	0.7	34.21	24.89	2
0.15	20	0.2	0.9	34.44	25.34	2
0.15	20	0.3	0.3	34.28	25.62	2
0.15	20	0.3	0.5	35.25	24.19	2
0.15	20	0.3	0.7	34.63	24.55	2
0.15	20	0.3	0.9	35.04	24.10	2
0.15	20	0.4	0.3	34.96	23.28	2
0.15	20	0.4	0.5	34.10	23.95	2
0.15	20	0.4	0.7	35.31	27.36	2
0.15	20	0.4	0.9	35.24	25.75	2
0.15	40	0.1	0.3	32.87	24.57	2
0.15	40	0.1	0.5	35.20	24.72	2
0.15	40	0.1	0.7	33.09	24.23	2
0.15	40	0.1	0.9	33.81	25.33	2
0.15	40	0.2	0.3	35.12	26.13	2
0.15	40	0.2	0.5	33.66	24.54	2
0.15	40	0.2	0.7	33.22	26.96	2
0.15	40	0.2	0.9	34.75	26.40	2
0.15	40	0.3	0.3	34.43	26.43	2
0.15	40	0.3	0.5	35.19	24.43	2
0.15	40	0.3	0.7	33.93	26.64	2
0.15	40	0.3	0.9	34.69	25.38	2
0.15	40	0.4	0.3	34.63	25.47	2
0.15	40	0.4	0.5	35.18	26.59	2
0.15	40	0.4	0.7	34.41	24.29	2
0.15	40	0.4	0.9	33.69	24.54	2
0.15	60	0.1	0.3	35.42	25.59	2
0.15	60	0.1	0.5	32.87	25.18	2

0.15	60	0.1	0.7	34.67	26.14	2
0.15	60	0.1	0.9	34.49	24.70	2
0.15	60	0.2	0.3	35.12	26.10	2
0.15	60	0.2	0.5	34.99	25.23	2
0.15	60	0.2	0.7	34.75	24.61	2
0.15	60	0.2	0.9	34.93	26.52	2
0.15	60	0.3	0.3	34.28	24.65	2
0.15	60	0.3	0.5	34.93	24.95	2
0.15	60	0.3	0.7	32.89	26.64	2
0.15	60	0.3	0.9	32.93	25.99	2
0.15	60	0.4	0.3	35.35	26.36	2
0.15	60	0.4	0.5	33.42	24.17	2
0.15	60	0.4	0.7	34.79	24.92	2
0.15	60	0.4	0.9	34.08	25.15	2
0.15	80	0.1	0.3	34.15	25.10	2
0.15	80	0.1	0.5	33.82	24.65	2
0.15	80	0.1	0.7	34.91	25.23	2
0.15	80	0.1	0.9	33.80	25.95	2
0.15	80	0.2	0.3	35.41	25.20	2
0.15	80	0.2	0.5	34.79	24.89	2
0.15	80	0.2	0.7	34.17	24.28	2
0.15	80	0.2	0.9	34.92	25.60	2
0.15	80	0.3	0.3	33.45	26.14	2
0.15	80	0.3	0.5	34.02	24.54	2
0.15	80	0.3	0.7	34.82	26.28	2
0.15	80	0.3	0.9	34.87	25.64	2
0.15	80	0.4	0.3	33.58	26.57	2
0.15	80	0.4	0.5	34.57	26.22	2
0.15	80	0.4	0.7	34.74	24.03	2
0.15	80	0.4	0.9	34.62	23.79	2
0.2	20	0.2	0.7	36.95	25.57	1
0.2	40	0.1	0.9	37.00	26.01	1
0.2	60	0.1	0.7	36.96	25.88	1
0.2	60	0.2	0.3	35.86	26.27	1
0.2	60	0.2	0.5	36.89	26.31	1
0.2	80	0.1	0.7	35.51	25.85	1
0.2	80	0.2	0.3	36.48	26.04	1
0.2	80	0.3	0.3	36.92	26.78	1
0.2	20	0.1	0.3	34.30	26.42	2
0.2	20	0.1	0.5	34.43	26.31	2
0.2	20	0.1	0.7	32.97	25.95	2
0.2	20	0.1	0.9	36.96	24.36	2
0.2	20	0.2	0.3	35.86	24.91	2

0.2	20	0.2	0.5	34.52	25.07	2
0.2	20	0.2	0.9	32.89	23.81	2
0.2	20	0.3	0.3	34.58	23.88	2
0.2	20	0.3	0.5	34.05	25.55	2
0.2	20	0.3	0.7	35.28	25.57	2
0.2	20	0.3	0.9	33.45	25.67	2
0.2	20	0.4	0.3	36.10	25.33	2
0.2	20	0.4	0.5	35.45	24.94	2
0.2	20	0.4	0.7	34.62	25.15	2
0.2	20	0.4	0.9	32.93	25.21	2
0.2	40	0.1	0.3	35.10	26.79	2
0.2	40	0.1	0.5	34.95	26.73	2
0.2	40	0.1	0.7	35.03	24.81	2
0.2	40	0.2	0.3	37.78	25.05	2
0.2	40	0.2	0.5	34.96	27.18	2
0.2	40	0.2	0.7	34.67	24.85	2
0.2	40	0.2	0.9	36.00	24.98	2
0.2	40	0.3	0.3	34.66	25.94	2
0.2	40	0.3	0.5	35.05	25.95	2
0.2	40	0.3	0.7	34.99	26.83	2
0.2	40	0.3	0.9	33.19	26.91	2
0.2	40	0.4	0.3	34.94	24.13	2
0.2	40	0.4	0.5	35.33	24.66	2
0.2	40	0.4	0.7	33.26	25.25	2
0.2	40	0.4	0.9	35.44	25.28	2
0.2	60	0.1	0.3	33.43	26.46	2
0.2	60	0.1	0.5	35.25	26.24	2
0.2	60	0.1	0.9	34.82	26.74	2
0.2	60	0.2	0.7	37.45	24.87	2
0.2	60	0.2	0.9	35.76	24.24	2
0.2	60	0.3	0.3	35.39	24.70	2
0.2	60	0.3	0.5	36.18	25.32	2
0.2	60	0.3	0.7	38.02	24.97	2
0.2	60	0.3	0.9	37.42	23.56	2
0.2	60	0.4	0.3	35.42	23.24	2
0.2	60	0.4	0.5	36.10	24.90	2
0.2	60	0.4	0.7	33.08	25.03	2
0.2	60	0.4	0.9	36.43	25.22	2
0.2	80	0.1	0.3	35.19	26.28	2
0.2	80	0.1	0.5	37.79	25.22	2
0.2	80	0.1	0.9	34.19	25.24	2
0.2	80	0.2	0.5	35.27	26.94	2
0.2	80	0.2	0.7	33.42	25.38	2

0.2	80	0.2	0.9	34.28	24.80	2
0.2	80	0.3	0.5	34.96	26.95	2
0.2	80	0.3	0.7	33.70	24.22	2
0.2	80	0.3	0.9	34.30	25.46	2
0.2	80	0.4	0.3	34.91	25.12	2
0.2	80	0.4	0.5	33.73	25.47	2
0.2	80	0.4	0.7	34.37	25.41	2
0.2	80	0.4	0.9	34.71	25.83	2
0.25	20	0.1	0.3	37.02	26.19	1
0.25	20	0.2	0.3	36.88	26.38	1
0.25	40	0.2	0.7	37.00	27.00	1
0.25	60	0.3	0.7	35.60	26.44	1
0.25	80	0.1	0.3	36.03	26.12	1
0.25	80	0.2	0.3	36.78	26.35	1
0.25	80	0.2	0.5	38.13	25.86	1
0.25	80	0.3	0.7	35.87	26.97	1
0.25	20	0.1	0.5	33.92	25.45	2
0.25	20	0.1	0.7	34.06	26.91	2
0.25	20	0.1	0.9	34.73	26.27	2
0.25	20	0.2	0.5	36.59	24.21	2
0.25	20	0.2	0.7	36.72	24.55	2
0.25	20	0.2	0.9	35.72	24.98	2
0.25	20	0.3	0.3	34.65	26.88	2
0.25	20	0.3	0.5	34.54	25.78	2
0.25	20	0.3	0.7	36.30	24.30	2
0.25	20	0.3	0.9	33.15	26.56	2
0.25	20	0.4	0.3	35.65	24.17	2
0.25	20	0.4	0.5	35.22	25.54	2
0.25	20	0.4	0.7	33.39	26.80	2
0.25	20	0.4	0.9	34.32	25.44	2
0.25	40	0.1	0.3	35.05	23.72	2
0.25	40	0.1	0.5	33.30	25.89	2
0.25	40	0.1	0.7	35.46	25.04	2
0.25	40	0.1	0.9	33.80	24.97	2
0.25	40	0.2	0.3	34.67	24.79	2
0.25	40	0.2	0.5	35.12	24.44	2
0.25	40	0.2	0.9	36.43	24.69	2
0.25	40	0.3	0.3	37.23	24.75	2
0.25	40	0.3	0.5	32.86	26.49	2
0.25	40	0.3	0.7	34.36	24.95	2
0.25	40	0.3	0.9	34.11	23.83	2
0.25	40	0.4	0.3	33.41	27.14	2
0.25	40	0.4	0.5	36.66	24.79	2

0.25	40	0.4	0.7	37.27	24.23	2
0.25	40	0.4	0.9	34.20	23.70	2
0.25	60	0.1	0.3	34.04	26.36	2
0.25	60	0.1	0.5	37.38	24.77	2
0.25	60	0.1	0.7	34.52	23.98	2
0.25	60	0.1	0.9	36.78	24.49	2
0.25	60	0.2	0.3	36.06	24.94	2
0.25	60	0.2	0.5	34.08	27.30	2
0.25	60	0.2	0.7	33.21	24.93	2
0.25	60	0.2	0.9	34.76	26.38	2
0.25	60	0.3	0.3	33.83	26.30	2
0.25	60	0.3	0.5	34.76	24.77	2
0.25	60	0.3	0.9	36.48	23.83	2
0.25	60	0.4	0.3	33.41	25.55	2
0.25	60	0.4	0.5	33.97	26.22	2
0.25	60	0.4	0.7	35.61	24.99	2
0.25	60	0.4	0.9	35.79	24.61	2
0.25	80	0.1	0.5	36.01	24.25	2
0.25	80	0.1	0.7	35.33	26.22	2
0.25	80	0.1	0.9	34.65	25.15	2
0.25	80	0.2	0.7	37.33	25.25	2
0.25	80	0.2	0.9	35.36	25.45	2
0.25	80	0.3	0.3	35.29	25.16	2
0.25	80	0.3	0.5	35.21	25.15	2
0.25	80	0.3	0.9	35.96	24.95	2
0.25	80	0.4	0.3	34.79	24.45	2
0.25	80	0.4	0.5	34.88	24.40	2
0.25	80	0.4	0.7	34.58	25.66	2
0.25	80	0.4	0.9	36.71	24.58	2
0.3	20	0.1	0.3	36.05	25.80	1
0.3	20	0.1	0.5	36.05	26.04	1
0.3	20	0.2	0.3	37.32	26.25	1
0.3	40	0.2	0.5	37.67	25.78	1
0.3	40	0.4	0.7	36.69	26.59	1
0.3	60	0.2	0.9	37.60	26.12	1
0.3	80	0.2	0.3	36.05	25.93	1
0.3	80	0.3	0.7	35.79	26.49	1
0.3	20	0.1	0.7	36.40	24.16	2
0.3	20	0.1	0.9	37.00	24.34	2
0.3	20	0.2	0.5	33.22	24.57	2
0.3	20	0.2	0.7	36.11	24.90	2
0.3	20	0.2	0.9	36.04	24.70	2
0.3	20	0.3	0.3	35.35	25.41	2

0.3	20	0.3	0.5	35.52	24.09	2
0.3	20	0.3	0.7	35.28	25.45	2
0.3	20	0.3	0.9	32.94	23.91	2
0.3	20	0.4	0.3	33.79	26.54	2
0.3	20	0.4	0.5	35.85	25.02	2
0.3	20	0.4	0.7	33.92	24.46	2
0.3	20	0.4	0.9	34.76	25.01	2
0.3	40	0.1	0.3	36.91	23.45	2
0.3	40	0.1	0.5	36.92	24.26	2
0.3	40	0.1	0.7	34.08	26.84	2
0.3	40	0.1	0.9	35.20	26.17	2
0.3	40	0.2	0.3	35.11	26.07	2
0.3	40	0.2	0.7	36.21	24.12	2
0.3	40	0.2	0.9	36.53	23.69	2
0.3	40	0.3	0.3	35.38	23.73	2
0.3	40	0.3	0.5	35.61	24.87	2
0.3	40	0.3	0.7	32.88	23.73	2
0.3	40	0.3	0.9	36.15	24.73	2
0.3	40	0.4	0.3	34.21	25.20	2
0.3	40	0.4	0.5	36.53	24.42	2
0.3	40	0.4	0.9	33.16	24.04	2
0.3	60	0.1	0.3	35.83	23.93	2
0.3	60	0.1	0.5	35.87	24.43	2
0.3	60	0.1	0.7	33.58	25.04	2
0.3	60	0.1	0.9	35.80	24.91	2
0.3	60	0.2	0.3	34.42	26.31	2
0.3	60	0.2	0.5	34.06	23.97	2
0.3	60	0.2	0.7	36.37	24.21	2
0.3	60	0.3	0.3	35.00	24.93	2
0.3	60	0.3	0.5	36.61	24.35	2
0.3	60	0.3	0.7	35.78	24.73	2
0.3	60	0.3	0.9	36.62	24.71	2
0.3	60	0.4	0.3	35.06	24.75	2
0.3	60	0.4	0.5	34.98	25.42	2
0.3	60	0.4	0.7	33.23	24.89	2
0.3	60	0.4	0.9	33.33	26.90	2
0.3	80	0.1	0.3	33.06	24.91	2
0.3	80	0.1	0.5	36.36	24.48	2
0.3	80	0.1	0.7	34.78	27.03	2
0.3	80	0.1	0.9	35.16	25.01	2
0.3	80	0.2	0.5	35.02	25.05	2
0.3	80	0.2	0.7	33.55	26.12	2
0.3	80	0.2	0.9	36.14	24.75	2

0.3	80	0.3	0.3	33.39	26.42	2
0.3	80	0.3	0.5	34.07	26.35	2
0.3	80	0.3	0.9	35.92	25.15	2
0.3	80	0.4	0.3	34.14	24.44	2
0.3	80	0.4	0.5	34.89	25.17	2
0.3	80	0.4	0.7	34.98	25.66	2
0.3	80	0.4	0.9	33.19	24.73	2

4.4 Deep neural network

Some of the limitations with other optimisation techniques are Genetic Algorithms (GA); computationally expensive and slow convergence for large datasets, requires careful tuning of parameters like population size and mutation rate. Particle Swarm Optimization (PSO); Prone to premature convergence, performance highly dependent on parameter settings (e.g., inertia weight, cognitive and social coefficients).Simulated Annealing (SA); Slow convergence rate, performance depends on the cooling schedule and initial temperature. Response Surface Methodology (RSM); Not suitable for high-dimensional problems with many variables, assumes a specific functional form (usually quadratic), which may not capture complex relationships. Taguchi Method assumes independence of input variables, limited in handling interactions between variables.

The DNN is a prominent technique in the computer version to optimize the parameters of any manufacturing processes [24]. The use of DL models in the optimization of process parameters offers several advantages over traditional optimization methods in FDM and other AM processes.

Capturing Complex Non-linear Relationships: DL models excel at capturing intricate non-linear behaviour between response variables and process parameters. In FDM, where parameters like nozzle temperature, print speed, and layer height interact in complex ways, deep learning models can effectively model these relationships.

Data-Driven Approach: DL models learn from large datasets, including experimental trials or simulations, to make predictions or optimize processes. This data-driven

approach allows deep learning models to identify optimal parameter settings based on desired outcomes such as print quality, mechanical properties, and material usage.

Flexibility and Adaptability: DL models are highly flexible and adaptable to different types of data and optimization tasks. They can handle high-dimensional input data, accommodate various process parameters and output variables, and adapt to changing conditions or requirements.

Automation and Efficiency: Deep learning-based optimization approaches automate parameter tuning and optimization, reducing the need for manual intervention and trial-and-error experimentation. By continuously learning from data, these models optimize manufacturing processes more efficiently, saving time and resources.

Scalability and Generalization: Well-trained DL models can scale across different manufacturing setups, materials, and applications. Once trained on a specific FDM setup, a DL model can generalize to similar setups and materials, enabling the transferability of optimization strategies across different environments.

Exploration of Novel Solutions: DNN can explore novel solutions and identify optimal parameter combinations that may not be apparent through traditional optimization methods. By exploring the entire parameter space and learning from data, DNN uncover hidden patterns and insights that lead to innovative process improvements and enhanced performance.

Supervised learning algorithms offer significant advantages for optimizing process parameters in FDM.

Supervised learning algorithms can construct predictive models that link process parameters (inputs) with desired outcomes or performance metrics (outputs). By training on historical data with known parameter-outcome relationships, these algorithms can accurately predict outcomes for new parameter settings. Once trained, supervised learning models can guide parameter optimization efforts. Engineers can input various parameter combinations into the model to quickly assess predicted

outcomes and identify optimal settings to achieve specific objectives, such as improving print quality or mechanical strength.

Supervised learning algorithms streamline parameter tuning by automating the search for optimal settings. Instead of relying on manual trial and error, engineers can use these models to systematically explore the parameter space and identify promising candidates for further testing. FDM processes involve numerous interrelated parameters that impact the quality of printed parts. Supervised learning, particularly DL models, can capture critical non-linear correlation between output variables and input parameters, enabling more accurate modeling of FDM dynamics.

Supervised learning models can adapt to new data and evolving process conditions, continuously improving their predictions over time. Engineers can update the model with new information as it becomes available, ensuring its relevance and effectiveness in guiding parameter optimization efforts. Supervised learning algorithms provide insights into the factors influencing process outcomes. Analysing model coefficients or feature importance can help engineers understand which parameters have the greatest impact, guiding optimization priorities.

Supervised learning models can be integrated with optimization techniques like Bayesian optimization or genetic algorithms to perform advanced optimization tasks. This integration enables efficient exploration of the parameter space while minimizing the number of experiments needed.

Supervised learning technique was used to execute the DL. This technique utilizes part of experimental data for training the model. Once the ML algorithm is trained it updates the parameters and the rest data can be used for testing. Prediction accuracy can be tested after validating the model. In this study, the training procedure of the DNNs is defined by using eqn. (4.4)

$$P = h\sum_{j=1}^{m} V_J x_j + a \qquad \text{---------- (4.4)}$$

Here, output of the training layer was determined by P, layer weight is represented as V_j, x_j was mentioned to denote the input values and the parameters of neural layer was expanded using the variable a. The sum of weights $V_j x_j$, bias a, and activation function h (Softmax, RELU) shown in equation (4.4). In every neuron which is connected to previous one input variable x_j is multiplied by weights and bias 'a' is added to control neuron activation. Output will be obtained after passing the weighted sum and bias to activation function. Figure 4.16 explains the inner layer of neural network model.

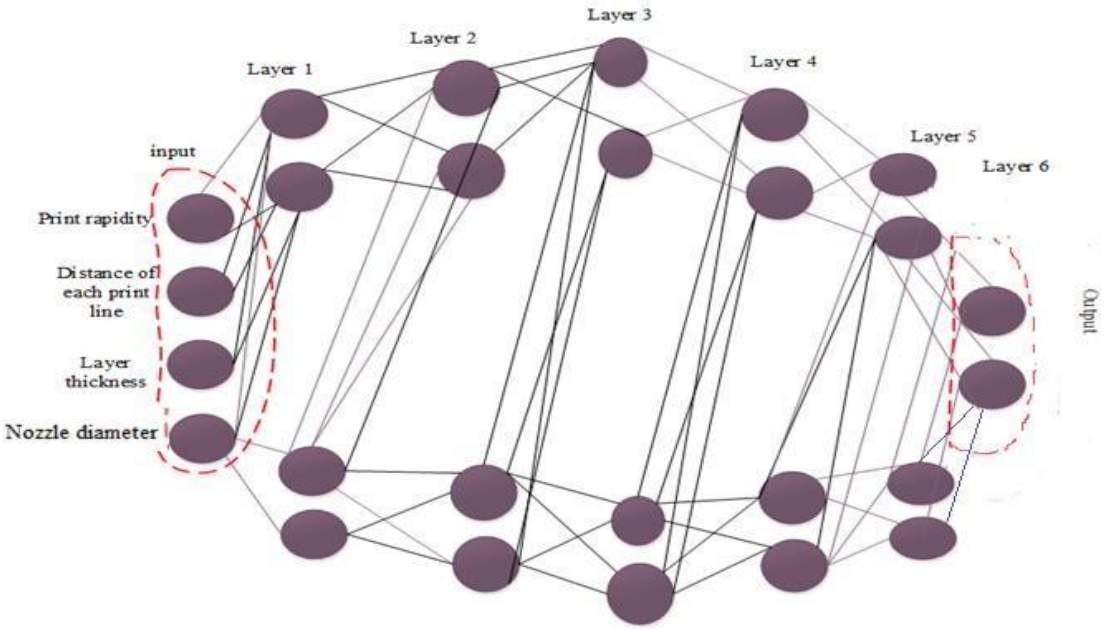

Figure 4.16 Inner layer of neural model

Here input variables are print speed, distance from each print line, layer thickness, and nozzle diameter. One input layer, 5 hidden layers and 1 output layer. Using a DL with five hidden layers, one input layer, and one output layer can be beneficial for tasks that require learning complex, hierarchical representations from data, such as image classification, natural language processing, and time-series prediction.

Rectified Linear Unit (RELU), activation function was used for hidden layers as it reaches to the convergence faster and no gradient vanishing issues [69] and Softmax

for output layer as it adds to sum 1 by normalizing the values in the range (0,1). The equations for computations of these activation functions are expressed by equations **4.5** and 4.6 respectively. Prediction accuracy in training data and testing data will be evaluated in. Categorical cross entropy was used as an objective function, Adam as an optimizer, batch size 10 for epochs 500.

$$\text{RELU } (x) = \max(x,0) = \begin{cases} x, & x > 0 \\ 0, & else \end{cases} \quad \text{---------- (4.5)}$$

$$\text{Softmax } (x_{k)} = \frac{e^{xk}}{\sum_{i=1}^{n} e^{xi}} \quad \text{---------- (4.6)}$$

Leveraging the features of Python with Jupyter Notebook in Anaconda, DL algorithm development process was effectively documented.

4.5 Developed algorithm

Adhering to ASTM standards with predefined dimensions total 256 experiments have been carried for each output, in which 204 result data used for training and 52 for testing the model using PYTHON programming language.

For the data preparation experimental data was organized by ensure that each experiment was properly labelled and contains all necessary input and output variables according to ASTM standards. Best performances were revealed by empirical studies that when we use 20-30% of the data for testing, and the remaining 70-80% for training [78]. Splitting of dataset we have divided the dataset into training and testing sets allocating 204 experiments for training and 52 experiments for testing. Data pre-processing was carried out by converting the dataset into a suitable format for training DL models using NumPy, arrays.

For defining model structure as per the model's architecture the number of input features, hidden layers, neurons per layer and activation functions were included. The loss function optimizer and evaluation metrics for training defined for compilation of

model. Model training has been carried out by fitting the model to the training data using the fit () method, specifying the number of epochs and batch size. Model Evaluation was further assessed by the trained model's performance on the testing data using evaluation metrics RM squared error. For visualization of predictions model predictions were tested against true values to visually inspect the model's performance and identify any discrepancies.

Figure 4.17 shows the developed neural network algorithm for the optimization of process parameters of FDM process.

In [1]:
```
import numpy as np
from keras.models import Sequential
from keras.layers import Dense
import xlrd
from sklearn.model_selection import train_test_split
import keras
import pandas as pd
from keras import utils
```

In [2]:
```
df=pd.read_csv(r"C:\Users\DS_USER\Downloads\newdata.csv")
```

In [3]:
```
df.columns
```

Out[3]:
```
Index(['Nozzle diameter(mm)', 'Print speed (mm/s) ', 'Layer thickness (mm) ',
       'Distance from each print line (mm) ', 'Classes'],
      dtype='object')
```

In [4]:
```
x_data=df[['Nozzle diameter(mm)', 'Print speed (mm/s) ', 'Layer thickness (mm) ','Distance from each print line (mm) ']]
```

In [5]:
```
 y_target=df["Classes"]
```

In [6]:
```
# y_target
```

In [7]:
```
# from tensorflow.keras.utils import to_categorical
from keras.utils import np_utils
```

```
In [8]:
y = np.array([y_target]).T
y.shape

Out[8]: (256, 1)

In [9]:
# y_target = np.array(y_target)
y_target = keras.utils.np_utils.to_categorical(y, num_classes=5)

In [10]:
# y_target=keras.utils.

In [11]:
#split data into train and test set
X_train, X_test, y_train, y_test = train_test_split(x_data, y_target, test_size = 0.2)

In [12]:
X_train.shape,X_test.shape

Out[12]: ((204, 4), (52, 4))

In [13]:
x_data = np.asarray(x_data).astype('float32')

In [14]:
#train the model
model = Sequential()
model.add(Dense(10, input_shape = (4,) ,activation = 'relu' ))
model.add(Dense(20, activation = 'relu'))
model.add(Dense(30, activation = 'relu'))
model.add(Dense(20, activation = 'relu'))
model.add(Dense(10, activation = 'relu'))
model.add(Dense(5, activation = 'softmax'))
model.compile(loss = 'categorical_crossentropy', optimizer = 'adam', metrics = ['accuracy'])
model.summary()

Model: "sequential"
```

```
In [15]:
model.fit(X_train, y_train, epochs = 500, batch_size = 10)

Epoch 459/500
21/21 [==============================] - 0s 2ms/step - loss: 0.2317 - accuracy: 0.8578
Epoch 460/500
21/21 [==============================] - 0s 2ms/step - loss: 0.2347 - accuracy: 0.8775
Epoch 461/500
21/21 [==============================] - 0s 2ms/step - loss: 0.2313 - accuracy: 0.8627
Epoch 462/500
21/21 [==============================] - 0s 2ms/step - loss: 0.2260 - accuracy: 0.8775
Epoch 463/500
21/21 [==============================] - 0s 2ms/step - loss: 0.2430 - accuracy: 0.8627
Epoch 464/500
21/21 [==============================] - 0s 3ms/step - loss: 0.2211 - accuracy: 0.8775
Epoch 465/500
21/21 [==============================] - 0s 2ms/step - loss: 0.2329 - accuracy: 0.8578
Epoch 466/500
21/21 [==============================] - 0s 3ms/step - loss: 0.2268 - accuracy: 0.8824
Epoch 467/500
21/21 [==============================] - 0s 2ms/step - loss: 0.2281 - accuracy: 0.8824
Epoch 468/500
21/21 [==============================] - 0s 2ms/step - loss: 0.2194 - accuracy: 0.8775

In [16]:
model.evaluate(X_test, y_test)

2/2 [==============================] - 0s 3ms/step - loss: 0.3389 - accuracy: 0.8846

Out[16]: [0.3389059901237488, 0.8846153616905212]
```

Figure 4.17 Developed DNN algorithm

CHAPTER 5

OPTIMIZATION AND VALIDATION

5.1 Optimization overview

The mechanical properties of the printed parts directly affect their ability to perform specific functions. For example, in engineering applications, parts may need to withstand certain loads, pressures, or temperatures without failure. Optimizing process parameters to enhance mechanical properties ensures that the printed parts meet these performance requirements.

Tensile strength, compressive strength and flexural properties determine the structural integrity and durability of printed parts. By optimizing process parameters to improve these properties, we can ensure that the parts can withstand mechanical stresses and environmental conditions over their intended lifespan. Mechanical properties are closely related to dimensional accuracy and part quality in FDM printing. Optimizing process parameters can help minimize defects such as warping, delamination, and dimensional inaccuracies, which can negatively impact mechanical properties. Optimizing process parameters to improve mechanical properties can also lead to more efficient use of materials. By producing parts with higher strength and durability, you can reduce material waste and minimize the need for post-processing or reinforcement techniques. Parts with optimized mechanical properties are less likely to fail prematurely or require frequent replacement or repair. This can lead to cost savings in terms of reduced downtime, maintenance, and replacement costs, making the manufacturing process more cost-effective in the long run.

Consistency in mechanical properties is essential for ensuring the reliability and repeatability of printed parts. By optimizing process parameters to achieve consistent mechanical properties across different batches or printing conditions, you can maintain high-quality standards and meet customer expectations. Prioritizing the optimization of mechanical properties in FDM process parameters is essential for producing high-quality, functional parts that meet performance requirements and

withstand real-world conditions. By focusing on enhancing mechanical properties, manufacturers can ensure the success and competitiveness of FDM manufacturing in various industries.

Flow for implementation of DNN model is followed by following process. Start → Data Collection & Pre-processing → DNN Model Initialization → Hyperparameter Tuning → Training → Evaluation → Optimization of Parameters → Real-Time Implementation → Validation → End

5.2 Parametric optimization using DNN model

Outlined steps for optimizing a DL model with 256 experiments were breakdown comprehensively for analyse the data.

Dataset is properly formatted with 256 samples, each containing the input parameters (nozzle diameter, print speed, layer thickness, width of each layer) and the corresponding output labels (connection status).Successively dividing the dataset into training and testing datasets, allocating 204 samples for training and 52 samples for testing DNN model has been defined the architecture according 5 hidden layers, 1 input layer, and 1 output layer.

The layers were designed with appropriate activation functions ReLU (Rectified linear unit) for hidden layers and Softmax for the output layer for binary classification with suitable numbers of neurons. RELU activation reaches to the convergence faster and no gradient vanishing issues [85] and Softmax function sum up to 1 with the normalization of the concerned values in the range zero to one. Model was compiled by specifying the appropriate loss function binary cross-entropy, optimizer Adam. After training the model using the training dataset, the hyperparameters are adjusted such as the number of epochs, batch size, and learning rate to achieve optimal convergence and performance. Training loss and validation accuracy as a function of the number of epochs were monitored to decide the number of epochs. The batch size conveys the count of samples used in each forward and backward pass during training. Smaller batch size 10 numbers was utilized can lead to faster convergence

and better generalization. The trained model was accessed using the testing dataset by compute relevant performance indices namely accuracy and precision to appraise its performance on unrevealed data. Visualisation of the model's predictions versus the true labels was done to identify any discrepancies or areas where the model may need improvement.

Experimentation carried out with model architecture by varying the number of hidden layers, activation functions and per layer neurons to find the configuration that yields the best performance. After tuning hyperparameters such as batch size, learning rate and regularity strength using techniques like grid search or random search to optimize the model's performance further.

5.3 Validation of DNN model

The obtained results during 256 experiments which consisting seventy percent data for training the proposed model and remaining for testing. The experimental results have been classified in classes on the basis of tensile & compressive strength measured with different combinations. Class 1 was for good connection status and Class 2 for others. Actual connection status and predicted connection status was interpreted as shown in Figure 5.1 and Figure 5.2.The real class and predicted class was shown by blue and orange points respectively. Overlaying points can be considered as no discrimination between actual and predicted class. Prediction accuracies after 500 epochs 0.8654 were obtained on trained data and 0.8846 achieved for test data.

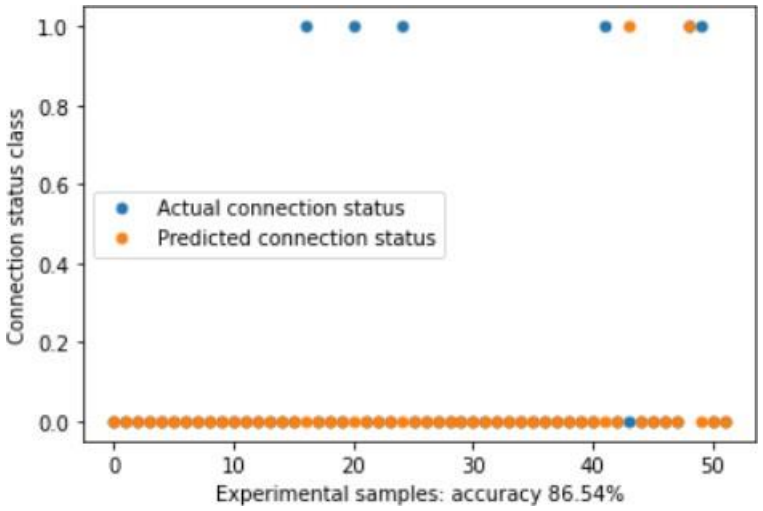

Figure 5.1 Performance of Prediction data after Training

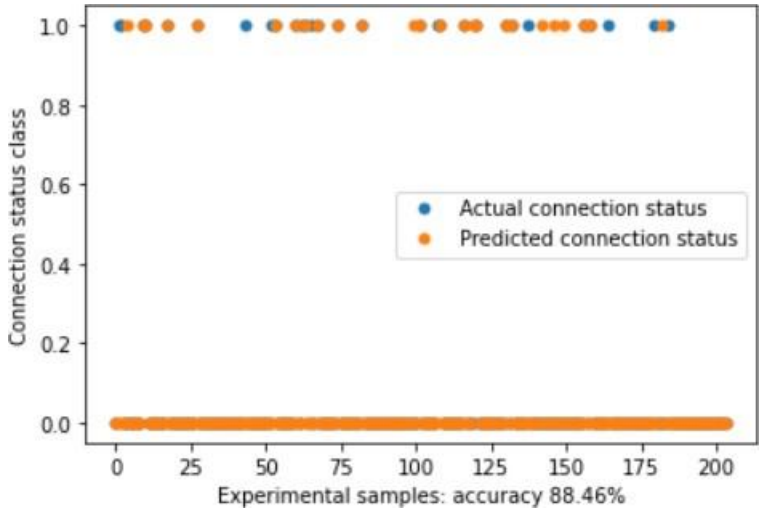

Figure 5.2 Performance of Prediction data after Testing

The training accuracy of 86.54% and testing accuracy of 88.46% indicate that the model has performed reasonably well and has generalized effectively to unseen data. Interpretation of the fit of the model based on these accuracies depicted below.

5.3.1 Training Accuracy (86.54%)

The training accuracy shows the proportion of properly classified samples within the training dataset. In this case, the model gained an accuracy of 86.54% on the training

dataset, indicating that it correctly classified approximately 86.54% of the samples. A training accuracy of 86.54% was relatively high, suggesting that the model has learned the underlying patterns and relationships present in the training data reasonably well.

However, it's important to note that the training accuracy was not excessively high, which indicates that the model has not memorized the training data or overfit to it.

5.3.2 Testing Accuracy (88.46%)

The testing accuracy depicts the proportion of precisely classified samples within the testing dataset, which consists of unseen data. The model achieved an accuracy of 88.46% on the testing dataset, indicating that it correctly classified approximately 88.46% of the samples. A testing accuracy of 88.46% was slightly higher than the training accuracy, which was generally an approving sign. This recommends that the model is fit for use on the training dataset and capability of generalizing well to unseen samples. The fact that the testing accuracy was close to the training accuracy further supports the notion that the model was not only memorizing the training data but also learning to generalize effectively.

5.3.3 Interpretation

The high training and testing accuracies suggest that the model has successfully learned to discriminate between the different classes based on the input parameters (nozzle diameter, print speed, layer thickness, width of each layer).The small difference between the training and testing accuracies indicates that the model is performing consistently well on both datasets, without exhibiting significant overfitting or underfitting behaviours. Overall, the fit of the model appeared to be satisfactory, as evidenced by the high accuracies on both the training and testing datasets. It suggests that the model was well-suited for predicting the connection status placed on the provided input parameters, and it can be deployed with confidence for future predictions.

5.3.4 RMSE value

RMSE depicts for Root Mean Squared Error. It is a metric can be used to evaluate the performance of models. RMSE measures the average magnitude of the errors between predicted values and actual values depicted in equation 5.1.

$$RMSE = \sqrt{\frac{1}{n}\sum_{i=1}^{n}(y_i - \hat{y}_i)^2}$$ .....(equation 5.1)

n = count of samples in the dataset

y_i = i^{th} sample actual value.

$\hat{y}_i$ = i^{th} sample predicted value.

5.3.5 R^2 value

R-squared (R^2) is a statistical metric that evaluates the contribution of the variance in the dependent variable that could be determined by the independent variables in a model. In other words, R-squared quantifies the wellness-of-fit of the model to the dataset.

Total Sum of Squares (SST): Computed the sum of squared differences between each perceived value and the mean of the dependent variable by equation 5.2

$$SST = \sum_{i=1}^{n}(y_i - \bar{y})^2$$ .....(equation 5.2)

$\bar{y}$ = mean of dependent variable.

Residual Sum of Squares (SSE): Computed the sum of squared differences between each perceived value and the estimated value from the model by equation 5.3

$$SSE = \sum_{i=1}^{n}(y_i - \hat{y}_i)^2$$ .....(equation 5.3)

$$R^2 = 1 - \frac{SSE}{SST}$$ ....(equation 5.4)

The values range of R-squared from 0-1. A higher R-squared value determines a wellness of the model fit to the data, with 1 indicating a perfect fit (the model explains all the variance) and 0 indicating that the model does not explain any variance beyond the mean of the dependent variable.

```
In [11]:
import numpy as np
import math
y_predicted=[0, 0, 0, 0, 0, 0, 0, 0, 0, 0, 0, 0, 0, 0, 0, 0, 0, 0, 0, 0, 0, 0, 0, 0, 0, 0, 0, 0, 0, 0, 0, 0, 0, 0, 0, 0, 0, 0,
y_actual=[0, 0, 0, 0, 0, 0, 0, 0, 0, 0, 0, 0, 0, 0, 0, 0, 1, 0, 0, 0, 1, 0, 0, 0, 1, 0, 0, 0, 0, 0, 0, 0, 0, 0, 0, 0, 0, 0,
MSE = np.square(np.subtract(y_actual,y_predicted)).mean()

RMSE = math.sqrt(MSE)
print("Root Mean Square Error:\n")
print(RMSE)

Root Mean Square Error:

0.3396831102433787
```

(a)

```
In [28]:
predicted=[2,1,2,2,1,2,2,2,2,2,2,2,2,2,1,1,2,2,2,2,2,2,2,2,2,2,2,2,2,2,2,2,2,2,2,2,2,2,2,2,2,2,2,2,2,2,2,2,2,2,2,2,2,1,2,2,1
actual=   [2,1,2,2,1,2,2,2,2,2,2,2,2,2,1,1,2,2,2,2,2,2,2,2,2,2,2,2,2,2,2,2,2,2,2,2,2,2,2,2,2,2,2,2,2,2,2,2,2,2,2,2,2,1,2,2,1
corr_matrix = np.corrcoef(actual, predicted)
corr = corr_matrix[0,1]
R_sq = corr**2

print(R_sq)

0.8796296296296325
```

(b)

Figure 5.3 Part program to calculate the a) RMSE value b) R^2 value

Python code snippet was utilized to calculate RMSE and R^2 value after obtaining the predicted classes from DNN model for the test dataset.

Table 5.1 Ranges of various error values matrices for discrimination [70]

METRIC	Very Good	Good	Satisfactory	Not Satisfactory
Coefficient of Determination (R^2)	$R^2 > 0.85$	$0.75 < R^2 <= 0.85$	$0.6 <= R^2 < 0.75$	$R^2 < 0.6$
Nash-Sutcliffe Efficiency (NSE)	NSE > 0.80	0.70 < NSE <= 0.80	0.50 < NSE <= 0.70	NSE < = 0.5
PBIAS (%)	|PBIAS| <= 5	5 < |PBIAS| <=10	10 < |PBIAS| <= 15	|PBIAS| > 15
Mean Error (ME) ft	|ME| <= 0.25'	0.25' < |ME| <= 0.5'	0.5' < |ME| <= 1.0'	|ME| > 1.0'
Mean Absolute Error (MAE) ft	MAE <= 0.5'	0.5' < MAE <= 0.75'	0.75' < MAE <= 1.5'	MAE > 1.5'
Root Mean Square Error (RMSE) ft	RMSE <= 0.75'	0.75' < RMSE <= 1.0'	1.0' < RMSE <= 2.0'	RMSE > 2.0'
Ratio "RMSE/SD-Observed" (RSR)	RSR <= 0.5	0.5 < RSR <=0.6	0.6 < RSR <= 0.7	RSR>0.7
1/2 Standard Deviation (Observed) ft	3 |ME|, MAE, RMSE	2 |ME|, MAE, RMSE	1 |ME|, MAE, RMSE	0 |ME|, MAE, RMSE

As per Table 5.1 RMSE $\leq$ 0.75 and R^2 > 0.85 shows very good fitting of the classification model. RMSE value for tested model observed is 0.3396 and R^2 value 0.8796 shown in Figure 5.3 which validates the performance of model and can predict the results under random circumstances.

5.4 Experimental validation by addition of performance matrix

Though evidently several researches have been carried out regarding optimisation of input parameters to upgrade the mechanical properties of FDM printed parts, eventually various studies reported the flimsy nature of 3D printed materials which should be taken care of. Flexural strength was less analysed compared to tensile and compressive strength. Grey relational analysis (GRA) associated with Principle component analysis (PCA) method fits for use to optimize multiple response

characteristics and can be further utilized for guidelines in design for manufacturing (DFM) in practical applications.

This study focuses the effect of input process parameters on the mechanical properties of PLA printed parts. Layer thickness, nozzle diameter, print speed, width of layer was considered as input parameters with four levels of each parameter. Subsequently, specimens were manufactured considering combinations of design variables strictly adhering to ASTM standards. 4 factors each of 4 levels Taguchi L16 orthogonal array of specific subset of input parameters combinations formed using MINITAB 16.0 were utilized to conduct the experimentation. Tensile strength, compressive strength and flexural strength were analysed by multi optimization using Taguchi and GRA combined with PCA. PCA assigns weight to each measurable significant response which affects the Grey relational grade (GRG). Validation of proposed study was carried out with experimental confirmation to find out significance of optimized parameters to enhance the mechanical behaviour of printed parts.

Table 5.2 depicts sixteen experiments have been carried out to investigate the effects of process parameters nozzle diameter (ND), print speed (PS), layer thickness (LT), width of each layer (DL) on each of the output parameter namely flexural strength (FS), tensile strength (TS), compressive strength (CS).

Table 5.2 Design of experiments L16 orthogonal array

A ND (mm)	**B PS (mm/s)**	**C LT (mm)**	**D DL (mm)**	**Experimental results**		
				FS (MPa)	**TS (MPa)**	**CS (MPa)**
0.15	20	0.1	0.3	52.3	33.9	26.07
0.15	40	0.2	0.5	51.5	33.7	24.54
0.15	60	0.3	0.7	49.4	32.9	26.64
0.15	80	0.4	0.9	50.1	35.6	23.79
0.2	20	0.2	0.7	54.2	37.0	25.57
0.2	40	0.1	0.9	54.2	37.0	26.01
0.2	60	0.4	0.3	51.1	37.4	26.24
0.2	80	0.3	0.5	52.8	35.0	26.95

0.25	20	0.3	0.9	53.9	33.2	26.56
0.25	40	0.4	0.7	53.3	37.3	24.23
0.25	60	0.1	0.5	57.9	37.38	24.77
0.25	80	0.2	0.3	58.7	36.78	24.35
0.3	20	0.4	0.5	52.6	35.85	26.02
0.3	40	0.3	0.3	54.6	35.38	23.73
0.3	60	0.2	0.9	60.5	37.6	26.12
0.3	80	0.1	0.7	58.7	34.78	27.03

5.4.1 GRA associated with PCA

Figure 5.4 details about the statistical approach of proposed methodology. Multiple response optimisations using statistical approach GRA associated with PCA shown as in was utilized. L16 orthogonal Taguchi array was used to carry out for experimentation and measurement of responses. Signal to noise ratio calculation carried out for quality response characteristics it possesses with greater value is better criterion for optimization. Normalization of S/N ratios in linear way leads to conversion reference sequence to comparable sequence in range of (0, 1). GRG and WGRG using first PC components values were calculated as discussed detailed in equation 3 and 5.Identical optimal conditions of process parameters using GRG and Weighted grey relational grade (WGRG) were used for individual response optimization.

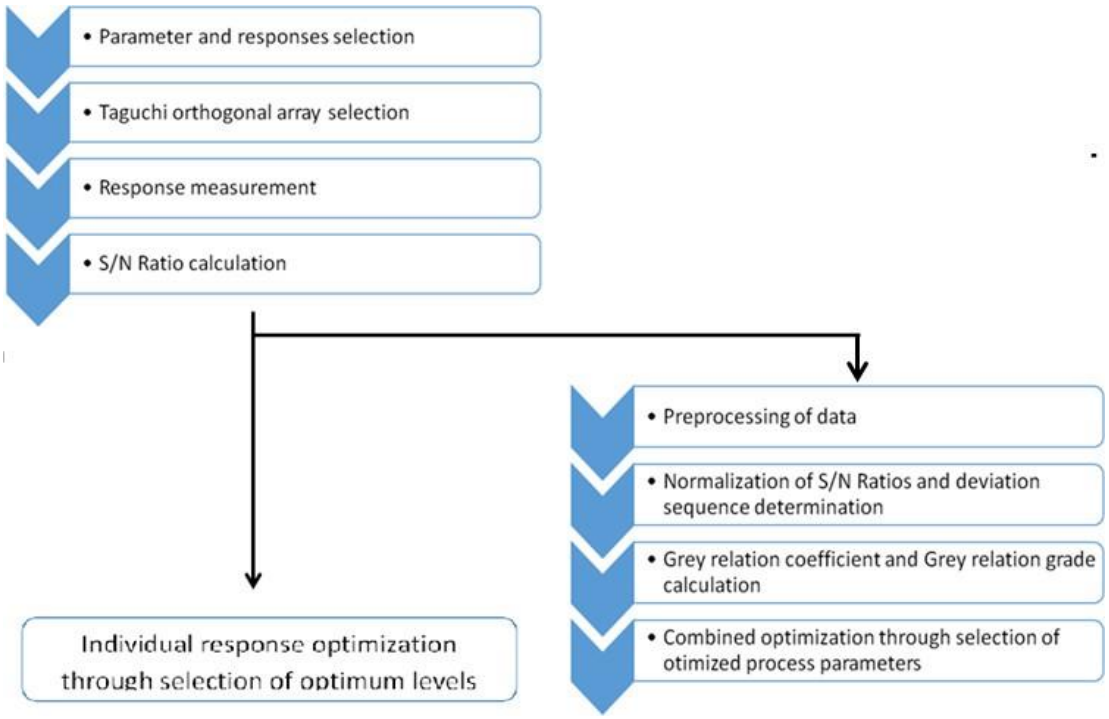

Figure 5.4 Statistical approach GRA associated with PCA

Combined optimization was validated through confirmatory experiment using optimized process parameters.

S/N ratio were calculated with larger the better criterion by equation 5.5,

$$\frac{S}{N}\text{Ratio} = -10 \text{ x } \log_{10} \frac{1}{x}\sum_{i=1}^{x}\frac{1}{y_{ij}^2} \quad \text{---------- (equation 5.5)}$$

Table 5.3 S/N Ratio calculation for L16 orthogonal array

ND (mm)	PS (mm/s)	LT (mm)	DL (mm)	S/N Ratio		
				FS (MPa)	TS (MPa)	CS (MPa)
0.15	20	0.1	0.3	34.363	30.596	28.323
0.15	40	0.2	0.5	34.233	30.542	27.797
0.15	60	0.3	0.7	33.868	30.341	28.511
0.15	80	0.4	0.9	34.000	31.034	27.528
0.2	20	0.2	0.7	34.683	31.352	28.155
0.2	40	0.1	0.9	34.678	31.364	28.303

0.2	60	0.4	0.3	34.170	31.462	28.379
0.2	80	0.3	0.5	34.449	30.871	28.611
0.25	20	0.3	0.9	34.632	30.410	28.485
0.25	40	0.4	0.7	34.535	31.427	27.687
0.25	60	0.1	0.5	35.254	31.453	27.879
0.25	80	0.2	0.3	35.373	31.312	27.730
0.3	20	0.4	0.5	34.420	31.090	28.306
0.3	40	0.3	0.3	34.744	30.975	27.506
0.3	60	0.2	0.9	35.635	31.504	28.339
0.3	80	0.1	0.7	35.373	30.827	28.637

As proposed area of interest was to maximize the flexural strength, tensile strength and compressive strength, the normalized results were interpreted by Larger the better criterion as shown in equation 5.6 for maximization.

$$x^*_j(p) = \frac{x_j(p) - \min x_j(p)}{\max x_j(p) - \min x_j(p)} \quad \text{(equation 5.6)}$$

Where, x∗j(p) is grey relational value, max $x_j(p)$ and min $x_j(p)$ are maximum and minimum values of $x_j(p)$for pth observation respectively. Here, response variables p=3 and sequential responses for $x_j(p)$for 16 experiments. j=1. 2, 3…..16. The best normalization will yield to the value 1, for good results normalized value should be high. The data is normalized to ensure comparability across different metrics and the scale effect has been removed.

Grey relational coefficient (GRC) is calculated by equation 5.7 which describes the discrimination between real normalization and desired normalized values.

$$\xi_j(p) = \frac{\Delta min + \xi \Delta max}{\Delta oi(p) + \xi \Delta max} \quad \text{(equation 5.7)}$$

Deviation sequence is denoted by $\Delta oi(p)$ and distinguishing coefficient ξ is taken 0.5 in this study and calculations are shown in Table 5.4.

$$\gamma_j = \frac{1}{n} \sum_{p=1}^{n} (\xi j(p)) \quad \text{(equation 5.8)}$$

Table 5.4 Normalization and deviation sequences of S/N Ratio responses

S/N Ratio response			Normalization			Deviation Delta		
FS	**TS**	**CS**	**FS**	**TS**	**CS**	**FS**	**TS**	**CS**
34.363	30.596	28.323	0.2603	0.2081	0.7091	0.7397	0.7919	0.2909
34.233	30.542	27.797	0.1903	0.1635	0.2455	0.8097	0.8365	0.7545
33.868	30.341	28.511	0.0000	0.0000	0.8818	1.0000	1.0000	0.1182
34.000	31.034	27.528	0.0682	0.5796	0.0182	0.9318	0.4204	0.9818
34.683	31.352	28.155	0.4363	0.8620	0.5576	0.5637	0.1380	0.4424
34.678	31.364	28.303	0.4336	0.8726	0.6909	0.5664	0.1274	0.3091
34.170	31.462	28.379	0.1571	0.9618	0.7606	0.8429	0.0382	0.2394
34.449	30.871	28.611	0.3070	0.4395	0.9758	0.6930	0.5605	0.0242
34.632	30.410	28.485	0.4075	0.0552	0.8576	0.5925	0.9448	0.1424
34.535	31.427	27.687	0.3537	0.9299	0.1515	0.6463	0.0701	0.8485
35.254	31.453	27.879	0.7666	0.9533	0.3152	0.2334	0.0467	0.6848
35.373	31.312	27.730	0.8384	0.8259	0.1879	0.1616	0.1741	0.8121
34.420	31.090	28.306	0.2908	0.6285	0.6939	0.7092	0.3715	0.3061
34.744	30.975	27.506	0.4704	0.5287	0.0000	0.5296	0.4713	1.0000
35.635	31.504	28.339	1.0000	1.0000	0.7242	0.0000	0.0000	0.2758
35.373	30.827	28.637	0.8384	0.4013	1.0000	0.1616	0.5987	0.0000

GRG γ_j was calculated by equation 5.8 which depicts the correlation between normalized value and corresponding experimental response value. Higher the GRG indicates ideal case.

Weights obtained from PCA were assigned to each quality response modifies this equation 5.9 to WGRG as below

$$\gamma^j = \frac{1}{n}\sum_{p=1}^{n} wq(\xi j(p)) \quad \text{---------- (equation 5.9)}$$

Where n is number of runs and $\sum_{p=1}^{n} wq = 1$

5.4.2 PCA (Principal component analysis)

PCA applies linear transformations to the original data to find new orthogonal axes (principal components) that capture the maximum variance in the data. These transformations aim to preserve the original information as much as possible while reducing the dimensionality of the dataset. PCA can be used to simplify multi-response optimization problems by transforming them into single-response optimization problems. By representing the data in terms of its principal components, PCA reduces the number of variables to be optimized while retaining essential information. This transformation helps in streamlining the optimization process.

Eigenvalues and Principal Components: After performing PCA, the eigenvalues and corresponding eigenvectors (principal components) are computed. These eigenvalues are arranged in descending order, indicating the amount of variance captured by each PC. The first eigenvalue associated with the first PC indeed accounts for the largest variance contribution in the data. [82]. The GRC's calculated for response variables was utilized to create a matrix, presented in equation 5.10

$$y = \begin{bmatrix} y_1(1) & y_1(2) & \cdots & y_1(k) \\ y_2(1) & y_2(2) & \cdots & y_2(k) \\ \cdots & \cdots & \cdots & \cdots \\ \cdots & \cdots & \cdots & \cdots \\ y_j\,(1) & y_j(2) & \ldots & y_j(k) \end{bmatrix}$$ .....(equation 5.10)

Here, $y_p(q)$ represents GRC of each quality responses, p = 1, 2, 3, . . . j, experiments and q = 1,2, 3, . . . k, quality responses. Values of study here were j = 16 and k = 3.

The correlation matrix coefficient was calculated as follows:

$$R_{jl=}\left(\frac{Cov\left(y_p(q), y_p(l)\right)}{\sigma_{yp}(q) * \sigma_{yp}(l)}\right) q = 1,2,\ldots k;\ l = 1,2,\ldots,k$$

---------- (equation 5.11)

Cov($y_p(q)$, $y_p(l)$ represents the covariance of sequences $y_p(q)$ and $y_p(l)$. $\sigma_{yp}(q)$ is standard deviation of sequence $y_p(q)$ and $\sigma_{yp}(l)$ is standard deviation of sequence $y_p(l)$. The eigen vectors and eigen values were calculated from R_{jl} array as per equation 5.12

$$(R - \lambda_k I_j)\, V_{pk} = 0 \text{----------} \quad \text{(equation 5.12)}$$

Successively, eigenvectors (V_{pk}) and eigenvalues (λ_k) of square matrix R were used to calculate the conflicting principal components (PC's) by using equation 5.13

$$Z_{jk} = \sum_{i=1}^{n} Yj(p) \times Vpk \text{ ----------} \quad \text{(equation 5.13)}$$

Here, Z_{jk} relates to k^{th} PC.

Table 5.5 Eigen analysis of the Correlation Matrix

Eigenvalue	1.6701	0.8409	0.4890
Proportion	0.557	0.280	0.163
Cumulative	0.557	0.837	1.000

Table 5.6 Eigenvectors

Variable	**PC1**	**PC2**	**PC3**
	0.552	-0.654	0.517
	0.657	-0.039	-0.753
	-0.512	-0.755	-0.408

Equal weights are assigned to response variables in GRA may lead to ambiguity in governing the process. PCA method assigns weight fraction for each individual characteristic [83]. For PCA, Eigen values and Eigen vectors of respective PCs were presented in Table 5.5 and 5.6. As shown in Table 5.5 first PC contribution was highest 55.7% for all quality characteristics. Contribution of each response variable was determined for PCA as shown in Table 5.7. Eigen vectors of first PC were squared to determine the relative weights of individual quality characteristic.

Table 5.7 Contribution of variance for first PC response variables.

Response Variable	Contribution
Flexural strength	0.3052
Tensile strength	0.4322
Compressive strength	0.2626

Sample calculation for contribution of response variable:

Flexural strength = $(0.552)^2 = 0.3052$

Tensile strength = $(0.657)^2 = 0.4322$

Compressive strength = $(-0.512)^2 = 0.2626$

GRG and Weighted GRG were calculated using equation 5.8 and 5.9 respectively. Successively according to their statistical values ranking of the experiments was done as depicted in Table 5.8

Table 5.8 GRG and WGRG for experimental results

Experiment No.	GRC			GRG	RANK	WGRG	RANK
1	0.410	0.390	0.643	0.481	13	0.463	13
2	0.387	0.377	0.403	0.389	16	0.387	16
3	0.333	0.333	0.818	0.495	12	0.460	14
4	0.351	0.553	0.338	0.414	15	0.435	15

5	0.481	0.793	0.540	0.605	8	0.632	7
6	0.480	0.806	0.629	0.638	5	0.660	6
7	0.376	0.933	0.687	0.665	4	0.699	3
8	0.427	0.479	0.956	0.621	7	0.589	9
9	0.468	0.347	0.788	0.534	11	0.500	11
10	0.445	0.884	0.373	0.567	9	0.616	8
11	0.698	0.919	0.427	0.682	3	0.723	2
12	0.771	0.752	0.384	0.636	6	0.661	5
13	0.421	0.584	0.631	0.545	10	0.547	10
14	0.498	0.524	0.333	0.452	14	0.466	12
15	1.000	1.000	0.655	0.885	1	0.909	1
16	0.771	0.462	1.000	0.744	2	0.698	4

GRCs were calculated as per equation 5.7 and average of three GRC were used to calculate the GRG. Higher the GRG, better the overall performance of that set of process parameters as depicted in experiment number 15.

Sample calculation for experiment 1 GRG= 1/3 (0.410+0.390+0.643) = 0.481

WGRG was then calculated by assigning weights to each response variable.

Sample calculation for experiment 1 WGRG = (0.410*0.3052 + 0.390*0.4322 + 0.643*0.2626) = 0.463

The experiments were ranked according to their corresponding values of GRG and WGRG respectively.

5.5 Response variable objective optimization

Table 5.9 S/N ratio results using L16 OA

S/N Ratio responses		
FS	**TS**	**CS**
34.363	30.596	28.323
34.233	30.542	27.797
33.868	30.341	28.511

34.000	31.034	27.528
34.683	31.352	28.155
34.678	31.364	28.303
34.170	31.462	28.379
34.449	30.871	28.611
34.632	30.410	28.485
34.535	31.427	27.687
35.254	31.453	27.879
35.373	31.312	27.730
34.420	31.090	28.306
34.744	30.975	27.506
* 35.635	* 31.504	28.339
35.373	30.827	* 28.637
A4B3C2D4	A4B3C2D4	A4B4C1D3

Optimized setting for every single objective was found was shown in Table 5.9.

The highest value for S/N ratio for flexural strength was 35.635, for tensile strength 31.504 and for compressive strength 28.637 respectively.

Nozzle diameter (ND) at level 4, print speed (PS) at level 3, layer thickness (LT) at level 2, width of each layer (DL) at level 4 was found to be highest for achieving good flexural as well as tensile strength.

Nozzle diameter (ND) at level 4, print speed (PS) at level 4, layer thickness (LT) at level 1, width of each layer (DL) at level 3 was found to be highest for achieving good compressive strength.

Table 5.10 Response table for average values of GRG and WGRG

AVG GRG

	LEVEL 1	LEVEL 2	LEVEL 3	LEVEL 4
ND (A)	0.445	0.632	0.605	*0.657
PS (B)	0.541	0.511	*0.682	0.604
LT (C)	*0.636	0.629	0.525	0.548
DL (D)	0.558	0.559	0.603	*0.618

AVG WGRG

LEVEL 1	LEVEL 2	LEVEL 3	LEVEL 4
0.358	0.645	0.625	*0.655
0.535	0.532	*0.698	0.596
0.636	*0.647	0.509	0.574
0.572	0.561	0.601	*0.626

An average value of GRG and WGRG of each input parameter at different levels is calculated in Table 5.10 determines means of GRG and W-GRG for unique optimal conditions.

Sample calculation of GRG for nozzle diameter at level 4:

AVG GRG = 1/4 (0.545 + 0.452 + 0.885 + 0.744) = 0.657

Sample calculation of WGRG for print speed at level 3:

AVG WGRG = 1/4 (0.460 + 0.699 + 0.723 + 0.909) = 0.698

Highest values of average WGRG were 0.655, 0.698, 0.647 and 0.626 for nozzle diameter (ND), print speed (PS), layer thickness (LT) and width of each layer (DL) respectively. Optimum set of input parameters can be concluded by the Table 5.10 as A4B3C2D4 namely nozzle diameter 0.3 mm, printing speed 60 mm/s, layer height 0.2 mm, width of each layer 0.7 mm.

5.6 Confirmatory experiment

Optimum parametric combination was found to enhance the mechanical properties of FDM process using GRA-PCA approach.

Predicted value of WGRG was calculated by equation 5.14

$$^{\gamma}pred = {}^{\gamma}a + \sum_{i=1}^{n} ({}^{\gamma}i - {}^{\gamma}a)\ )$$ ---------- (equation 5.14)

Sample calculation of predicted value of WGRG:

$^{\gamma}i$	$^{\gamma}i$-$^{\gamma}a$
0.570588	0.084
0.590132	0.108
0.591289	0.056
0.590132	0.036

$^{\gamma}a = 0.585535$ and $\sum_{i=1}^{n} ({}^{\gamma}i - {}^{\gamma}a)\ ) = 0.284$

Where $^{\gamma}pred$ is predicted value of WGRG, $^{\gamma}a$ is average value of WGRG and $^{\gamma}i$ is average WGRG at optimum value of i^{th} input parameter and n are total number of significant input parameters**.**

Table 5.11 Comparison of Experimental confirmation

	Optimal condition	Predicted Value	Confirmatory Experiment Value
Flexural strength (Mpa)	60.5		60.7
Tensile strength (Mpa)	37.6		37.7
Compressive strength (Mpa)	26.12		26.1
Optimal Condition	A4B3C2D4		A4B3C2D4
WGRG		0.869	0.910

$^{\gamma}$pred value was observed as 0.869. Successively experimental verification was carried out for optimum combination of input parameters. Table 5.11 depicts confirmatory experimental values for flexural strength 60.7 Mpa, tensile strength 37.7 Mpa and compressive strength 26.1 Mpa respectively which shows 4.71 % improvement in WGRG was observed. The optimized parameters suggested by the DNN model through physical experimentation, confirming improvements in the mechanical properties.

5.7 Results and discussion

Present study proposed a DNN strategy to predict the best parametric combination with optimized mechanical properties (Flexural, tensile and compressive strength) of printed parts. In the present research, less analysed design variables parameters like nozzle diameter, width of print line and layer thickness, print speed are considered as input parameters with their levels values that are trained to the proposed system. Adhering to ASTM standards with predefined dimensions total 256 experiments have been carried for each output, in which 204 result data used for training and 52 for testing the model using PYTHON programming language. Subsequently, Prediction accuracies after 500 epochs 0.8654 were obtained on trained data and 0.8846 achieved for test data. RMSE value 0.3396 and R2 value 0.8796 is validated by relating the performance with existing models. Hence, the efficient outcomes of the developed model have been verified by

gaining the best combination of process parameters and Taguchi analysis interpreted their influence on the flexural, tensile and compressive strength of FDM printed parts.

5.7.1 Taguchi Analysis

5.7.1.1 Flexural strength analysis

Table 5.12 Response table for means

Level	ND	PS	LT	DL
1	50.80	53.24	55.76	54.17
2	53.07	53.39	56.22	53.69
3	55.95	54.72	52.66	53.89
4	56.60	55.08	51.78	54.68
Delta	5.79	1.83	4.44	0.99
Rank	1	3	2	4

Table 5.13 Response table for S/N ratio

Larger is better

Level	ND	PS	LT	DL
1	34.12	34.52	34.92	34.66
2	34.50	34.55	34.98	34.59
3	34.95	34.73	34.42	34.61
4	35.04	34.80	34.28	34.74
Delta	0.93	0.27	0.70	0.15
Rank	1	3	2	4

The mean effect plot in Figure 5.5 illustrates the effects of input variables on the response variable, showing both the mean values and signal-to-noise (S/N) ratios. From this plot, we can observe the impact of each input parameter on the response variable, providing insights into their relative importance. Table 5.12 presents the rank-wise influential parameters based on their effects on the response variable. The parameters are ranked in terms of their impact on the response variable as nozzle diameter, layer thickness, print speed, width of print layer respectively. The analysis indicates that the nozzle diameter has a significant impact on the response variable, particularly flexural strength. An increment in the nozzle diameter range leads to a drastic increase in flexural strength. The layer thickness is identified as the second most influential parameter affecting

flexural strength. Lower layer thickness and higher print speed contribute to higher flexural strength. However, a decrement in layer thickness from 0.2 to 0.3 mm results in a drop in part strength. This implies that optimizing the layer thickness within a specific range is crucial for achieving the desired strength characteristics. The analysis indicates that print speed also plays a significant role in determining flexural strength. Higher print speeds contribute to higher flexural strength, suggesting that adjusting the print speed parameter can impact the mechanical properties of the printed parts. While the width of each print layer is included as a parameter, the analysis suggests that it does not have a dominant effect on flexural strength. This indicates that variations in the width of each print layer may not significantly influence the strength characteristics of the printed parts compared to other parameters.

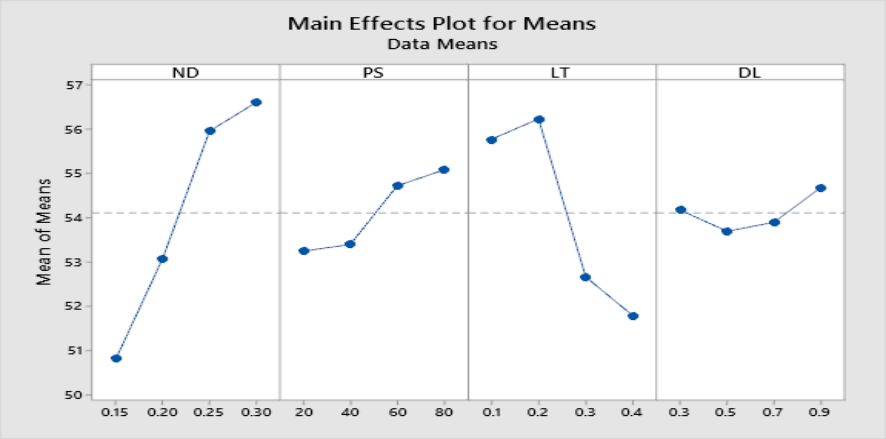

(a)

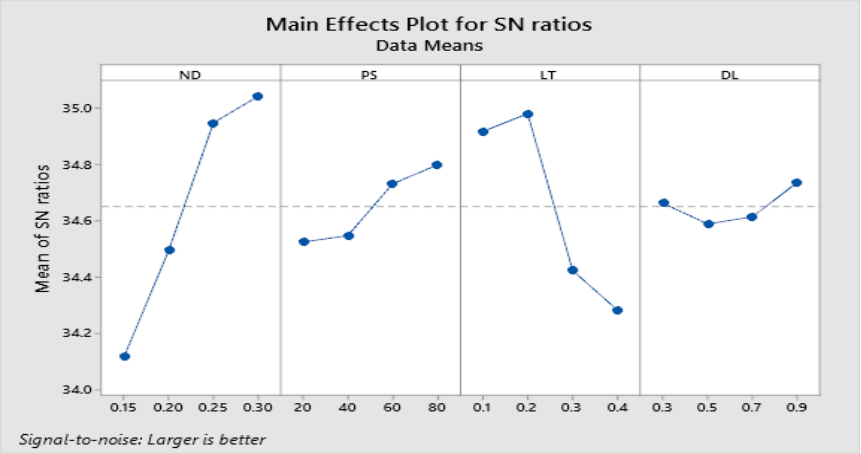

(b)

Figure 5.5 Main effect plots for (a) means (b) SN ratios of FS

5.7.1.2 Tensile strength analysis

Table 5.14 Response table for means

Level	ND	PS	LT	DL
1	34.01	34.95	35.76	35.86
2	36.58	35.83	36.16	35.46
3	36.15	36.23	34.09	35.47
4	35.81	35.53	36.54	35.76
Delta	2.57	1.28	2.45	0.40
Rank	1	3	2	4

Table 5.15 Response table for S/N ratio

Larger is better

Level	ND	PS	LT	DL
1	30.63	30.86	31.06	31.09
2	31.26	31.08	31.16	30.99
3	31.15	31.17	30.65	30.99
4	31.08	31.01	31.25	31.06
Delta	0.63	0.31	0.60	0.10
Rank	1	3	2	4

Figure 5.6 depicts for tensile strength Nozzle diameter is most influential parameter and then after layer thickness, print speed, width of each print line respectively. Tensile strength increased by raising the value of nozzle diameter from 0.15 to 0.2 mm and

further decreased. Layer thickness is identified as the second most influential parameter affecting tensile strength. The analysis reveals a significant increase in tensile strength as the layer thickness value transitions from the low range to the higher range. However, there is a decrease in tensile strength observed when the layer thickness falls from 0.2 to 0.3 mm. Tensile strength increased from varying print speed from 20 to 60 mm/s while distance of each print line has no significant effect.

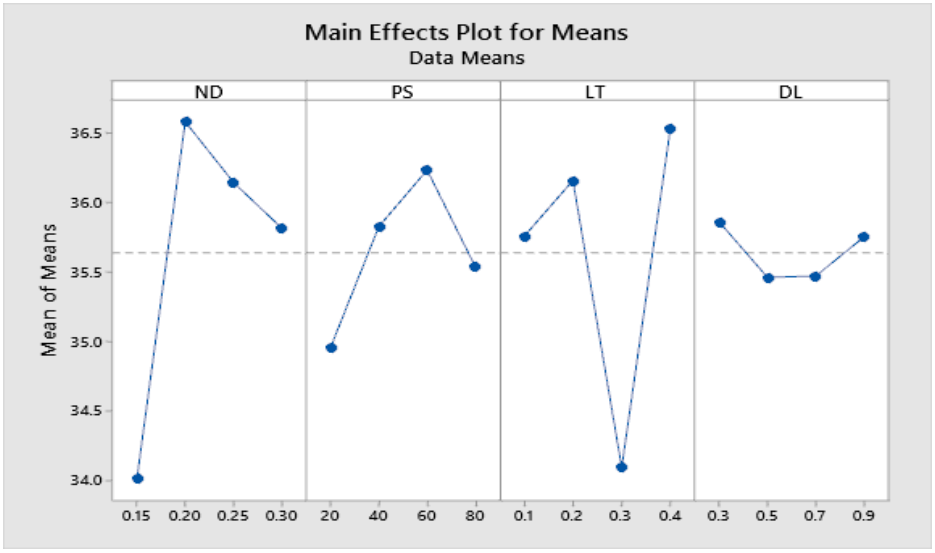

(a)

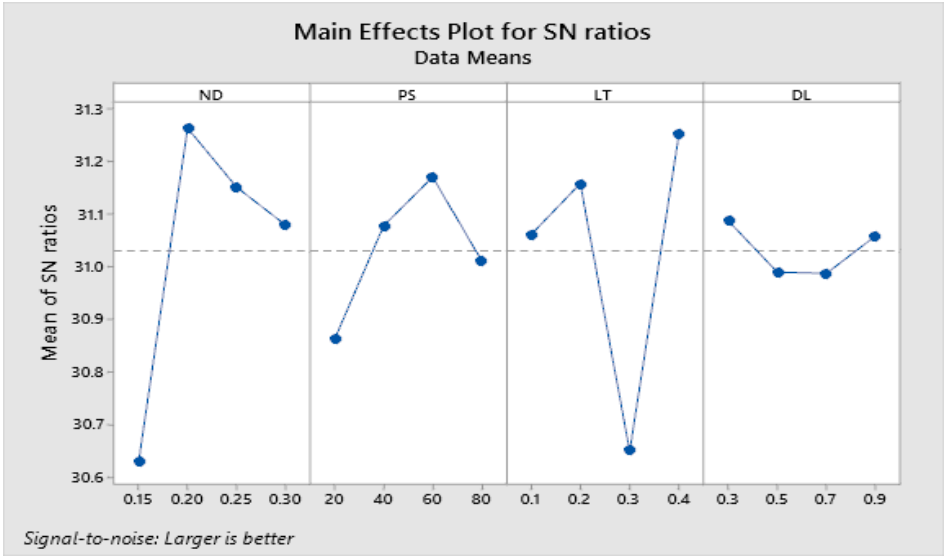

(b)

Figure 5.6 Main effect plots for (a) means (b) SN ratios of TS

5.7.1.3 Compressive strength analysis

Table 5.16 Response table for means

Level	ND	PS	LT	DL
1	25.26	26.05	25.97	25.10
2	26.19	24.63	24.76	25.57
3	24.98	25.56	25.97	25.87
4	25.34	25.53	25.07	25.23
Delta	1.21	1.43	1.21	0.77
Rank	2	1	3	4

Table 5.17 Response table for S/N ratio

Larger is better

Level	ND	PS	LT	DL
1	28.04	28.32	28.29	27.98
2	28.36	27.82	27.87	28.15
3	27.95	28.15	28.28	28.25
4	28.07	28.13	27.98	28.03
Delta	0.42	0.49	0.41	0.26
Rank	2	1	3	4

Figure 5.7 depicts for compressive strength print speed is dominant parameter and nozzle diameter, layer thickness, width successively. The analysis identifies print speed as the dominant parameter affecting compressive strength. It reveals a decrease in compressive strength as print speed increases. This suggests that higher print speeds may negatively impact the structural integrity and compressive strength of printed parts. Part strength shows highest at the nozzle diameter at 0.2 mm, layer thickness at 0.1 and 0.3 mm. While included as a parameter, the width of each print layer shows a relatively lower influence on compressive strength compared to print speed, nozzle diameter, and layer thickness. Nonetheless, the analysis suggests that optimizing the width of each print layer, particularly at a value of 0.7 mm, can contribute to improved compressive strength characteristics.

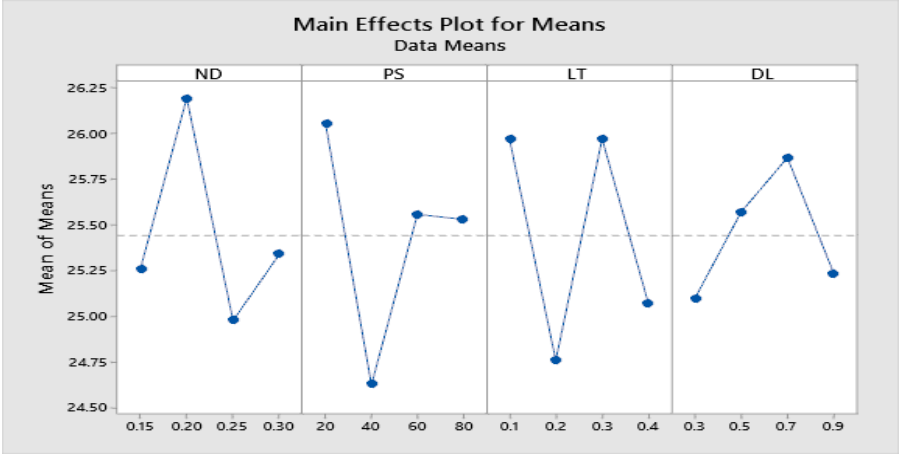

(a)

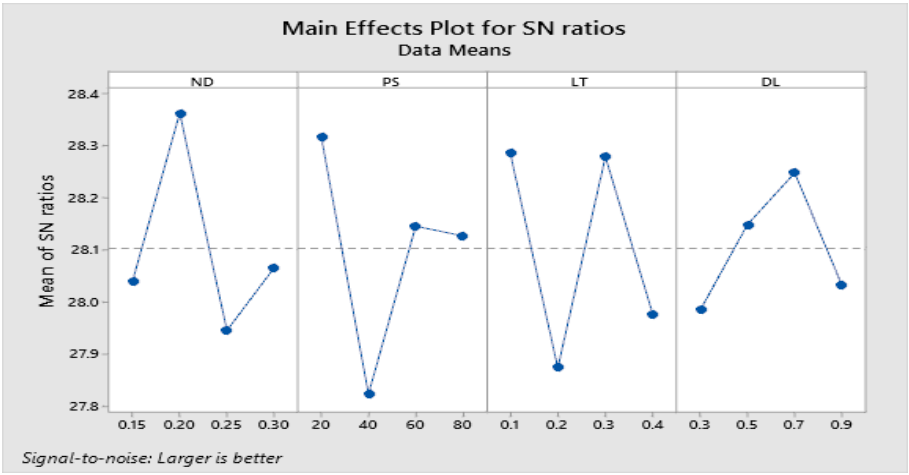

(b)

Figure 5.7 Main effect plots for (a) means (b) SN ratios of CS

5.7.2 Probability plots

Normally probability plots are the graphical presentation to interpret the data set is distributed normally or not. Outlier detection from normal distribution can be significantly tested by the Anderson Darling (ADT) test. In a probability plot, each data point from the sample is plotted against its corresponding percentile (probability) within the dataset. The percentile represents the proportion of data points in the sample that are less than or equal to the value being plotted. This creates a scatter plot where each point represents a data value and its associated percentile.

The probability plot often includes curved blue lines, which represent the approximate 95% confidence intervals for a normal distribution. These lines help assess the goodness of fit of the data to a normal distribution. Points falling within these confidence intervals indicate agreement with the expected distribution, while points outside the intervals suggest deviations from normality. Points that fall outside the confidence intervals, particularly in the tails of the distribution, represent extreme values or outliers in the dataset. These outliers may indicate deviations from the expected distribution or the presence of unusual data points that warrant further investigation.

By examining the arrangement of points relative to the confidence intervals and the overall pattern of the plot, analysts can assess the distributional characteristics of the dataset. A close alignment of points with the confidence intervals suggests that the data closely follows the expected distribution, while deviations may indicate departures from normality or other distributional assumptions.

From Figure 5.8 it was evident that ADT values are in lower range .P value for flexural strength was 0.178, for tensile strength 0.095 and 0.140 for compressive strength successively. P-values were greater than 0.05 depicts the normal distribution was followed by the data set. Also all the data points lay beside the fitted line. Hence it was feasible to perform optimization and analysis on this data further.

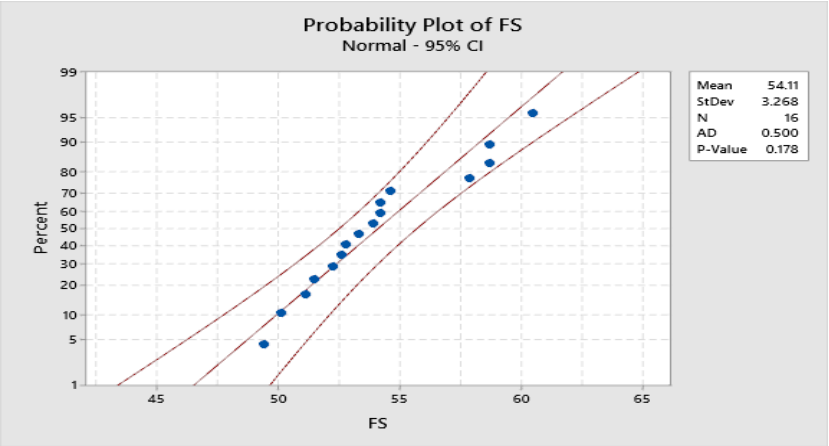

(a)

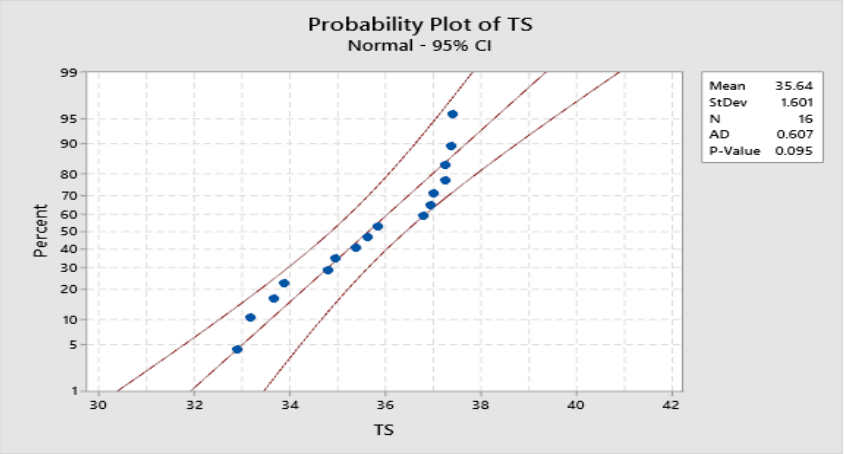

(b)

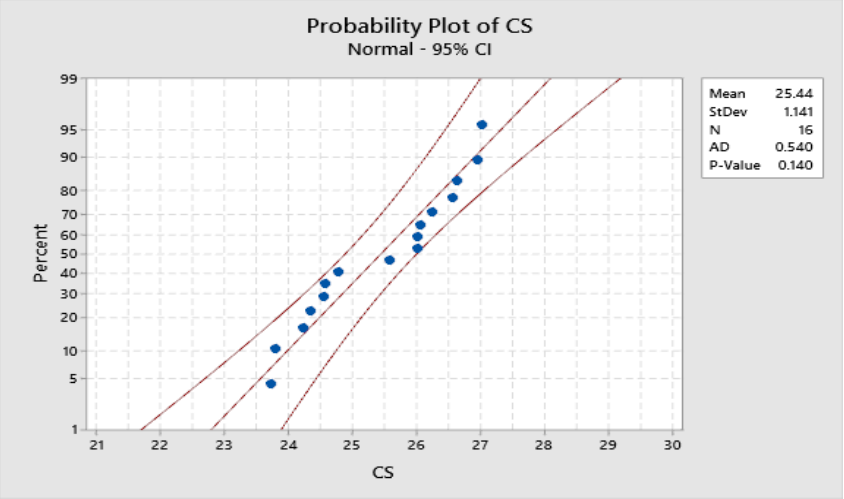

(c)

Figure 5.8 Normal probability plots for mechanical strength (a) Flexural (b) Tensile (c) Compressive

5.7.3 Contour plots

Figure 5.9 depicts the contour maps which visualize the correlation between two continuous variables and one dependent variable.

Figure 5.9 (a) illustrates the impact of two influential parameters, nozzle diameter and layer thickness, on flexural strength. It's evident from the plot that a higher range of

nozzle diameter (0.25 to 0.3 mm) and a lower layer thickness (0.1 to 0.2 mm) lead to higher flexural strength.

When the nozzle diameter increases, fewer extruded strands are needed to fill a given specimen width. This results in wider extruded lines per layer. While wider lines reduce the number of intralayer bonds, they can actually enhance interstrand interaction, leading to stronger bonds. The increased spacing between strands within a layer due to wider extruded lines facilitates better interlayer bonding, which contributes to overall part strength.

Flexural strength, which measures a material's resistance to deformation under bending, is influenced by layer thickness as well. Thicker layers tend to produce rougher surface finishes and weaker interlayer bonding compared to thinner layers. Therefore, thinner layers often result in better flexural strength due to improved interlayer adhesion and surface quality. Poor interlayer bonding can lead to delamination between layers and reduced flexural strength. Additionally, thicker layers may have more pronounced layer lines, which can act as stress concentrators and reduce flexural strength.

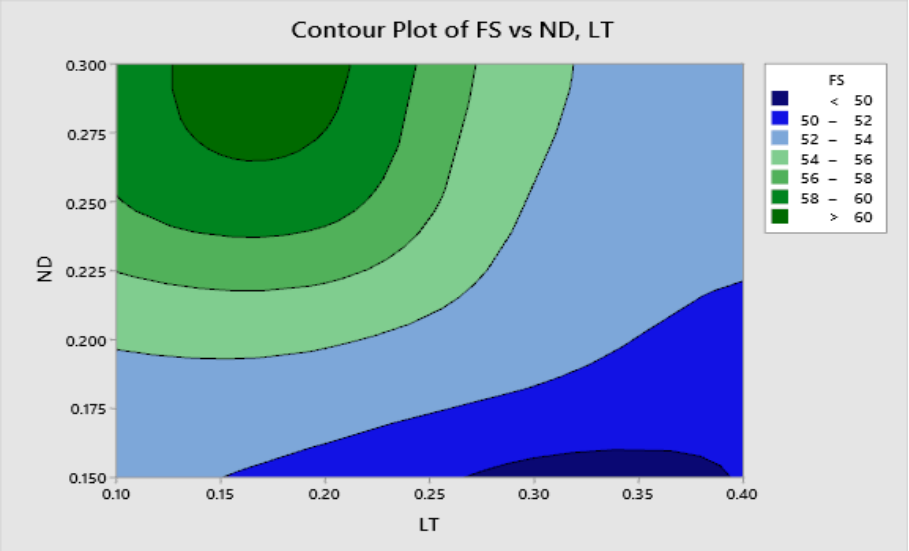

(a)

Figure 5.9 (b) shows the effect of most influential parameters nozzle diameter and layer thickness on tensile strength. Here it is evident that higher range of nozzle diameter 0.2 to 0.3 mm and lower layer thickness 0.1 to 0.2 mm results in higher tensile strength.

The observed trend can be attributed to several factors. Firstly, the larger nozzle hole allows for greater overlap between raster or infill lines, resulting in stronger interfacial bonding. When raster or infill lines overlap more extensively, they create a denser and more interconnected structure, enhancing horizontal bonds and overall part strength.

Conversely, smaller nozzle holes lead to barely touching or minimal overlap between infill lines within plane, weakening horizontal bonds and reducing interfacial bonding. This can result in a less robust structure and lower mechanical properties. Moreover, by lowering the ratio of layer thickness to nozzle size, it is possible to enhance bonding between layers and reduction in voids and interstitial gaps as well to minimize anisotropy. This optimization strategy promotes better adhesion between adjacent layers, resulting in improved tensile strength.

Tensile strength, which exhibits capability of material to withstand maximum stress before breaking under tension, is influenced by layer thickness. Thicker layers typically yield reduced tensile strength compared to thinner layers due to several reasons. Firstly, thicker layers create larger interfaces between adjacent layers, which can lead to weaker interlayer bonding and lower tensile strength. Additionally, thicker layers may contain more voids or trapped air pockets within the material, acting as defects that can compromise tensile strength.

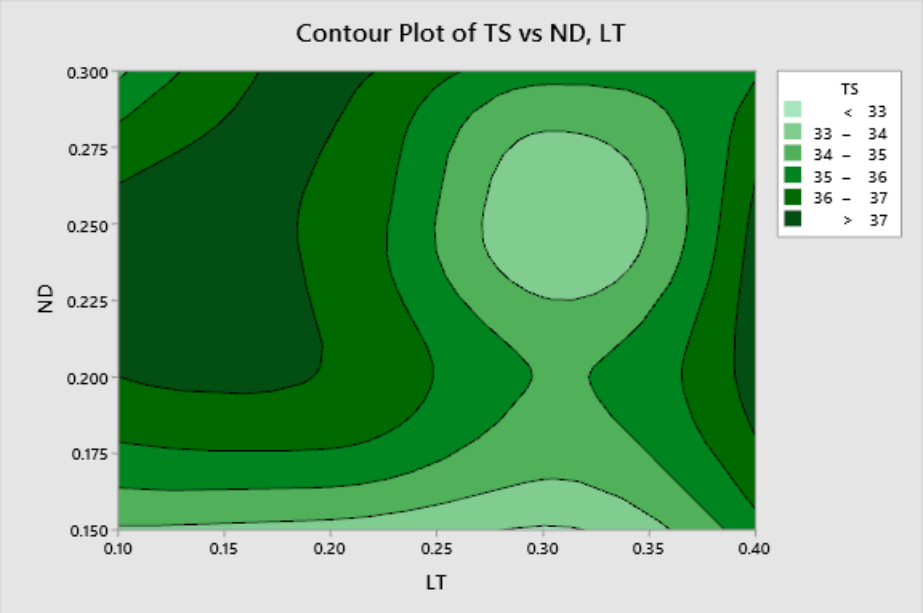

(b)

Figure 5.9 (c) shows the effect of most influential parameters print speed and nozzle diameter on compressive strength. Here it is evident that higher range of nozzle diameter 0.15 to 0.2 mm and higher print speed 60 to 80 mm/s results in higher compressive strength.

Finer layer resolution achieved with smaller nozzle diameters can contribute to higher compressive strength in FDM-printed parts. Smaller nozzles allow for the deposition of thinner layers, resulting in smoother surfaces and better interlayer bonding. This improved bonding between layers enhances the overall structural integrity of the part, making it more resistant to compressive forces. Factors such as infill pattern, infill density, and print orientation may have graceful traces on compressive strength.

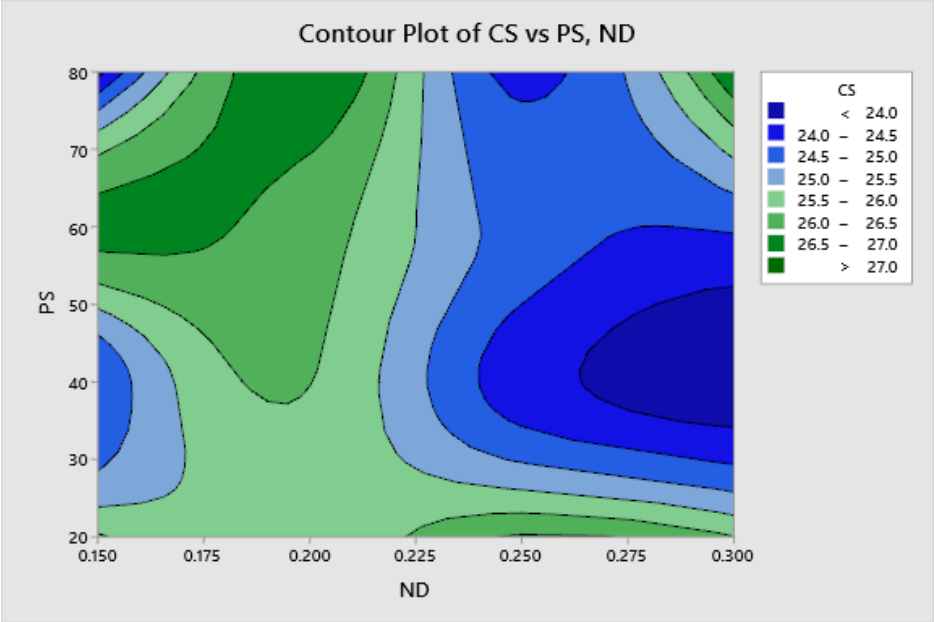

(c)

Figure 5.9 Contour plots for mechanical strength (a) Flexural (b) Tensile (c) Compressive

After applying the optimized parameters provided by the DNN model, the results from the experiments were compared with the model's predictions. Accuracy of the DNN model was assessed by calculating the difference between predicted and experimental results. A close match indicates that the model accurately optimized the parameters. It has been analysed whether the optimized parameters consistently yield improved performance across multiple experiments.

5.8 State of art of comparison

B.M. Castro et al. [25] utilized 3D printing scheme using ML web-based pharmaceutical software for pharmaceutical application which helps to improve the fabrication procedure. But it lacks in predicted key fabrication parameters with low accuracies of 76% and 67% for the printability and the filament characteristics. Proposed model of Adaptive fuzzy logic by R.K Gupta et al [13] error rate recorded during the design

process. Grace et al [48] proposed autonomous correction structure but the design process is complex. Mohamed et al [24] proposed Dimension optimization of modeling scheme and Artificial neural network (ANN) Optimization Definitive screening design (DSD). This study confirmed the capability of an integrated DSD and the ANN for optimizing AM conditions to avoid problems typically encountered in multiple experiments. Error recorded in Predicted and actual results 8.7%.Kaushik Yanamandra, et al [53] utilized Imaging strategy where high similarity rates was recorded for original and reconstruction model but it takes more duration to execute the function. M. Samie Tootooni et al [51] utilized Laser-Scanned 3D Point Cloud Data using ML. Here Sampling was done with Sparse Representation-based Classification (SRC), k-Nearest Neighbors (kNN), Naïve Bayes (NB), Neural Network (NN), Support Vector Machine (SVM), Decision Tree (Tree) but required large real time data. Scanning an entire part, which can be time consuming and inefficient. For sample size 500 the maximum accuracy was 84.71%. John M. Gardner et al [52] implemented Image classification; here experiments were performed to improve the part quality in better extent. This work focuses on using the tool to optimize for visible print flaws, but other metrics, such as road width and dimensional stability, could also be addressed assuming the effects can be measured locally. Correlations between local flaws and overall part performance, such as mechanical properties can be addressed. Ashutosh Kumar Gupta et al. [27] investigated the effect of process parameters on dimensional accuracy of FDM printed parts and results show that ANN model predicts the results with very less error in comparison of existing models. Jayant Giri et al. [28] optimized critical process parameters using ANN, Mohammad Shirmohammadi et al. [29] investigated the effect of FDM 3D printing process parameters on the surface roughness of printed parts using ANN Hybrid algorithm and RSM. Jingchao Jiang et al [8] proposed DL model where Different complex problems are studied with short duration and wide range of accuracy. Accuracy rate recorded was 83%. Proposed using DNN is trained with less analysed input variables as nozzle diameter, width of each print line helped to gain better result 88.64% in terms of prediction accuracy by detecting the finest combination in the printing layer.

Table 5.18 State of art of comparison

Reference	Methods	Merits	Limitations
Jianjing Zhang et al. [40]	Deep learning (LSTM)	Layer-wise Relevance Propagation (LRP) was found useful for interpreting the prediction result.	Predictive model RMSE values are at satisfactory levels.
Grace et al [48]	Autonomous correction structure using computer vision and deep learning	Attain high performance like accuracy and fast response	Design process is too complex
M. Samie Tootooni et al [51]	Sparse Representation-based Classification (SRC), k-Nearest Neighbors (kNN), Naïve Bayes (NB), Neural Network (NN), Support Vector Machine (SVM), Decision Tree (Tree)	Utilized Laser-Scanned 3D Point Cloud Data using ML.	Scanning an entire part, which can be time consuming and inefficient. For sample size 500 the maximum accuracy was 84.71%.
Jingchao Jiang et al [8]	DL model	Different complex problems are studied with short duration and wide range of accuracy.	Accuracy rate recorded was 83%.
B.M. Castro et al. [25]	3D printing scheme using ML for pharmaceutical application	Helps to improve the fabrication procedure	It lacks in predicted key fabrication parameters with low accuracies of 76% and 67% for the printability and the filament characteristics.
R.K Gupta et al [13]	Adaptive fuzzy logic	Error rate recorded during the design process and attained high accuracy	Design process is complex
John M. Gardner et al [52]	Image classification	This work focuses on using the tool to optimize for visible print flaws	Correlations between local flaws and overall part performance, such as mechanical properties can be

			addressed.
Ashutosh Kumar Gupta et al. [27]	ANN model	Effect of process parameters on dimensional accuracy of FDM printed parts visualised. Results show that ANN model predicts the results with very less error in comparison of existing models.	Prediction on unseen data achieving different aims could be concentrated due to flimsy nature of FDM printed parts.
Kaushik Yanamandra [53]	Imaging strategy	High similarity rates was recorded for original and reconstruction model	Takes more duration to execute the function.
Ru Chen et al [46]	FDM based 3D printing design	used to enhance the 3D printing parts by combining the in-situ strain calculation	But the fabrication process is difficult
Mohamed et al [24]	Dimension optimization of modeling scheme and ANF	Study confirmed the capability of an integrated DSD and the ANN for optimizing AM conditions to avoid problems typically encountered in multiple experiments.	Error recorded in Predicted and actual results 8.7%. Design properties are not suitable for ANF module
Proposed	Deep learning model	It has helped to gain better result by detecting the finest connection lines in the printing layer. Also faults were detected with good accuracy	This study limits its use as standard test parts fabrication were done adhering to ASTM standards.

CHAPTER 6

CONCLUSION AND FUTURE SCOPE

By including a comprehensive summary of results, conclusive remarks, and thoughtful recommendations for future work, this chapter aims to provide a comprehensive overview of the study's findings and contribute to the advancement of knowledge in the field of AM and process optimization.

6.1 Brief

FDM is a model of AM which uses layer by layer-based methodology to fabricate a component. Today in the digital manufacturing era FDM process is widely used as it can construct intricate and complex part geometries in short time as compared to conventional manufacturing, its simplicity and economical bahaviour. Despite of such advantages, literature argued various machine learning approaches adopted to increase the performance of FDM addressing the issues of irregularities in part properties, accuracy, and reliability due to challenging task of best parametric selection. In this context, the present study proposed a DNN strategy to predict the best parametric combination with optimized mechanical properties of printed parts. In the present research, less analysed design variables parameters like nozzle diameter, width of print line and layer thickness, print speed are considered as input parameters with their levels values that are trained to the proposed system. Adhering to ASTM standards with predefined dimensions total 256 experiments have been carried for each output, in which 204 result data used for training and 52 for testing the model using PYTHON programming language. Subsequently, the proposed model has gained the accuracy of 88.46% and RMSE value 0.3396 is validated by relating the performance with existing models. Hence, the efficient outcomes of the developed model have been verified by gaining the best combination of process parameters and ANOVA analysis interpreted their influence on the tensile and compressive strength of FDM printed parts.

Case study utilized which aims to optimize multiple responses of FDM process of PLA printed parts through best combination of selected design variables using Grey regression Taguchi based method associated with PCA. Taguchi L16 array of specific subset of input parameters combinations was utilized to conduct the experimentation. Tensile strength, compressive strength and flexural strength were analysed by multi optimization adopting Taguchi and Grey relation analysis combined with PCA. Validation of proposed study was carried out with experimental confirmation to find out significance of optimized parameters to enhance the mechanical behaviour of printed parts.

6.2 Summary of results

- Though evidently several researches have been carried out regarding optimisation of input parameters to optimize the mechanical properties of FDM printed parts, eventually various studies reported the flimsy nature of 3D printed materials which should be taken care of.
- AM mechanism is the process of fabrication, which includes the connection of materials commonly layer-by-layer to generate the structure from FDM. Advantages of this technology involve new design structures, low economic volumes, etc. Moreover, the AM mechanism includes numerous types of machinery to manufacture flexible materials. Nevertheless, during the 3D printing process, if the printing parameter selection at the same time is mismatched, the raise of faulty connection is tremendously affecting the entire performance. Therefore, in this research, a DL model was developed for detecting the best connection between process parameters.
- For example, high dimensional accuracy, high surface finish and better tensile strength can be achieved by setting low layer thickness but can affect the compressive strength adversely. Print speed affects the mechanical properties; build time affects the overall cost of product. Multi response optimisation of FDM process based PLA components was investigated using design variables as nozzle diameter, print speed, layer thickness and width of each print layer

with the selection of level values based on previous literature and customized 3D printed FDM machine.

- Experimentation carried out with model architecture by varying the number of hidden layers, neurons per layer, and activation functions to find the configuration that yields the best performance. After tuning hyperparameters such as learning rate, batch size; prediction accuracies after 500 epochs 0.8654 were obtained on trained data and 0.8846 achieved for test data. The training accuracy was not excessively high, which indicates that the model has not memorized the training data or overfit to it. A testing accuracy of 88.46% was slightly higher than the training accuracy, which was generally an approving sign. This recommends that the model is fit for use on the training dataset and capability of generalizing well to unseen samples. It interprets that the model is well-suited for predicting the connection status based on the provided input parameters, and it can be deployed with confidence for future predictions.
- RMSE value for tested model observed was 0.3396 and R^2 value 0.8796 which validates the performance of model and can predict the results under random circumstances.
- The rank-wise influential parameters based on their effects on the response variable were nozzle diameter, layer thickness, print speed, width of print layer respectively for flexural and tensile strength analysed by Taguchi analysis. For compressive strength print speed is dominant parameter and nozzle diameter, layer thickness, width successively.
- From probability plots it was evident that ADT values are in lower range .P value for flexural strength was 0.178, for tensile strength 0.095 and 0.140 for compressive strength successively. P-values were greater than 0.05 depicts the normal distribution was followed by the data set. Also all the data points lay beside the fitted line. Hence it was feasible to perform optimization and analysis on this data further.
- To investigate the relationship between nozzle diameter, layer thickness and flexural strength contour plots were mapped which revealed that a higher range of nozzle diameter (0.25 to 0.3 mm) and a lower layer thickness (0.1 to

0.2 mm) lead to higher flexural strength. When the nozzle diameter increases, fewer extruded strands are needed to fill a given specimen width. This may results in wider extruded lines per layer. While wider lines reduce the number of intralayer bonds, they can actually enhance interstrand interaction, leading to stronger bonds. Thinner layers often result in better flexural strength due to improved interlayer adhesion and surface quality.

- In the context of impact of nozzle diameter and layer thickness on tensile strength; the higher range of nozzle diameter 0.2 to 0.3 mm and lower layer height 0.1 to 0.2 mm showed higher tensile strength. Larger nozzle hole allows for greater overlap between raster or infill lines, resulting in stronger interfacial bonding. When raster or infill lines overlap more extensively, they create a denser and more interconnected structure, enhancing horizontal bonds and overall part strength. Thicker layers create larger interfaces between adjacent layers, which may lead to weaker interlayer bonding and lower tensile strength.
- The effect of most influential parameters print speed and nozzle diameter on compressive strength depicted that higher range of nozzle diameter 0.15 to 0.2 mm and higher print speed 60 to 80 mm/s results in higher compressive strength. Finer layer resolution achieved with smaller nozzle diameters may contribute to higher compressive strength in FDM-printed parts.
- Tensile strength, compressive strength and flexural strength were analysed by multi optimization using Taguchi and Grey relation analysis associated with PCA. PCA assigns weight to each measurable significant response which affects the GRG. PCA determined the contribution of tensile strength (43.22%), flexural strength (30.52%) and compressive strength (26.26%) respectively.
- WGRG values depicted the most influential factor as print speed followed by nozzle diameter, layer thickness and width of each print layer successively.
- Optimum combination of input parameters was analysed by GRA associated with PCA approach as nozzle diameter 0.3 mm, print speed 60 mm/s, layer thickness 0.2 mm and width of each layer 0.9 mm which was classified into

class 1 in DNN. Confirmatory experimental values for flexural strength were 60.7 Mpa, tensile strength 37.7 Mpa and compressive strength 26.1 Mpa which demonstrated 4.71 % improvement in predicted WGRG.

- GRA associated with PCA is graceful optimisation technique which can be used to determine best combination of design variables of FDM process to improve significant quality responses. GRA associated with PCA method fits for use to optimize multiple response characteristics and can be further utilized for guidelines in design for manufacturing (DFM) for practical applications.
- By establishing a robust interface between AM and DL, we have shown that machine learning models can effectively predict and optimize key parameters influencing mechanical properties such as tensile, compressive, and flexural strengths. This approach not only improves the quality and consistency of FDM-printed parts but also paves the way for the use of intelligent systems to automate and enhance additive manufacturing processes. Through continuous learning from experimental data, the model offers real-time adaptability, reducing trial-and-error in parameter selection and enhancing the efficiency of the FDM process.
- The developed deep learning model successfully performed fault detection and behaviour analysis during the FDM process, providing a substantial advancement over traditional methods. The model was able to identify potential faults and deviations in the manufacturing process in real-time, which helped to mitigate errors and reduce material wastage. By training the model on a comprehensive dataset, it achieved high accuracy in detecting faults and predicting the behaviour of the system, which translated into improved part quality and consistency. This optimized model opens new avenues for deploying smart monitoring systems in FDM processes, which can self-correct and ensure reliable production of high-quality parts.
- The results obtained from the optimized deep learning model were compared with existing optimization techniques, including traditional statistical methods and machine learning approaches. The deep learning model outperformed these methods in terms of prediction accuracy, mechanical strength

optimization, and control of overflow rates. In particular, the optimized parameters yielded significant improvements in tensile, compressive and flexural strength, enhancing prediction accuracy compared to traditional approaches. This comprehensive comparison highlights the superiority of deep learning-based optimization for FDM, offering a more accurate and efficient approach to achieving desired mechanical properties in printed parts.

6.3 Limitations and future scope

The model is expected to achieve higher prediction accuracy as more data is fed into it. This indicates that the model has the capability to learn from a large dataset and make more accurate predictions. The model can be applied to analyse and optimize other mechanical properties beyond those studied in the current research. This suggests the versatility and scalability of the model for addressing different objectives and requirements.

One limitation mentioned is the need for a large amount of data to accurately train and process the neural network model. This could be challenging and resource-intensive, particularly in cases where obtaining sufficient data may be difficult or expensive.

GRA associated with PCA is graceful optimisation technique which can be used to determine best combination of design variables of FDM process to improve significant quality responses. GRA associated with PCA method fits for use to optimize multiple response characteristics and can be further utilized for guidelines in design for manufacturing (DFM) for practical applications.

This study limits its use as standard test parts fabrication were done adhering to ASTM standards. In futuristic direction the optimum combination of FDM process design variables can be used to build smart manufacturing based real time components using highly customized 3D printers. The model can be further optimized and tuned by adjusting parameters such as the number of neurons and layers, activation functions, optimizers, dropouts, normalization techniques, and batch size.

Ongoing refinement and improvement of the model can enhance performance. Depending on the specific objectives of an application, the model can be customized and fine-tuned to achieve different aims, such as improving part quality characteristics, reducing build time, or minimizing costs. This highlights the adaptability and flexibility of the model for various applications. The study suggests the integration of other artificial intelligence (AI) techniques such as cloud computing, big data analytics and Internet of Things (IoT) technologies. This indicates a broader scope for future research and potential synergies between different AI methodologies.

REFERENCES

1) V. Chowdary Boppana and Fahraz Ali, "Improvement of tensile strength of fused deposition modelling (FDM) part using artificial neural network and genetic algorithm techniques", International Journal of Industrial Engineering and Operations Management (2023), Emerald Publishing Limited, https://doi.org/10.1108/IJIEOM-01-2023-0006.

2) A.Karad, P. Sonawwanay, "Experimental study of effect of infill density on tensile and flexural strength of 3D printed parts", Journal of Engineering and Applied Science (2023) 70:104, https://doi.org/10.1186/s44147-023-00273-x

3) Eujin Pei, Alain Bernard, Dongdong Gu, Christoph Klahn, "Handbook of Additive Manufacturing", https://doi.org/10.1007/978-3-031-20752-5

4) W. Lao, M. Li, T.N. Wong, M.J. Tan, and T. Tjahjowidodo, "Improving surface finish quality in extrusion-based 3D concrete printing using machine learning-based extrudate geometry control," *Virtual and Physical Prototyping*, vol. 15, no.2,pp. 178-193, 2020, https://doi.org/10.1080/17452759.2020.1713580.

5) Gao, G.; Xu, F.; Xu, J.; Tang, G.; Liu, Z. "A Survey of the Influence of Process Parameters on Mechanical Properties of Fused Deposition Modeling Parts", Micromachines (2022),13, 55, https://doi.org/10.3390/mi13040553.

6) Mohd Nizam Sudin, Nazri Md Daud, "The Effect of Nozzle Size on the Tensile and Flexural Properties of PLA Parts Fabricated Via FDM" Science, Engineering and Technology (2023), https://doi.org/10.54327/set2023/v3.n1.71

7) N. Naveed, "Investigate the effects of process parameters on material properties and microstructural changes of 3D-printed specimens using fused deposition modelling (FDM)", Materials Technology (2020), https://doi.org/10.1080/10667857.2020.1758475

8) J. Jiang, C. Yu, X.Xu, Y. Ma, and J. Liu, "Achieving better connections between deposited lines in additive manufacturing via machine learning," Mathematical Biosciences and Engineering, vol. 17, no. 4, 2020.

9) Chamil Abeykoon*, Pimpisut Sri-Amphorn, Anura Fernando, "Optimization of fused deposition modeling parameters for improved PLA and ABS 3D printed structures", International Journal of Lightweight Materials and Manufacture (2020), https://doi.org/10.1016/j.ijlmm.2020.03.003

10) S.Esslinger, and R.Gadow, "Additive manufacturing of bio ceramic scaffolds by combination of FDM and slip casting," Journal of the European Ceramic Society, vol. 40, no. 11,pp. 3707-3713, 2020, doi: https://doi.org/10.1016/j.jeurceramsoc.2019.10.029.

11) Rahul Roy, Abhijit Mukhopadhyay, "Tribological studies of 3D printed ABS and PLA plastic parts", Materials Today: Proceeding (2021) https://doi.org/10.1016/j.matpr.2020.09.235

12) Ranakoti L, Gangil B, Mishra SK, Singh T, Sharma S, Ilyas RA, El-Khatib S, "Critical Review on Polylactic Acid: Properties, Structure, Processing, Biocomposites, and Nanocomposites", Materials (Basel). 2022 Jun 17;15(12):4312. doi: https://doi.org/10.3390/ma15124312.

13) D.Yadav, D.Chhabra, R.K. Gupta, A.Phogat, and A. Ahlawat, "Modeling and analysis of significant process parameters of FDM 3D printer using ANFIS," Materials Today: Proceedings, vol. 21,pp. 1592-1604, 2020, doi: https://doi.org/10.1016/j.matpr.2019.11.227.

14) M.Goudswaard, B. Hicks, and A.Nassehi, "The creation of a neural network based capability profile to enable generative design and the manufacture of functional FDM parts," The International Journal of Advanced Manufacturing Technology, vol. 113, no. 9,pp. 2951-2968, 2021, doi: https://doi.org/10.1007/s00170-021-06770-8.

15) K.Yanamandra, G.L. Chen, X.Xu, G. Mac, and N. Gupta, "Reverse engineering of additive manufactured composite part by tool path reconstruction using imaging and machine learning," *Composites Science and Technology*, vol. 198,pp. 108318, 2020, doi: https://doi.org/10.1016/j.compscitech.2020.108318.

16) S.Dev, and R.Srivastava, "Experimental investigation and optimization of FDM process parameters for material and mechanical strength," *Materials Today:*

Proceedings, vol. 26,pp. 1995-1999, 2020, doi: https://doi.org/10.1016/j.matpr.2020.02.435.

17) K. Rajan, M. Samykano, K. Kadirgama, "Fused deposition modeling: process, materials, parameters, properties and applications", The International Journal of Advanced Manufacturing Technology (2022) 120:1531–1570, https://doi.org/10.1007/s00170-022-08860-7

18) A. Gupta, M.Taufiq, "Improvement of part strength prediction modelling by artificial neural networks for filament and pellet based additively manufactured parts", Australian Journal of Mechanical Engineering(2022), https://doi.org/10.1080/14484846.2022.2047472

19) Vicki May, "The History Of Additive Manufacturing: From The 1980s to Today", https://prototaluk.com/blog/history-of-additive-manufacturing/

20) L.Beng, B.Mcwilliams, W. Jaronsinski, "Machine Learning in Additive Manufacturing: A Review", JOM, Vol. 72, No. 6, (2020),The Minerals, Metals & Materials Society https://doi.org/10.1007/s11837-020-04155-y

21) Azhar Iqbal, Anoop Kumar Sood "Application of Machine Learning in Fused Deposition Modeling: A Review Chapter , 2021, https://doi.org/10.1115/1.4042084

22) Arup Dey and Nita Yodo, "A Systematic Survey of FDM Process Parameter Optimization and Their Influence on Part Characteristics", Journal Manuf. Mater. Process. 2019, 3, 64; doi: https://doi.org/10.3390/jmmp3030064.

23) L.Suárez, and M.Domínguez, "Sustainability and environmental impact of fused deposition modelling (FDM) technologies," *The International Journal of Advanced Manufacturing Technology*, vol. 106, no.3,pp. 1267-1279, 2020, doi: https://doi.org/10.1007/s00170-019-04676-0.

24) O.A. Mohamed, S.H.Masood, and J.L.Bhowmik, "Modeling, analysis, and optimization of dimensional accuracy of FDM-fabricated parts using definitive screening design and deep learning feed-forward artificial neural network," Advances in Manufacturing, vol. 9, no. 1,pp. 115-129, 2021, doi: https://doi.org/10.1007/s40436-020-00336-9.

25) M.Elbadawi, B.M. Castro, F.K.H.Gavins, J.J.Ong, S.Gaisford, G. Perez, A.W.Basit, P.Cabalar, and A. Goyanes, "M3DISEEN: A novel machine learning

approach for predicting the 3D printability of medicines," International Journal of Pharmaceutics, vol. 590,pp. 119837, 2020, doi: https://doi.org/10.1016/j.ijpharm.2020.119837.

26) Ravi Butola, Ranganath M. Singari, Lakshya Tyagi, "Comparison of response surface methodology with artificial neural network for prediction of the tensile properties of friction stir-processed surface composites", Proceedings of the Institution of Mechanical Engineers, Part E: Journal of Process Mechanical EngineeringVolume 236, Issue 1, February 2022, Pages 126-137, https://doi-org.imeche.idm.oclc.org/10.1177/09544089211036833

27) Ashutosh Kumar Gupta, Mohammad Taufik, "Investigation of dimensional accuracy of material extrusion build parts using mathematical modelling and artificial neural network", International Journal on Interactive Design and Manufacturing (IJIDeM) (2023) 17:869–885 https://doi.org/10.1007/s12008-022-01186-4

28) Jayant Giri, Pranay Shahane, Shrikant Jachak, Rajkumar Chadge, Pallavi Giri, "Optimization of FDM process parameters for dual extruder 3d printer using Artificial Neural network", Materials Today: Proceedings, 2214-7853- 2021 Elsevier Ltd, https://doi.org/10.1016/j.matpr.2021.01.899

29) Mohammad Shirmohammadi, Saeid Jafarzadeh Goushchi, Peyman Mashhadi Keshtiban, "Optimization of 3D printing process parameters to minimize surface roughness with hybrid artificial neural network model and particle swarm algorithm", Progress in Additive Manufacturing (2021) 6:199–215 , https://doi.org/10.1007/s40964-021-00166-6

30) Mahmood, M.A.; Visan, A.I.; Ristoscu, C.; Mihailescu, I.N. "Artificial Neural Network Algorithms for 3D Printing", Materials 2021, 14, 163. https://doi.org/10.3390/ma14010163

31) Omar Ahmed Mohamed1, Syed Hasan Masood, Jahar Lal Bhowmik, "Modeling, analysis, and optimization of dimensional accuracy of FDM-fabricated parts using definitive screening design and deep learning feedforward artificial neural network", Adv. Manuf. (2021) 9:115–129, https://doi.org/10.1007/s40436-020-00336-9.

32) Demei Lee, Guan-Yu Wu, “Parameters Affecting the Mechanical Properties of Three-Dimensional (3D) Printed Carbon Fiber-Reinforced Polylactide Composites”, Polymers 2020, 12, 2456; doi: https://doi.org/10.3390/polym12112456

33) M. Ajay Kumar, M.S. Khan, “Effect of fused deposition machine parameters on tensile strength of printed carbon fiber reinforced PLA thermoplastics”, Materials Today: Proceedings, 2020, https://doi.org/10.1016/j.matpr.2020.03.033

34) Atefeh Rajabi Kafshgar, “Optimization of Properties for 3D Printed PLA Material Using Taguchi, ANOVA and Multi-Objective Methodologies”, Procedia Structural Integrity 34 (2021) 71–77, doi: https://doi.org/10.1016/j.prostr.2021.12.011

35) Peter Kayode Farayibi, Babatunde Olamide Omiyale, “Mechanical Behaviour of Polylactic Acid Parts Fabricated via Material Extrusion Process: A Taguchi-Grey Relational Analysis Approach”, International Journal of Engineering Research in Africa, 2020, Vol. 46, pp 32-44, doi: https://doi.org/10.4028/www.scientific.net/JERA.46.32

36) Pooja Patil, Dharmendra Singh, “Multi-objective optimization of process parameters of Fused Deposition Modeling (FDM) for printing Polylactic Acid (PLA) polymer components”, Materials Today: Proceedings, (2021), https://doi.org/10.1016/j.matpr.2021.01.353

37) J Mogan, L Sandanamsamy, “A review of FDM and graphene-based polymer composite”, Materials Science and Engineering 1078 (2021) 012032, https://doi.org/10.1088/1757-899X/1078/1/012032

38) Ganesh Chate, Raviraj Kulkarni, “Study of the Effect of Nano-silica Particles on Resin-Bonded Moulding Sand Properties and Quality of Casting”, Silicon, Springer Nature 2018, https://doi.org/10.1007/s12633-017-9705-z.

39) M. Birosz, M. Ando, “Effect of infill pattern scaling on mechanical properties of FDM-printed PLA specimens”, Progress in Additive Manufacturing (2023), https://doi.org/10.1007/s40964-023-00487-8

40) Jianjing Zhang, Peng Wang, Robert X. Gao, “Deep learning-based tensile strength prediction in fused deposition modeling” Computers in Industry” https://doi.org/10.1016/j.compind.2019.01.011m

41) M.F. Khan, A.Alam, M.A.Siddiqui, M.S.Alam, Y. Rafat, N. Salik, and I. Al-Saidan, “Real-time defect detection in 3D printing using machine learning,” *Materials Today: Proceedings*, 2020, doi: https://doi.org/10.1016/j.matpr.2020.10.482.

42) J.M. Mercado-Colmenero, C. Martin-Doñate, V. Moramarco, M.A. Attolico, G. Renna, M.R. Santiago, and C. Casavola, “Mechanical characterization of the plastic material GF-PA6 manufactured using FDM technology for a compression uniaxial stress field via an experimental and numerical analysis,” *Polymers*, vol. 12, no.1,pp. 246, 2020, doi: https://doi.org/10.3390/polym12010246.

43) S.Garzon-Hernandez, D. Garcia-Gonzalez, A. Jerusalem, and A. Arias, “Design of FDM 3D printed polymers: An experimental-modelling methodology for the prediction of mechanical properties,” Materials & Design, vol. 188,pp. 108414, 2020, doi: https://doi.org/10.1016/j.matdes.2019.108414.

44) S.Garzon-Hernandez, A. Arias, and D. Garcia-Gonzalez, “A continuum constitutive model for FDM 3D printed thermoplastics,” Composites Part B: Engineering, vol. 201,pp. 108373, 2020, doi: https://doi.org/10.1016/j.compositesb.2020.108373.

45) V.Shanmugam, O. Das, K.Babu, U.Marimuthu, A.Veerasimman, D.J. Johnson, R.E. Neisiany, M.S. Hedenqvist, S. Ramakrishna, and F. Berto, “Fatigue behaviour of FDM-3D printed polymers, polymeric composites and architected cellular materials,” International Journal of Fatigue, vol. 143,pp. 106007, 2021, doi: https://doi.org/10.1016/j.ijfatigue.2020.106007.

46) R. Chen, W. He, H.Xie, and S. Liu, “Monitoring the strain and stress in FDM printed lamellae by using Fiber Bragg Grating sensors,” Polymer Testing, vol. 93,pp. 106944, 2021, doi: https://doi.org/10.1016/j.polymertesting.2020.106944.

47) L. Di Angelo, P. Di Stefano, A. Dolatnezhadsomarin, E. Guardiani, and E. Khorram, “A reliable build orientation optimization method in additive manufacturing: The application to FDM technology,” The International Journal of

Advanced Manufacturing Technology, vol. 108,pp. 263-276, 2020, doi: https://doi.org/10.1007/s00170-020-05359-x.

48) Z. Jin, Z. Zhang, and G.X.Gu, "Autonomous in-situ correction of fused deposition modeling printers using computer vision and deep learning," *Manufacturing Letters*, vol. 22,pp. 11-15, 2019, doi: https://doi.org/10.1016/j.mfglet.2019.09.005.

49) A.Majeed, Y. Zhang, S.Ren, J.Lv, T.Peng, S. Waqar, and E. Yin, "A big data-driven framework for sustainable and smart additive manufacturing," *Robotics and Computer-Integrated Manufacturing*, vol. 67,pp. 102026, 2021, doi: https://doi.org/10.1016/j.rcim.2020.102026.

50) V.Wankhede, D.Jagetiya, A. Joshi, and R. Chaudhari, "Experimental investigation of FDM process parameters using Taguchi analysis," Materials Today: Proceedings, vol. 27,pp. 2117-2120, 2020, doi: https://doi.org/10.1016/j.matpr.2019.09.078.

51) M. Samie Tootooni, Ashley Dsouza "Classifying the Dimensional Variation in Additive Manufactured Parts from Laser-Scanned 3D Point Cloud Data using Machine Learning Approaches" Journal of Manufacturing Science and Engineering, doi: https://doi.org/10.1115/1.4036641

52) John M. Gardner, Kevin A. Hunt, "Machines as Craftsmen: Localized Parameter Setting Optimization for Fused Filament Fabrication 3D Printing" dv. Mater. Technol. 2019, 1800653, DOI: https://doi.org/10.1002/admt.201800653

53) Kaushik Yanamandra,Jun Yung Choi, "Measurement of viscoelastic constants and Poisson's ratio of carbon fiber reinforced composites using in-situ imaging" , Journal of reinforced plastics and composites,2020, https://doi.org/10.1177/07316844221136843.

54) Saty Dev , Rajeev Srivastava, "Optimization of fused deposition modeling (FDM) process parameters for flexural strength", Materials Today: Proceedings 44 (2021) 3012–3016, https://doi.org/10.1016/j.matpr.2021.02.436

55) Anhua Peng, Xingming Xiao, "Process parameter optimization for fused deposition modelling using response surface methodology combined with fuzzy

inference system", Int J Adv Manuf Technol (2014) 73:87–100, doi: 10.1007/s00170-014-5796-5

56) Dinesh Yadav, Deepak Chhabra, "Optimization of FDM 3D printing process parameters for multi-material using artificial neural network", Materials Today: Proceedings (2019), https://doi.org/10.1016/j.matpr.2019.11.225

57) K.N. Gunasekaran, "Investigation of mechanical properties of PLA printed materials under varying infill density", Materials Today: Proceedings, https://doi.org/10.1016/j.matpr.2020.09.041

58) Anoop Kumar Sood , R.K. Ohdar, "Improving dimensional accuracy of Fused Deposition Modelling processed part using grey Taguchi method", Materials and Design 30 (2009) 4243–4252, doi: https://doi.org/10.1016/j.matdes.2009.04.030

59) Achyut Trivedi, Pavan Kumar Gurrala, "Fuzzy logic based expert system for prediction of tensile strength in Fused Filament Fabrication (FFF) process", Materials Today: Proceedings 44 (2021), 1344–1349. https://doi.org/10.1016/j.matpr.2020.11.391

60) Anhua Peng, Xingming Xiao, "Process parameter optimization for fused deposition modelling using response surface methodology combined with fuzzy inference system", Int J Adv Manuf Technol (2014) 73:87–100, doi: https://doi.org/10.1007/s00170-014-5796-5

61) Mohammed Hikmat, Sarkawt Rostam, "Investigation of tensile property-based Taguchi method of PLA parts fabricated by FDM 3D printing technology", Results in Engineering 11 (2021) 100264, https://doi.org/10.1016/j.rineng.2021.100264

62) Amna Mazen, Brendan McClanahan, "Factors affecting ultimate tensile strength and impact toughness of 3D printed parts using fractional factorial design", The International Journal of Advanced Manufacturing Technology (2022) 119:2639–2651, https://doi.org/10.1007/s00170-021-08433-0

63) Fuda Ning, Weilong Cong, "Additive manufacturing of carbon fiber-reinforced plastic composites using fused deposition modeling: Effects of process parameters on tensile properties", Journal of Composite Materials 2017, Vol. 51(4) 451–462, doi: https://doi.org/10.1177/0021998316646169

64) M Heidari-Rarani, N Ezati, “Optimization of FDM process parameters for tensile properties of polylactic acid specimens using Taguchi design of experiment method”, Journal of Thermoplastic Composite Materials 1–18, 2020, https://doi.org/10.1177/0892705720964560

65) Ge Gao, Fan Xu and Jiangmin Xu, “Parametric Optimization of FDM Process for Improving Mechanical Strengths Using Taguchi Method and Response Surface Method: A Comparative Investigation”, Machines 2022, 10, 750. https://doi.org/10.3390/machines10090750

66) Manohar Singh, Pushpendra S. Bharti, “Grey relational analysis based optimization of process parameters for efficient performance of fused deposition modelling based 3D printer”, Journal of Engg. Research, ICMET Special Issue, https://doi.org/10.36909/jer.ICMET.17159

67) Charalampous Paschalis, Kostavelis Ioannis, “Learning-based error modeling in FDM 3D printing process”, Rapid Prototyping Journal, 27/3 (2021) 507–517, doi: https://doi.org/10.1108/RPJ-03-2020-0046

68) Mahmoud Moradi, Reza Beygi, Noordin Mohd. Yusof, Ali Amiri, L.F.M. da Silva, and Safian Sharif, “3D Printing of Acrylonitrile Butadiene Styrene by Fused Deposition Modeling: Artificial Neural Network and Response Surface Method Analyses”, JMEPEG (2023) 32:2016–2028, https://doi.org/10.1007/s11665-022-07250-0

69) K. Arulkumaran, M. P. Deisenroth, M. Brundage, A. A. Bharath, Deep reinforcement learning: A brief survey, IEEE Signal Process. Mag., 34 (2017), 26–38.

70) D. N. Moriasi, J. G. Arnold, M. W. Van Liew, “MODEL EVALUATION GUIDELINES FOR SYSTEMATIC QUANTIFICATION OF ACCURACY IN WATERSHED SIMULATIONS”, 2007 American Society of Agricultural and Biological Engineers, Vol. 50(3): 885−900, https://swat.tamu.edu/media/1312/moriasimodeleval.pdf

71) J.P. Oliveira, A.D.LaLonde, and J. Ma, “Processing parameters in laser powder bed fusion metal additive manufacturing,” *Materials & Design*, vol. 193,pp. 108762, 2020, https://doi.org/10.1016/j.matdes.2020.108762.

72) C. Gamboa, S. Bejar, F. Trujillo Vilches, L. Hurtado, “Geometrical analysis in material extrusion process with polylactic acid (PLA)1carbon fiber”, Rapid Prototyping Journal29/11 (2023) 21–39Emerald Publishing Limited, https://doi.org/10.1108/RPJ-09-2022-0294

73) Y. Wang, J. Huang, Y. Wang , S. Feng,T. Peng , H. Yang, J. Zou, “A CNN-Based Adaptive Surface Monitoring System for Fused Deposition Modeling” IEEE/ASME TRANSACTIONS ON MECHATRONICS, VOL. 25, NO. 5, OCTOBER 2020, Accessed on April 20,2021 at 01:45:26 UTC from IEEE Xplore.

74) Mojtaba Khanzadeha, Prahalada Raob, “Quantifying Geometric Accuracy with Unsupervised Machine Learning: Using Self-Organizing Map on Fused Filament Fabrication Additive Manufacturing Parts” Journal of Manufacturing Science and Engineering, 2017. doi: https://doi.org/10.1115/1.4038598

75) Ribin Varghese Pazhamannil , P. Govindan, P. Sooraj, “Prediction of the tensile strength of polylactic acid fused deposition models using artificial neural network technique” Materials Today: Proceedings,2020, https://doi.org/10.1016/j.matpr.2020.01.199

76) S. Muthu Nataraja , S. Senthil, P. Narayanasamy, “Investigation of Mechanical Properties of FDM-Processed Acacia concinna–Filled Polylactic Acid Filament” , International Journal of Polymer Science, Volume 2022, Article ID 4761481, https://doi.org/10.1155/2022/4761481

77) Rama Srikar Mutyala, Kijung Park, Elif Elçin Günay, Gayeon Kim, Sharon Lau, John Jackman, Gül E. Okudan Kremer, “Effect of FFF process parameters on mechanical strength of CFR-PEEK outputs”, International Journal on Interactive Design and Manufacturing (IJIDeM) (2022) 16:1385–1396 https://doi.org/10.1007/s12008-022-00944-8

78) Qi Zhu, Kang Yu, Hanqiao Li, Qingqing Zhang, Dawei Tu, “Rapid residual stress prediction and feedback control during fused deposition modeling of PLA”,

The International Journal of Advanced Manufacturing Technology (2022) 118:3229–3240, https://doi.org/10.1007/s00170-021-08158-0

79) X. Li, X.Jia, Q. Yang, and J. Lee, “Quality analysis in metal additive manufacturing with deep learning,” Journal of Intelligent Manufacturing, vol. 31, no. 8,pp. 2003-2017, 2020, doi: https://doi.org/10.1007/s10845-020-01549-2.

80) N.A. Fountasa, P. Kostazos, “Experimental investigation and statistical modelling for assessing review the tensile properties of FDM fabricated parts”, Procedia Structural Integrity 26 (2020) 139–146, doi: https://doi.org/10.1016/j.prostr.2020.06.017

81) Afshin Gholamy, Vladik Kreinovich, Olga Kosheleva, “Why 70/30 or 80/20 Relation Between Training and Testing Sets: A Pedagogical Explanation”, . Departmental Technical Reports (CS). 1209, https://scholarworks.utep.edu/cs_techrep/1209

82) Tesfaye Mengesha Medibew, “A Comprehensive Review on the Optimization of the Fused Deposition Modeling Process Parameter for Better Tensile Strength of PLA-Printed Parts”, Advances in Materials Science and Engineering, Volume 2022, Article ID 5490831 https://doi.org/10.1155/2022/5490831.

83) Dey Arup, Nita Yodo. 2019. "A Systematic Survey of FDM Process Parameter Optimization and Their Influence on Part Characteristics" Journal of Manufacturing and Materials Processing 3, no. 3: 64. https://doi.org/10.3390/jmmp3030064

84) Qazi, M.I.; Akhtar, R.; Abas, M.; Khalid, Q.S.; Babar, A.R.; Pruncu, C.I. “An Integrated Approach of GRA Coupled with Principal Component Analysis for Multi-Optimization of Shielded Metal Arc Welding (SMAW) Process”, Materials 2020, 13, 3457. https://doi.org/10.3390/ma13163457

85) Anusree T.G., Anjan R.Nair, “Process Parameter Optimization of Fused Deposition Modeling for Helical Surfaces Using Grey Relational Analysis”, Materials Science Forum Online: 2016-11-15 Vol. 879, pp 861-866, https://doi:10.4028/www.scientific.net/MSF.879.861

86) Sukindar N. A., Mohd ariffin, Mohd khairol anuar, “Analyzing the effect of nozzle diameter in fused deposition modeling for extruding polylactic acid using open source 3D printing”, Teknologi,2016, https://doi.org/10.11113/jt.v78.6265.

LIST OF PUBLICATIONS

1) Nitin N. Gotkhindikar, Mahipal Singh, Ravinder Kataria, “Optimized deep neural network strategy for best parametric selection in fused deposition modelling”, International Journal on Interactive Design and Manufacturing (IJIDeM), (Published, Indexing: SCI, Impact factor: 2.2), (2023), ISSN- 19552513, https://doi.org/10.1007/s12008-023-01369-7

2) Nitin N. Gotkhindikar, Mahipal Singh, Ravinder Kataria, “Parametric optimization of fused deposition modelling process using integrated GRA-PCA approach”, OPSEARCH Journal, (Under review, Indexing: Scopus, SJR: 0.5), (2024), ISSN-00303887.

3) Nitin N. Gotkhindikar, Mahipal Singh, Ravinder Kataria, “A comprehensive study on material and performance characteristics of fused deposition modelling: Current scenario and future research direction”, AIP Conf. Proc. 2986, 030010 (2024) https://doi.org/10.1063/5.0192764

4) Nitin N. Gotkhindikar, Mahipal Singh, Ravinder Kataria, “Deep Neural Network Model for Better Print Line Connection in Fused Deposition Modeling”, AIP Conf. Proc. 2986, 030010 (2024) https://doi.org/10.1063/5.01927647

LIST OF WORKSHOPS/ FDP/ COURSES

1) Faculty development programme on “Artificial Intelligence”, organized by AICTE Training and Learning (ATAL) Academy from 14.09.2020 to 18.09.2020

2) Faculty development programme on “3D Printing and design”, organized by AICTE Training and Learning (ATAL) Academy from 01.02.2021 to 05.02.2021

3) NPTEL Course on “Fundamentals of Additive Manufacturing Technologies”, from Jul-Oct 2023, (12 week course).

4) Training course on “Generative AI”, at Pantech Learning Pvt Ltd from 08.01.2024 to 27.01.2024.